LEVEL II

A CAVITY-TYPE BROADBAND ANTENNA WITH A STEERABLE CARDIOID PATTERN

B. A. Munk and C. J. Larson

OSU
The Ohio State University

The Ohio State University
ElectroScience Laboratory
Department of Electrical Engineering
Columbus, Ohio 43212

FINAL REPORT 711559-2

Contract N00014-78-C-0855

December 1979

Department of the Navy
Office of Naval Research
Arlington, Virginia 22217

Approved for public release;
distribution unlimited

NOTICES

When Government drawings, specifications, or other data are used for any purpose other than in connection with a definitely related Government procurement operation, the United States Government thereby incurs no responsibility nor any obligation whatsoever, and the fact that the Government may have formulated, furnished, or in any way supplied the said drawings, specifications, or other data, is not to be regarded by implication or otherwise as in any manner licensing the holder or any other person or corporation, or conveying any rights or permission to manufacture, use, or sell any patented invention that may in any way be related thereto.

UNCLASSIFIED

SECURITY CLASSIFICATION OF THIS PAGE *(When Data Entered)*

REPORT DOCUMENTATION PAGE

READ INSTRUCTIONS BEFORE COMPLETING FORM

1 REPORT NUMBER	2. GOVT ACCESSION NO. / 3. RECIPIENT'S CATALOG NUMBER
4. TITLE *(and Subtitle)*: A CAVITY-TYPE BROADBAND ANTENNA WITH A STEERABLE CARDIOID PATTERN	5. TYPE OF REPORT & PERIOD COVERED: Final Report
	6. PERFORMING ORG. REPORT NUMBER: ESL-711559-2
7. AUTHOR(s): B. A. Munk, C. J. Larson	8. CONTRACT OR GRANT NUMBER(s): Contract N00014-78-C-0855
9. PERFORMING ORGANIZATION NAME AND ADDRESS: The Ohio State University ElectroScience Laboratory, Department of Electrical Engineering, Columbus, Ohio 43212	10. PROGRAM ELEMENT, PROJECT, TASK AREA & WORK UNIT NUMBERS
11. CONTROLLING OFFICE NAME AND ADDRESS: Department of the Navy, Office of Naval Research, 800 North Quincy St., Arlington, Virginia 22217	12. REPORT DATE: DEC 1979
	13. NUMBER OF PAGES: 87
14. MONITORING AGENCY NAME & ADDRESS *(If different from Controlling Office)*	15. SECURITY CLASS. *(of this report)*: Unclassified
	15a. DECLASSIFICATION/DOWNGRADING SCHEDULE

16. DISTRIBUTION STATEMENT *(of this Report)*

This document has been approved for public release and sale; its distribution is unlimited.

17. DISTRIBUTION STATEMENT *(of the abstract entered in Block 20, if different from Report)*

18. SUPPLEMENTARY NOTES

19. KEY WORDS *(Continue on reverse side if necessary and identify by block number)*

Flushmounted Antenna
Steerable Antenna
Cardioid Pattern
IFF Antenna
Hybrid Design
Loop Design
Push push traps

20. ABSTRACT *(Continue on reverse side if necessary and identify by block number)*

This report describes a new vertically polarized cavity-type antenna with a cardioid pattern steerable in the horizontal plane. The front-to-back ratio is better than 15 dB over a 25% bandwidth and better than 20 dB within half that total bandwidth. The average gain is approximately 2 dB above a monopole and the VSWR<? except at the very end of the band. The beamwidth in the front as well as the nullwidth in the back is so wide that the beam is directed only in the four cardinal directions in the horizontal plane. A working model will be delivered to NRL as part of the contract.

DD FORM 1 JAN 73 1473 EDITION OF 1 NOV 65 IS OBSOLETE

UNCLASSIFIED

SECURITY CLASSIFICATION OF THIS PAGE *(When Data Entered)*

ACKNOWLEDGMENT

The discussions with and suggestions by Messrs. Gerry Hart and Paris Coleman of NRL throughout this investigation were most helpful and are deeply appreciated.

The authors also wish to acknowledge the contribution of Mr. Dale Woodside in the early phases of this investigation.

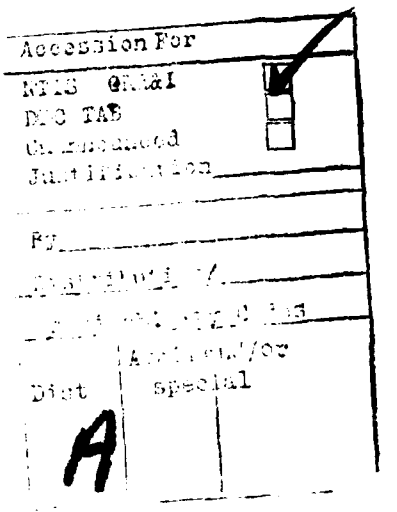

TABLE OF CONTENTS

I. INTRODUCTION

This report describes the basic development of a flush-mounted antenna with a cardioid pattern and a 25% bandwidth. By use of diode switches, the beam can be directed in four directions. However, the feed system can be relatively easily modified to scan in 45^{o} steps.

The simplest and most widely known method of producing a cardioid pattern is to place two dipoles (or monopoles) at a distance of one quarter wavelength and feed them 90^{o} out of phase, see Figure 1. However, this approach could not be used in the present situation for essentially two reasons:

1. The antenna must be flush-mounted on an airplane.

2. The bandwidth must be 25%.

The first of these discrepancies can be resolved by using a flush-mounted cavity which is excited either by monopoles or loops, see Figure 2. The number of these depend on how we wish to steer the beam. The second problem also leads us to consider an alternate approach as illustrated in Figure 3. Here we have mounted four loops in the cavity and fed them with a linear phase delay of 360^{o} around the circumference, i.e., the four loops are excited with the phases 0^{o}, 90^{o}, 180^{o} and 270^{o}. Further, we have in the center of the cavity mounted a top-loaded monopole. Further, we have a top loaded monopole mounted in the center of the cavity.

The radiation pattern in the horizontal plane of the four loops will be omnidirectional and so will the pattern of the monopole. However, while the phase of the radiated signal from the monopole will remain constant as we go around the antenna in the horizontal plane, the phase of the signal from the four loops will change 360^{o}. Thus, at some direction the signal from the four loops and the one from the monopole will be out of phase. If at the same time the amplitudes of the two signals

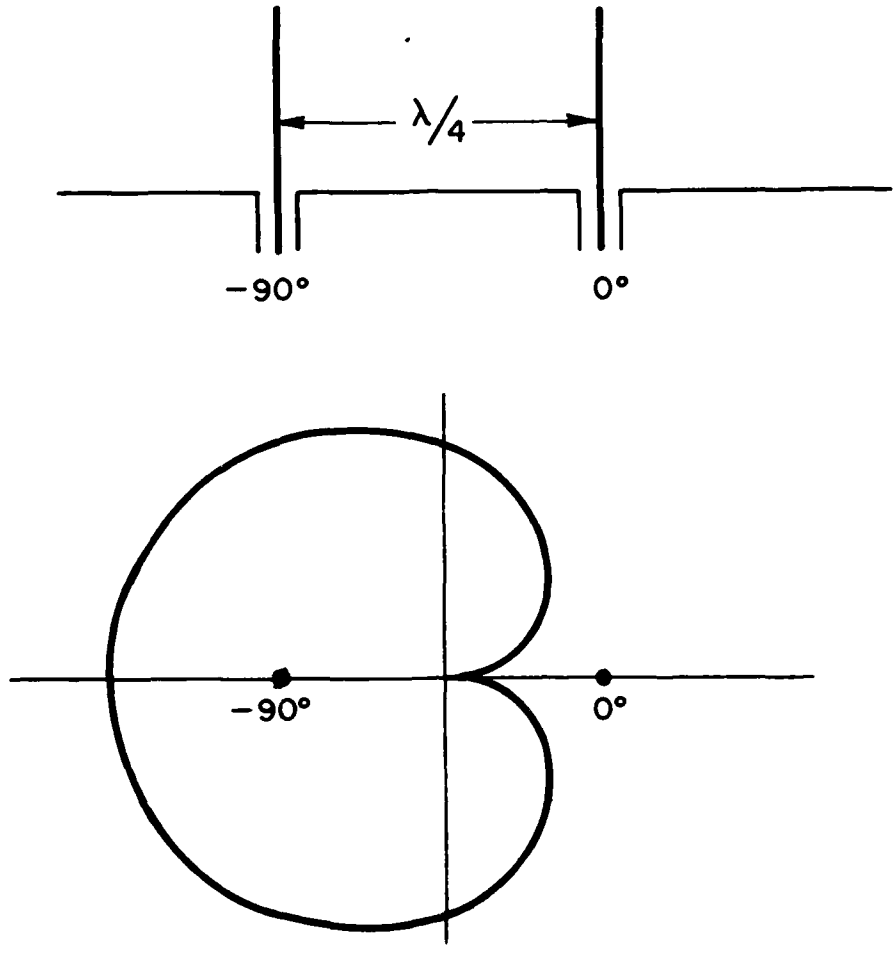

Figure 1. The well known way of producing a cardioid Pattern: Two monopoles fed in quadrature and spaced λ/4 apart.

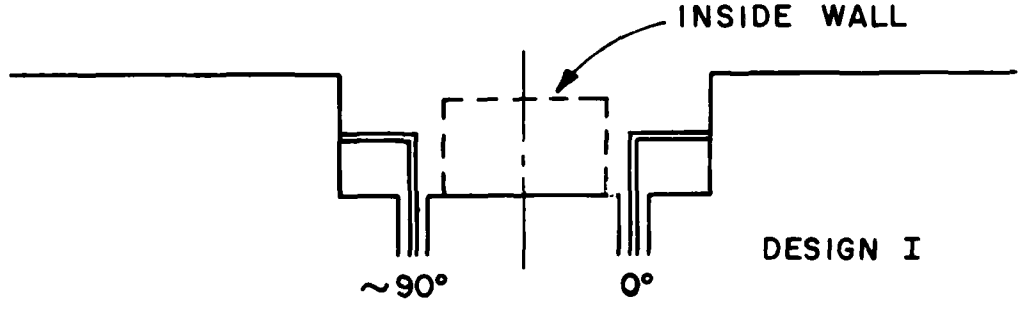

Figure 2. An alternate way to produce a cardioid pattern: Two loops located in a flush mounted cavity. Design I.

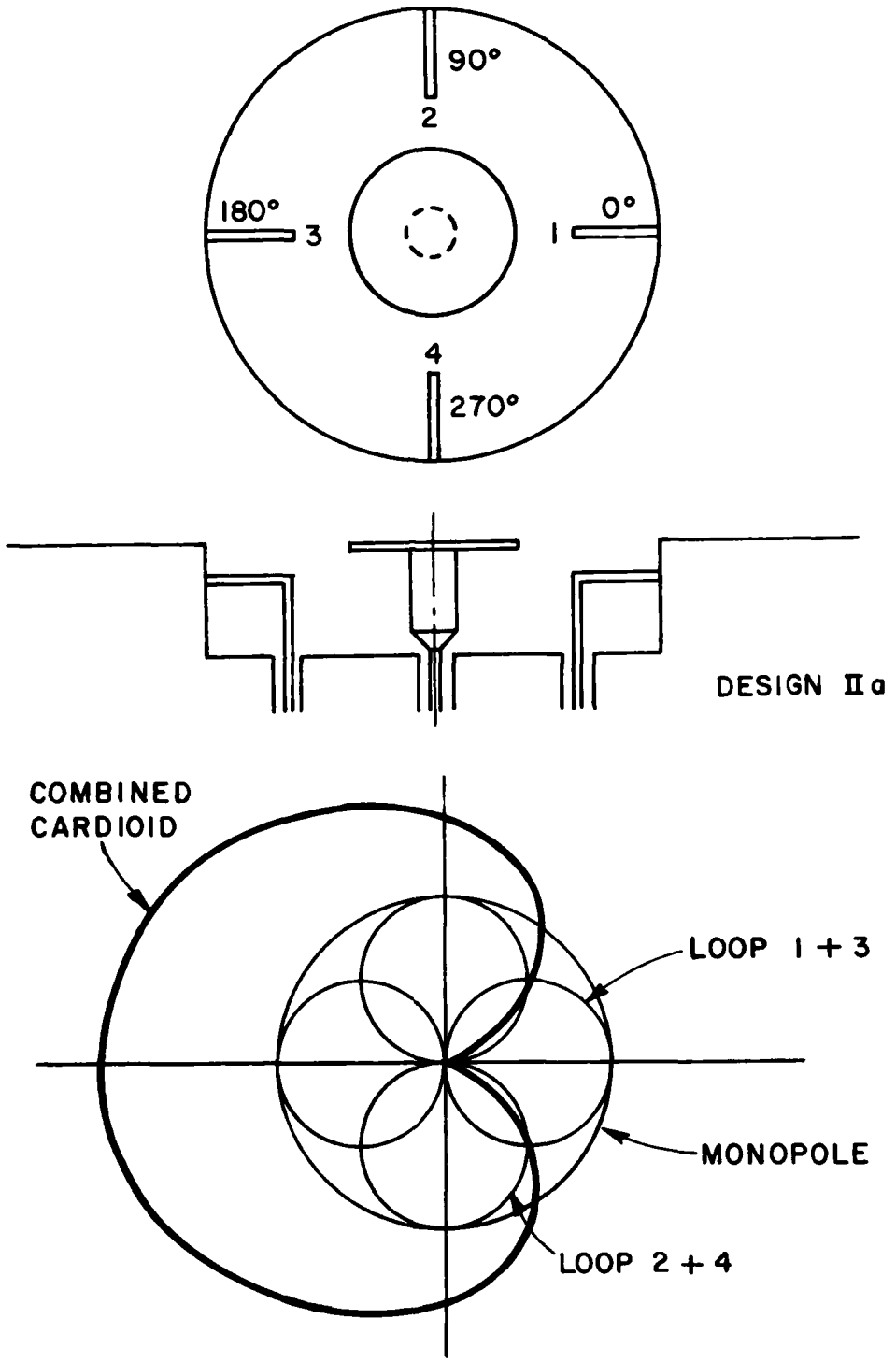

Figure 3. Four loops fed in phase progression with a monopole in the middle can also produce a cardioid pattern. The beam can be steered by changing the relative phase of the monopole. Design IIa.

are equal, we will obtain a null in the combined radiation pattern in that direction. By changing the phase relationship between the monopole and the four loops, we are able to steer the beam in the horizontal plane. A fundamental advantage of this configuration as compared to the one in Figure 2 is that no coupling exists between the monopole and the four loops, while a strong mutual coupling is present between the two excited loops in Figure 2.

A variation of the approach in Figure 3 is shown in Figure 4. Instead of exciting all four loops, we are here exciting only two opposing loops 180^{0} out of phase. Thus, the radiation pattern from these two loops will be a figure eight as indicated in Figure 4. If we now adjust the phase of the monopole such that the two signals cancel in the back direction, a null is obtained while a maximum is obtained in the front direction.

The advantage of the approach in Figure 4 is that it yields a broader null than the one in Figure 3, and also a higher gain. However, while the Figure 3 approach can easily be scanned continuously in the horizontal plane, the approach in Figure 4 rotates in 90^{0} steps (or 45^{0} steps if the loops are excited in pairs).

In the following we shall investigate these various designs in more detail; in particular the one given in Figure 4.

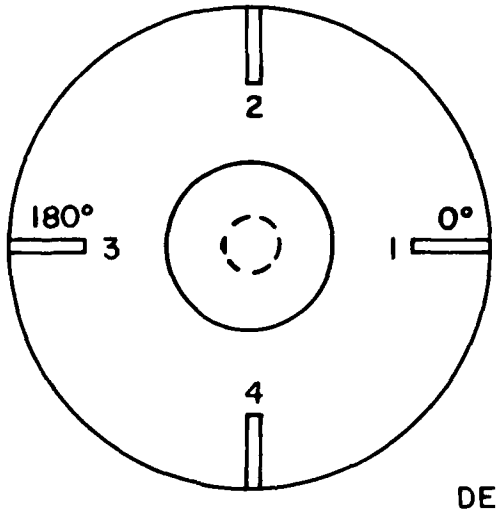

DESIGN II b

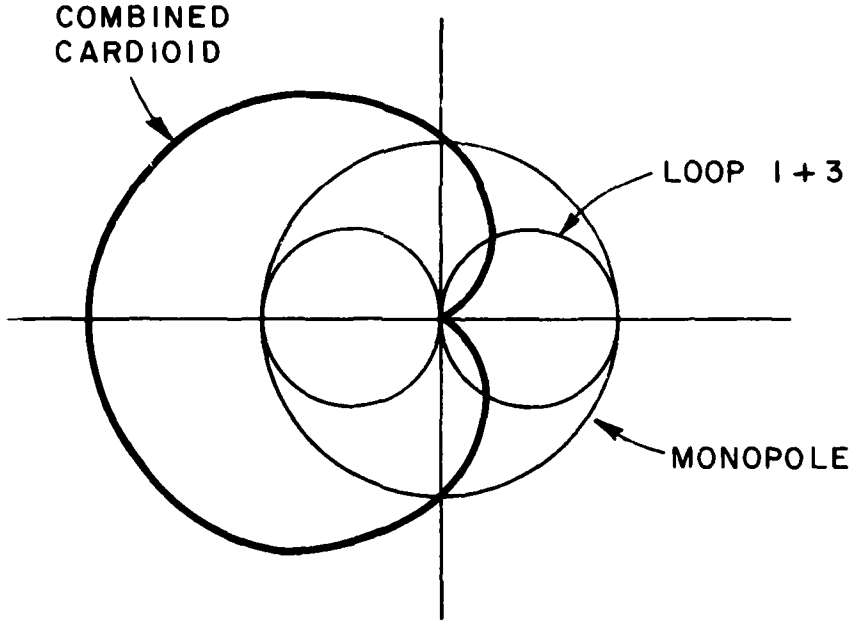

Figure 4. Same antenna as in Figure 3 but exciting only loop 1+3 and the monopole resulting in a sharper cardioid pattern. Design IIb.

II. DESIGN I

Design I shown in Figure 2 consists of four loops mounted in a cavity. Only two opposing loops are excited at a time and by controlling the relationship between these two active loops we can obtain a null either to the left or right along the line connecting the two active loops. The other two loops are simply not connected. They are of course being parasitically excited and in order to minimize this effect they must be reactively loaded as explained later.

However, before attempting to phase the two loops they must first be properly matched. A direct measurement of a single loop mounted in the cavity as shown in Figure 5 showed a very bad impedance as indicated in Figure 6, curve a. Enlargement of the loops produces a typical impedance curve b, i.e., pushed it around somewhat on the Smith chart without much improvement as one might expect. However, if we enlarge the center post from a diameter of ½" to 2½" (and retain the original loops) we obtain curve c in Figure 6, which shows some improvement. Although the accuracy of the various curves in Figure 6 is rather poor, it was later confirmed by curves transformed to the central part of the Smith chart that a conducting body mounted in the center of the cavity increased the bandwidth potential of the loops significantly. The exact cause of this observation is not clear at this time, but is believed to be related to elimination of part of the stored energy surrounding the loops.

It is recognized that the presence of a center conductor permits the lowest order coaxial mode to propagate out of the cavity and also that this particular mode is indeed being excited by the two opposite loops excited 180^{o} out of phase. However, it was repeatedly observed that it was the distance between the loops and the center conductor in the cavity that gave the improvement in impedance, not the actual diameter of the center conductor which determines the cut-off frequency of the coaxial mode.

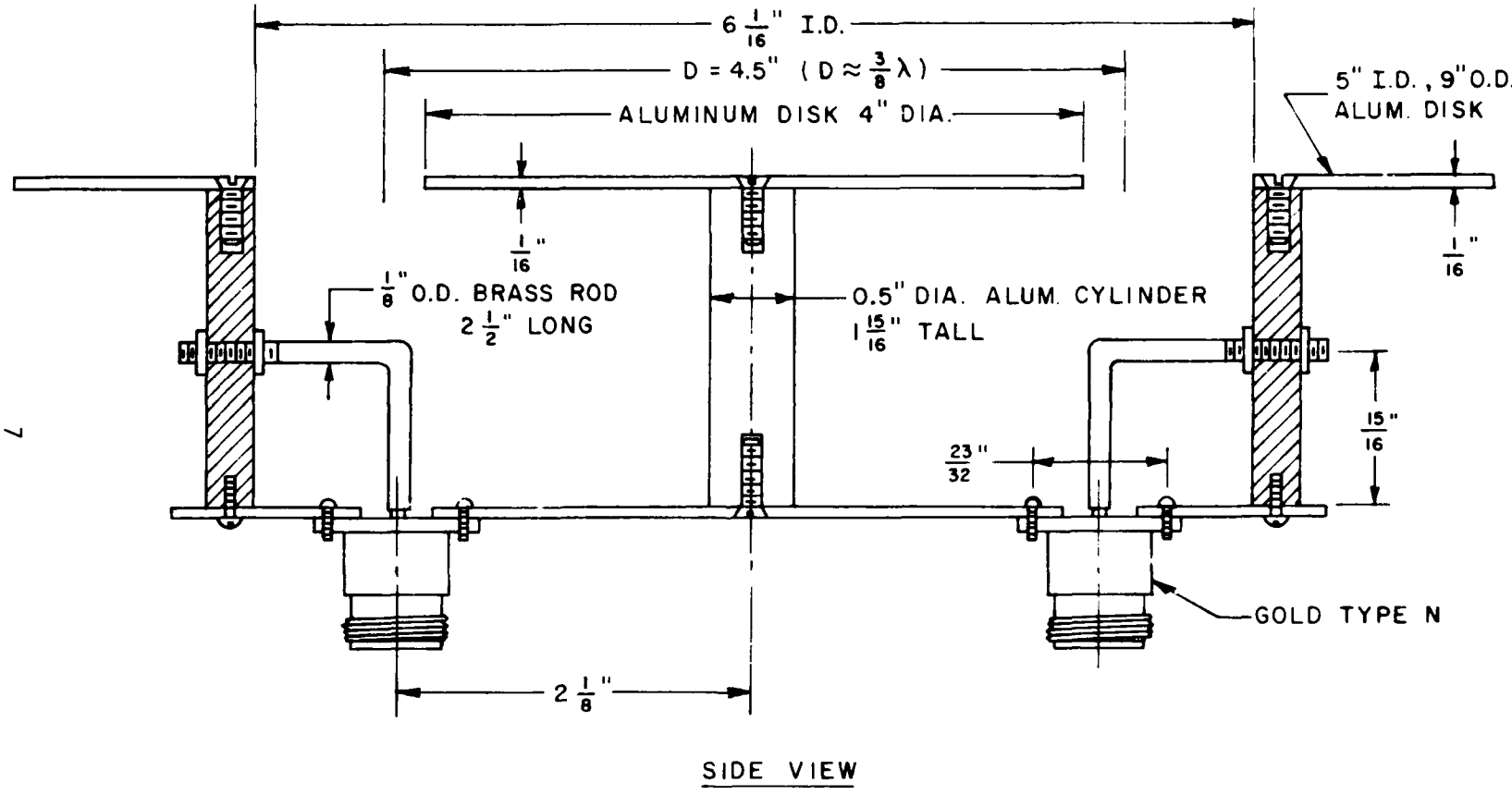

Figure 5. The detailed drawing of the first design I consisting of merely four loops (no monopole).

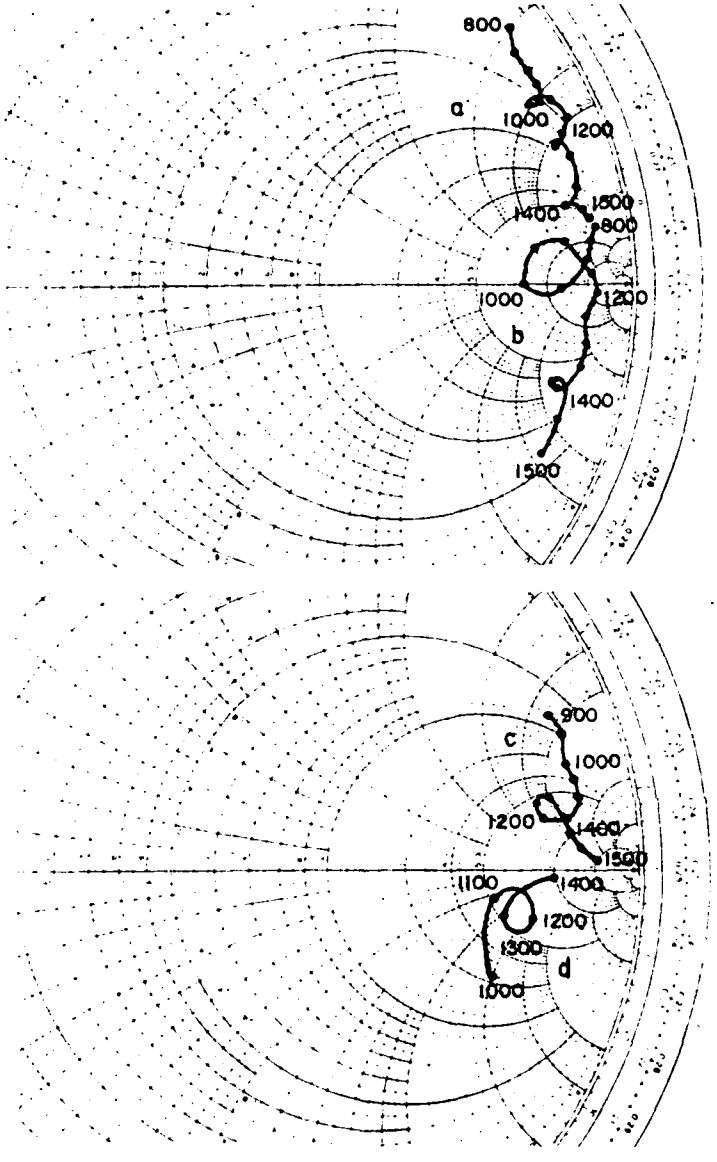

Figure 6. The loop impedance of design I.

Curve a: With dimensions as shown in Figure 5.
Curve b: With larger loops.
Curve c: With loops as shown in Figure 5 but a $2\frac{1}{2}$" center post instead of $\frac{1}{2}$".
Curve d: The impedance of curve c in series with a capacitor.

Obviously some matching network has to be introduced at the loop terminal in order to bring the impedance down to a lower impedance level. It is important here to remind the reader that any successful matching usually is preceeded by reversing the impedance curve, i.e., instead of the impedance curves moving clockwise on the Smith chart with increasing frequency, we should try to make them run counter clockwise (obviously this is only possible over a limited frequency range). Since transmission lines and many other components naturally run clockwise on the Smith chart with increasing frequency, a natural compensation of a reversed impedance curve may take place.

Reversing of the typical impedance curves in Figure 6 can be accomplished in a number of ways. One of the simplest approaches consists of the insertion of a series capacitance. Typically this would move curve c in Figure 6 into a typical curve d which, when observed from the center of the Smith chart, is seen to run counter clockwise as a function of frequency. In our present situation we have chosen that approach with one minor modification; instead of inserting a series capacitance directly at the output terminals yielding curve "d" we inserted a series capacitance at the 90^{0} bend (point A in Figure 5). There are two reasons for this:

a. It is mechanically convenient.

b. The impedance as seen at point A in Figure 5 by the capacitor will be moved slightly counter clockwise on the Smith chart as compared to the impedance seen directly at the input terminals. This may be important if the loop impedance is of the general form represented by curve b in Figure 6 where a series capacitor would be ineffective in reversing the impedance curve for frequencies above 1200 MHz.

The construction of a loop with a series capacitance is seen in Figure 7. By screwing the horizontal rod A further into the hole of

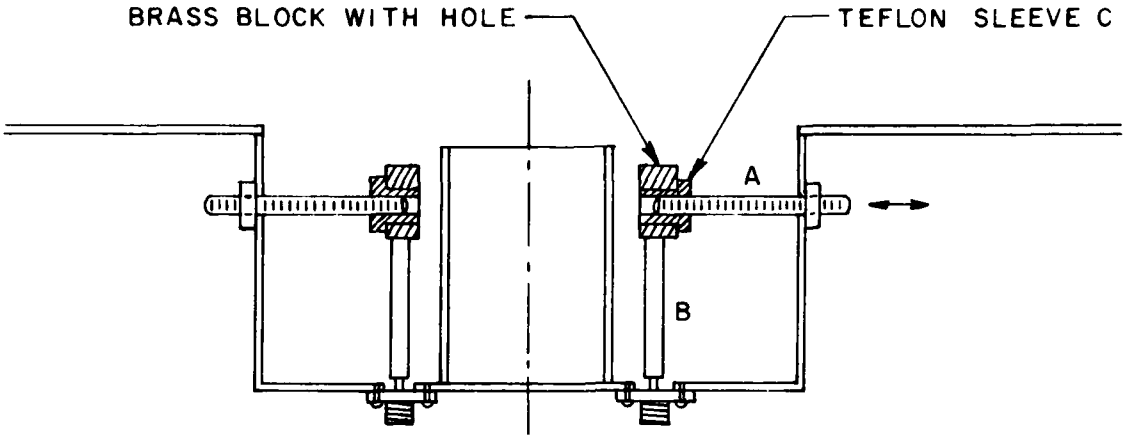

Figure 7. The mechanical design of loops containing a series capacitance created between rod A and the hole in the brass block lined with a teflon sleeve C.

the brass block attached to the top of the vertical rod B, the capacitance is increased. The hole is seen to be lined by a dielectric teflon sleeve C providing a good sturdy mechanical design. The effect of varying the capacitance upon the input impedance of a single loop is illustrated in Figure 8. All four loops were provided with N-connectors, and the input impedance of a single loop measured with the other three loops opencircuited. Also shown in Figure 8 is the beneficial effect of a dielectric slab put about ¼" on top of the loops and simulating a radome.

We should emphasize that the input impedances shown in Figure 8 are only typical since they depend very much on the load condition of the other three parasitic loops. This is demonstrated in Figure 9 where we show the input impedance of a single loop with the other three loops opencircuited as in Figure 8 but also with the three loops short circuited. The big difference in impedance between the open and

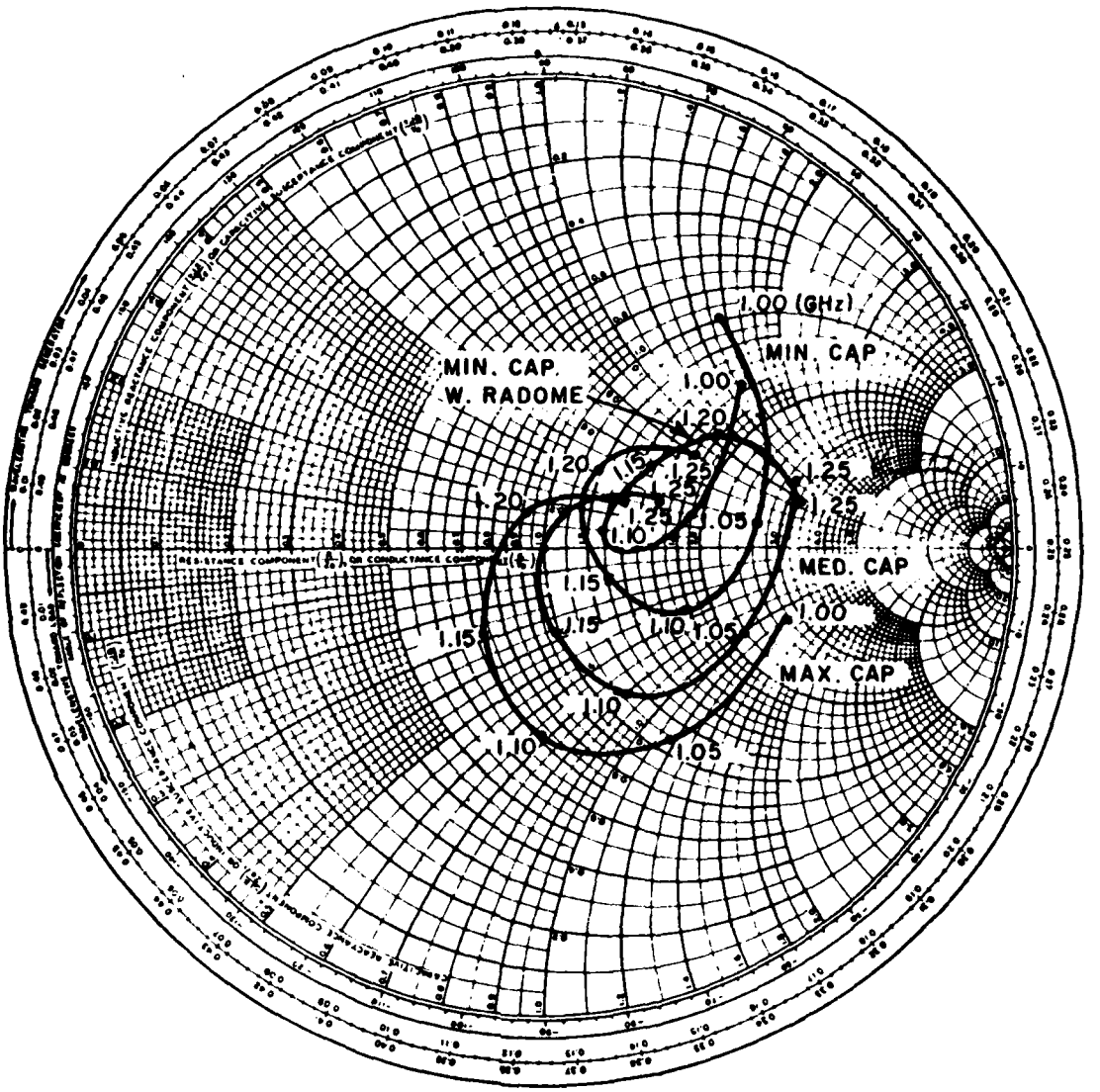

Figure 8. The input impedance of a single loop for positions of the capacitor shown in Figure 7. The other three loops were open circuited.

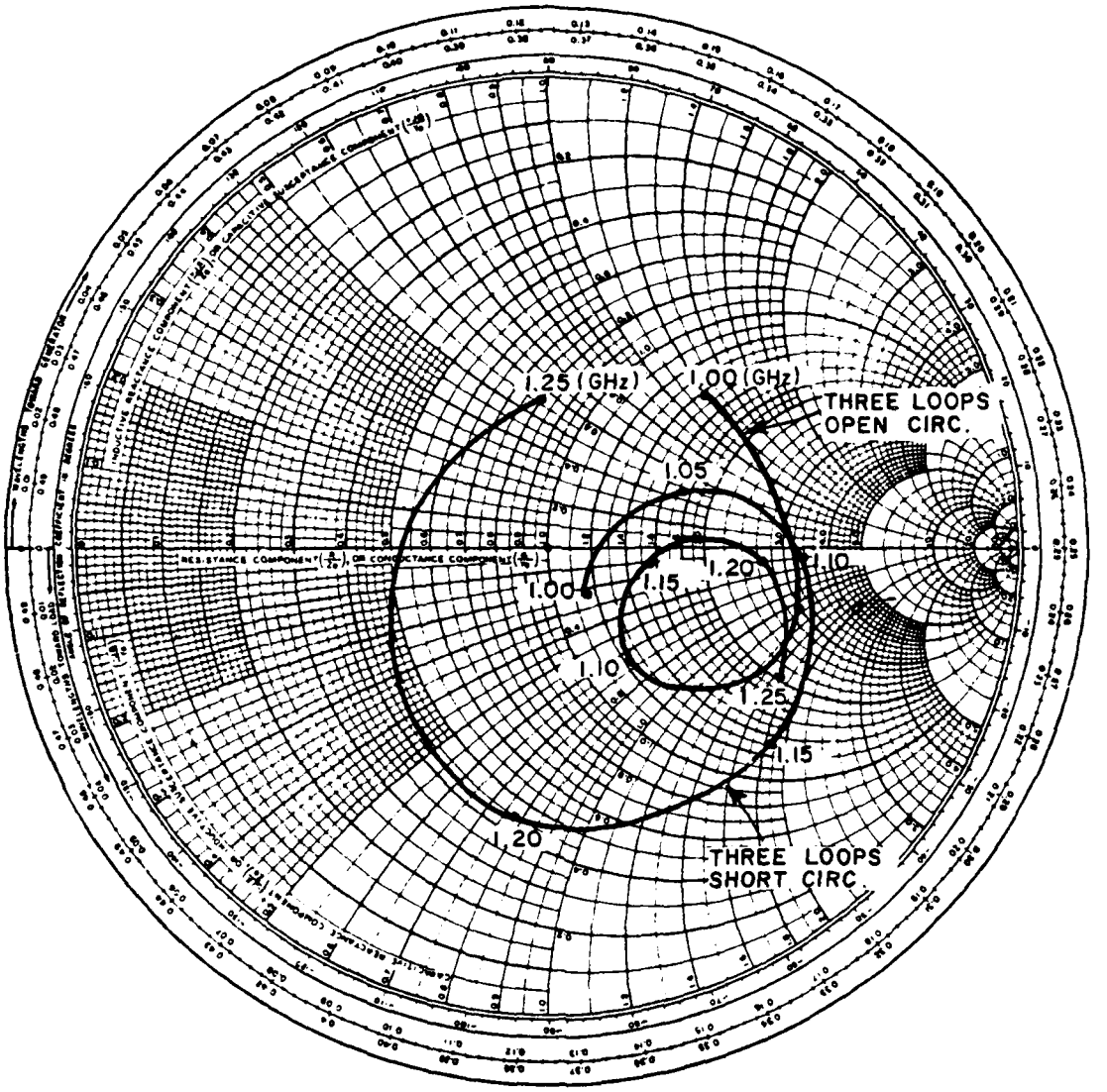

Figure 9. The input impedance of a single loop for fixed capacitance but with the other three loops being open circuited or short circuited.

short circuit impedance case is a testimony to the very strong mutual coupling that ultimately would be the Waterloo for this approach (but not for another version).

Thus, although the present design fell short in meeting the entire spec, we nevertheless feel it would be of interest to report the results before moving on to present another design that did meet the specifications. In Figure 10 we show a schematic depicting how the four loops were fed. Note that there are four input ports, and adjacent to each is a $\lambda/4$-trap terminated in a switching diode. When this diode is conducting, the other end of the $\lambda/4$-trap attains a high impedance and a signal will flow freely on the line. If on the other hand the diode is open, we will obtain a short curcuit at the other end of the $\lambda/4$-trap, and no signals can flow on the line. Note further, that the $\lambda/4$-traps are positioned $\lambda/4$ away from the lines connecting two opposing loops. This insures no "disturbance" on this interconnecting line when the $\lambda/4$-trap produces a short circuit at the input terminals (i.e., diodes open). Finally, the point where the input line attaches to the line connecting two opposing loops is important in as much as it determines the phase and amplitude ratio between two opposing loops, i.e., their radiation pattern. This optimum position was found after some experimenting and a typical set of radiation pattern is shown in Figure 11. Note that the scale is linear, i.e., the front-to-back ratio is only of the order of 10-14 dB. Considering that our design goal was 20 dB, it was decided to tune the antenna up to the absolute maximum front-to-back ratio. To this end we mounted two monopole antennas at the edge of the standard 4' circular groundplane, one in front and the other in back direction. By measuring the ratio between the voltages induced in the two monopoles from the antenna, we obtained the front-to-back ratio in the near field, which turned out to be remarkably well correlated with the far field values. The maximum FB-ratio was now obtained by varying two parameters, namely:

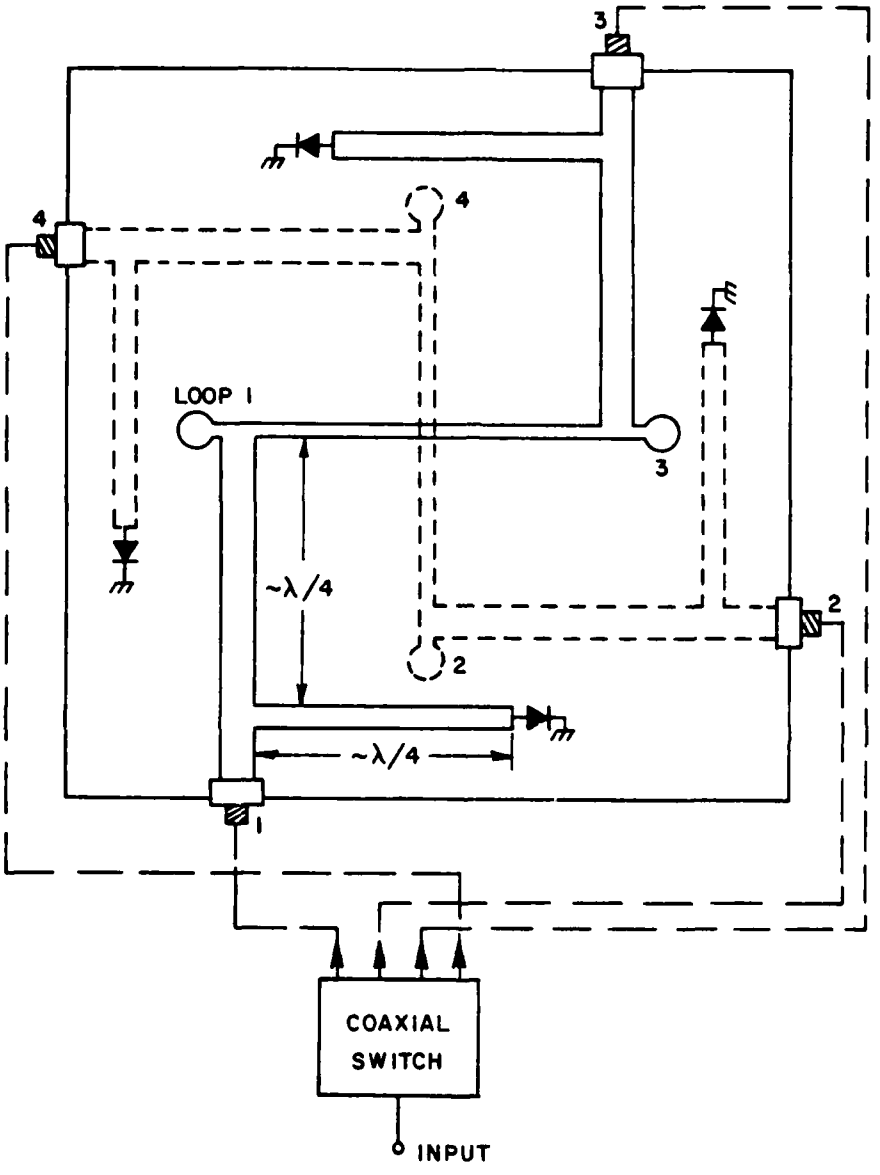

Figure 10. The strip lines that feed the four loops via a coaxial switch. Quarter wave traps terminated in diodes activates one set of loops only.

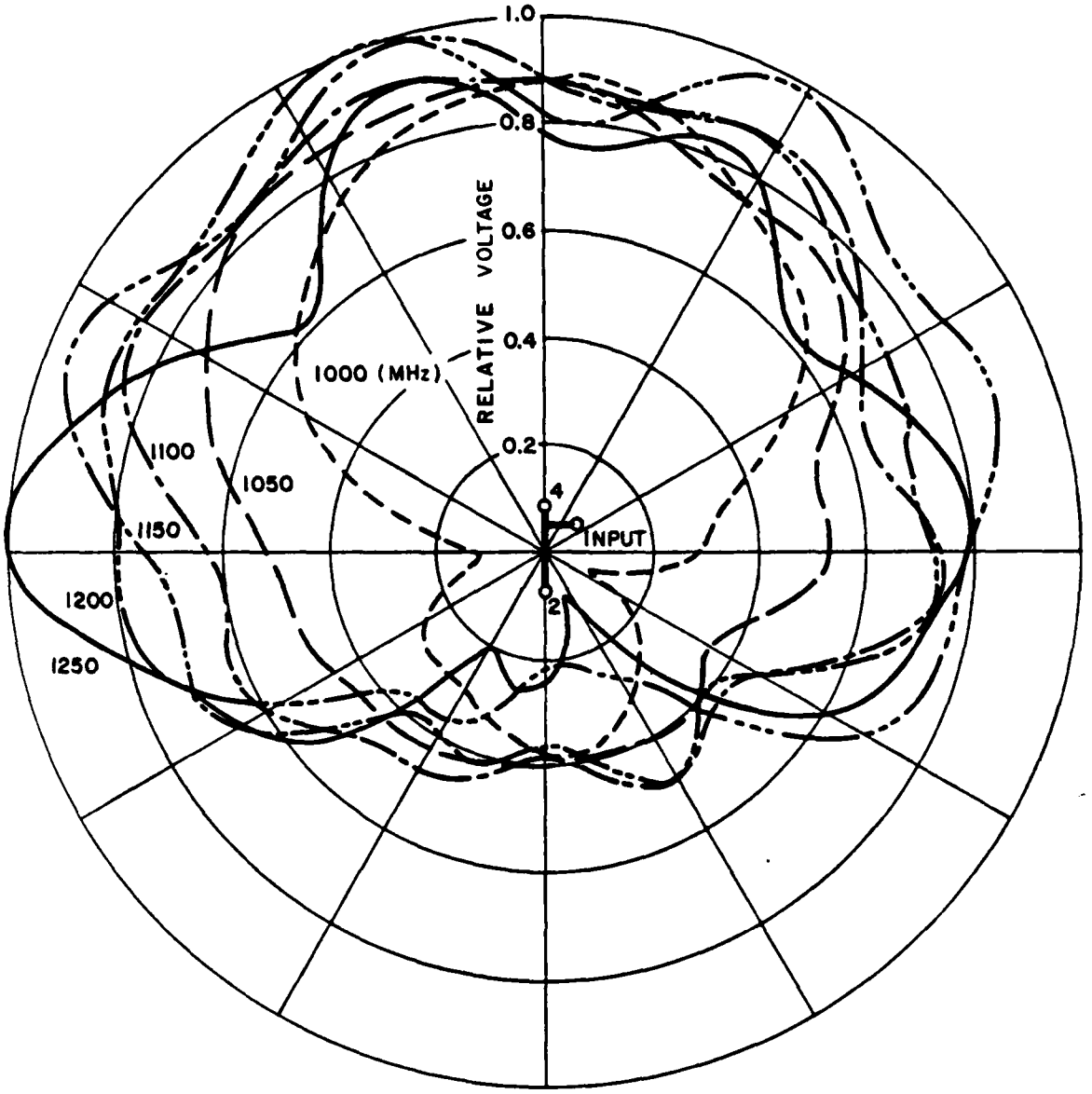

Figure 11. The radiation pattern of the first version of design I. Front-to-back ratio is insufficient (note linear scale).

1. A sliding contact as shown on the insert of Figure 12.

2. A stub adjustable in length and mounted approximately $\lambda/8$ away from the sliding contact, see insert in Figure 12.

Adjustment of the sliding contact effects essentially the phase ratio between the two active loops, while adjustment of the stub affects their amplitude ratio and as is illustrated in Figure 12, it was indeed possible to obtain "infinite" high FB-ratios at one specific frequency. As can also be seen in Figure 12, however, the bandwidth is lacking considerably. This appeared to be the case with several combinations of line length between two opposing loops, variation of the characteristic impedance and for various loadings of the two other loops. Typical far field radiation patterns are seen in Figure 13 which again indicate the narrow bandedness of this design, although very high FB-ratio can be obtained at one frequency.

After some further frustrating experimentation, it was decided to abandon this design. However, it was decided first to gain some insights into why this antenna was so narrow banded patternwise, while the combined input impedance of the two loops was very nicely within 2:1 (VSWR) over the entire band (1.0-1.25 GHz). To that end we decided to measure the input impedance of each of the two loops 1 and 3 under <u>working</u> condition, i.e., the input impedance consisting of the self impedance plus the mutual impedance multiplied with the current ratio I_1/I_3.

The setup is shown in Figure 14 and is seen to consist of a generator feeding one loop through a Smith chart plotter and the other loop through an attenuator and trombone. The two latter are adjusted for maximum FB-ratio at each frequency as being monitored by the two monopoles mounted close to the edge on the 4' ground plane. The impedances of the two loops are shown in Figures 15a and b for a number of load conditions of the two parasitic loops. Note that the impedance of the loop in

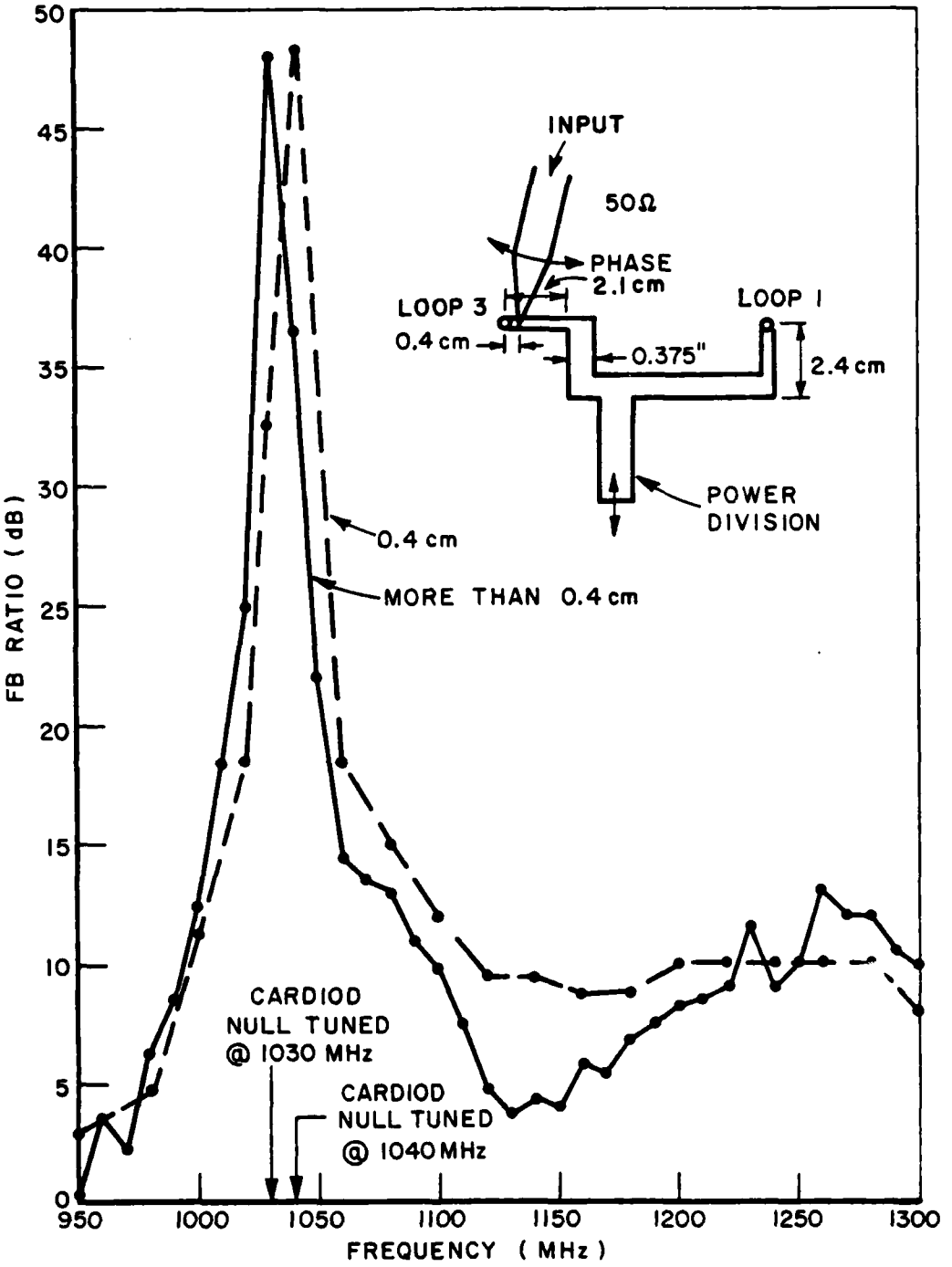

Figure 12. The FB-ratio obtained by feeding two loops as shown in insert. The sliding contact adjusts the phase, the open circuit stub power division between the two active loops. The two passive loops are terminated in open circuited transmission lines 0.8 cm long.

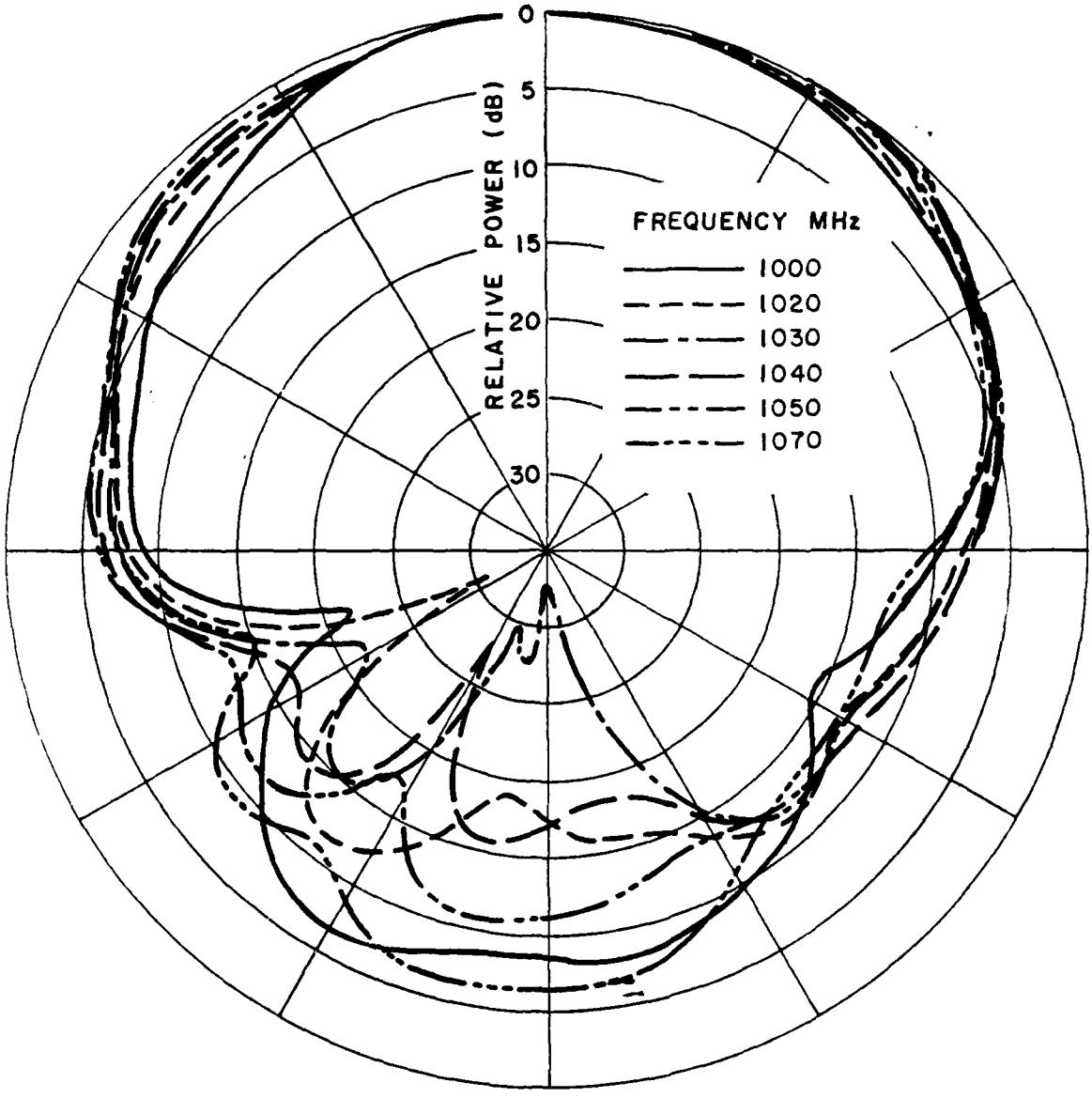

Figure 13. Typical radiation pattern for design I when FB-ratio is peaked at one frequency as shown in Figure 12.

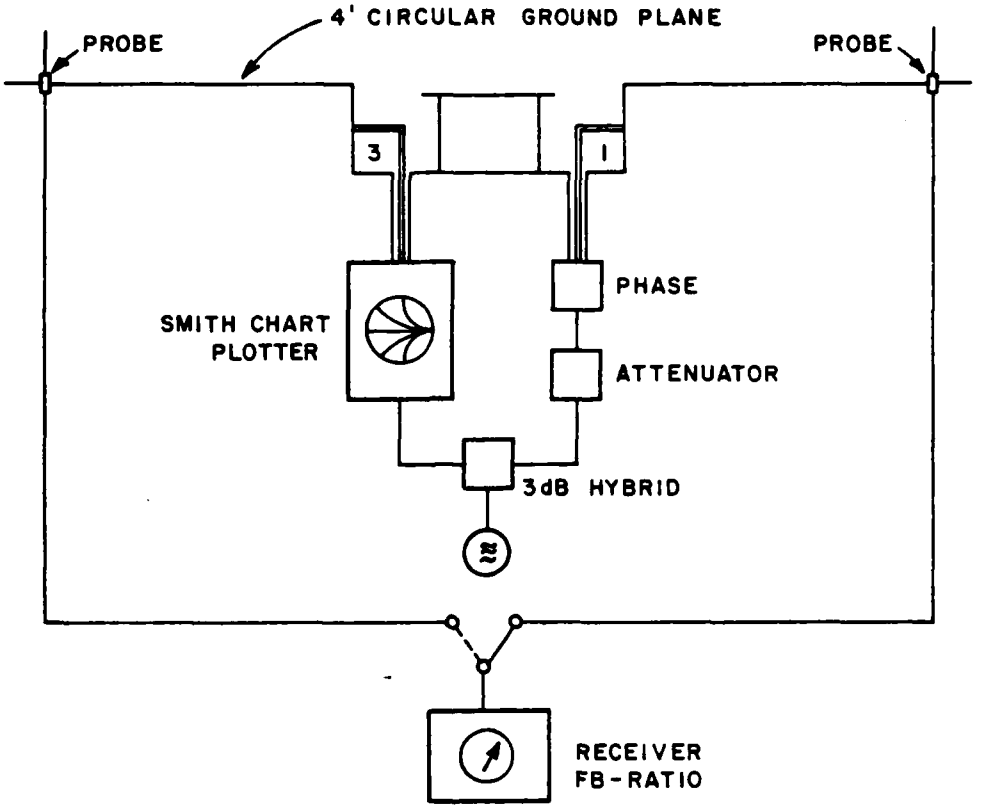

Figure 14. The loop currents I_3 and I_1 are adjusted for max. FB-ratio by varying phase and amplitude to loop 1. Then the impedance for loop 3 is read on the network analyzer.

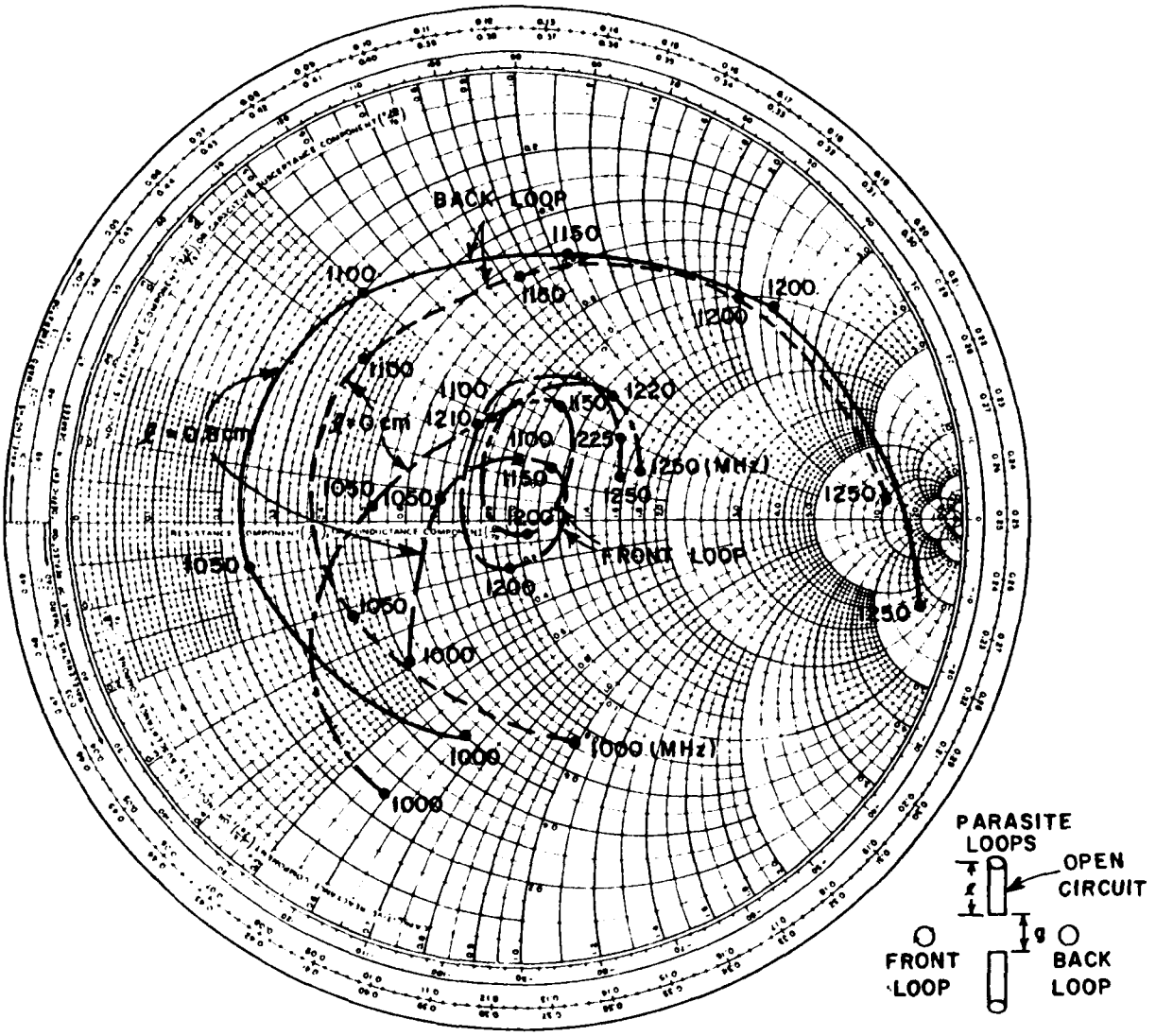

Figure 15a. The input impedance of the front and back loops with their current ratio adjusted for maximum FB-ratio as shown in Figure 14. The two parasitic loops are reactively loaded with open circuited transmission lines of length ℓ as shown.

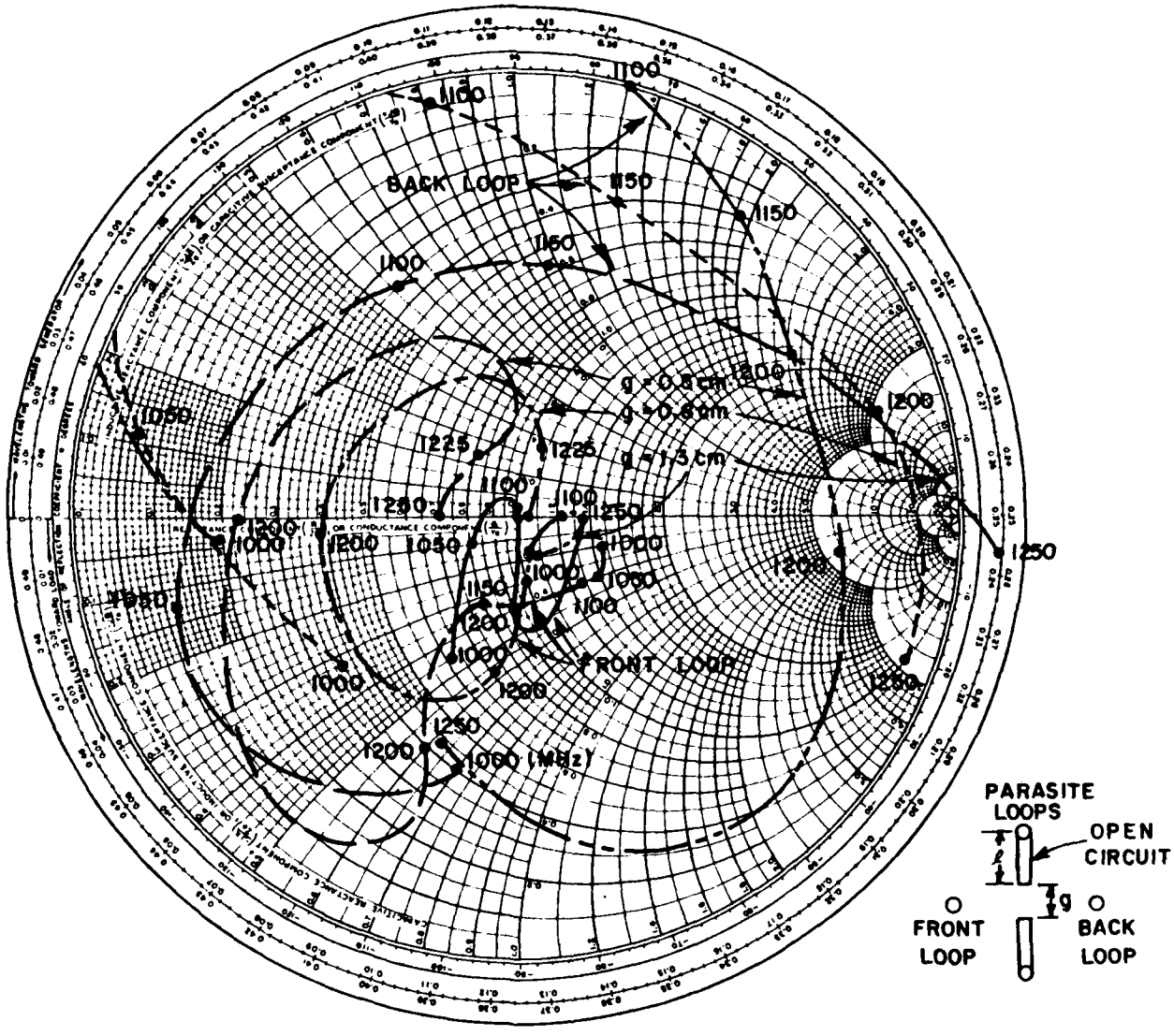

Figure 15b. The input impedance of the front and back loops with their current ratio adjusted for maximum FB-ratio as shown in Figure 14. The two parasitic loops are reactively loaded with open circuited transmission lines with gap g as shown.

the forward direction is always behaving relatively nicely while the impedance of the loop in the backward direction is so bad that it sometimes is outside the Smith chart. As mentioned above, these impedances are obtained for maximum FB-ratio, and although this condition constitutes an ideal situation, it seems fairly safe to conclude that matching the back loop to a VSWR<2 across the band 1.0 to 1.25 GHz is pretty much out of the question. (A VSWR<2 of each loop is about what is required even if we obtain a helping hand from a hybrid.)

III. DESIGN II

Although the results revealed above represent only a small portion of a rather long series of experimental work, we may quite safely conclude that the lack of pattern bandwidth can be traced back to a very strong mutual coupling between the loops in the cavity. It was further felt that the asymmetric nature of design I was primarily to blame for this calamity. Consequently we concentrated on obtaining a more symmetrical design, namely as shown in Figure 16. It consists of four loops similar to design I above, however, in addition it has a top loaded monopole mounted in the center. In addition any two opposing loops are always excited with currents being equal and exactly 180^{o} out of phase. This assures that the coupling between the monopole and any two opposing pairs of loops will ideally be zero. The cardioid shaped pattern is now created in the following way:

If we feed the four loops with equal amplitude but with a progressive phase, namely 0^{o}, 90^{o}, 180^{o} and 270^{o}, it can be shown that the radiation pattern for these four loops will essentially be circular in the horizontal plane provided the average cavity diameter is less than $\sim.6\lambda$. So will of course the radiation pattern of the monopole in the middle. However, if we would record the phase of the far field of the monopole as we move around the antenna once at a certain distance, we would find it to be constant, while the phase of the field from the

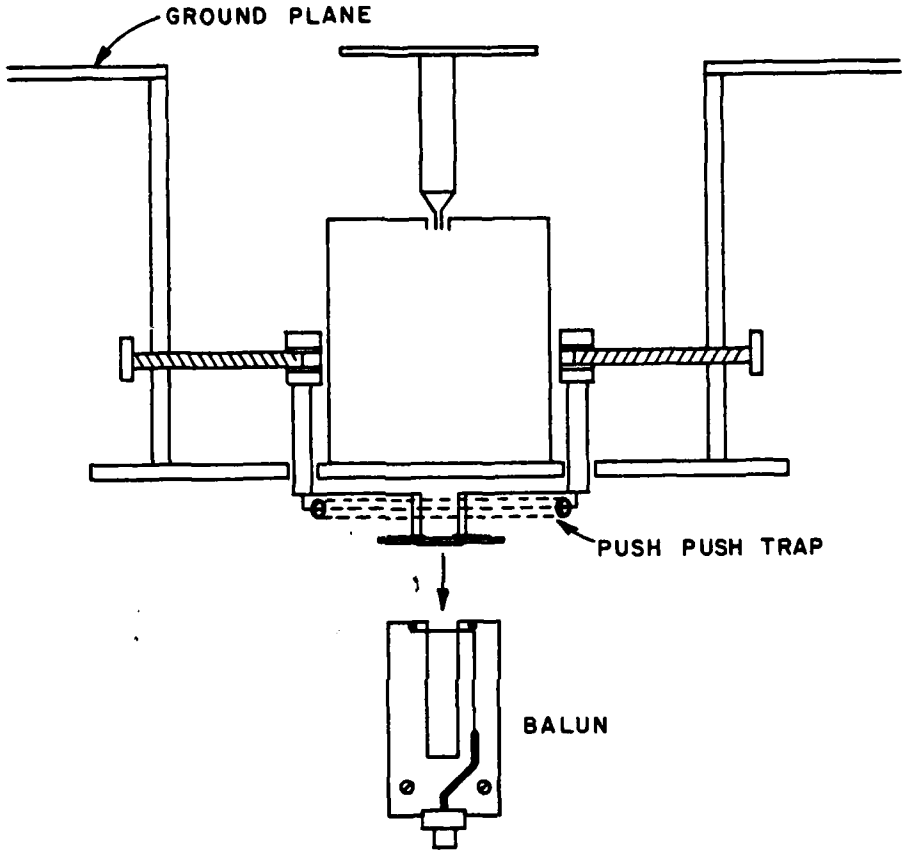

Figure 16. Design II consisting of four loops with a monopole in the middle. Feeding opposing loops in series from a balun assures the two loops to be exactly 180^{0} out of phase.

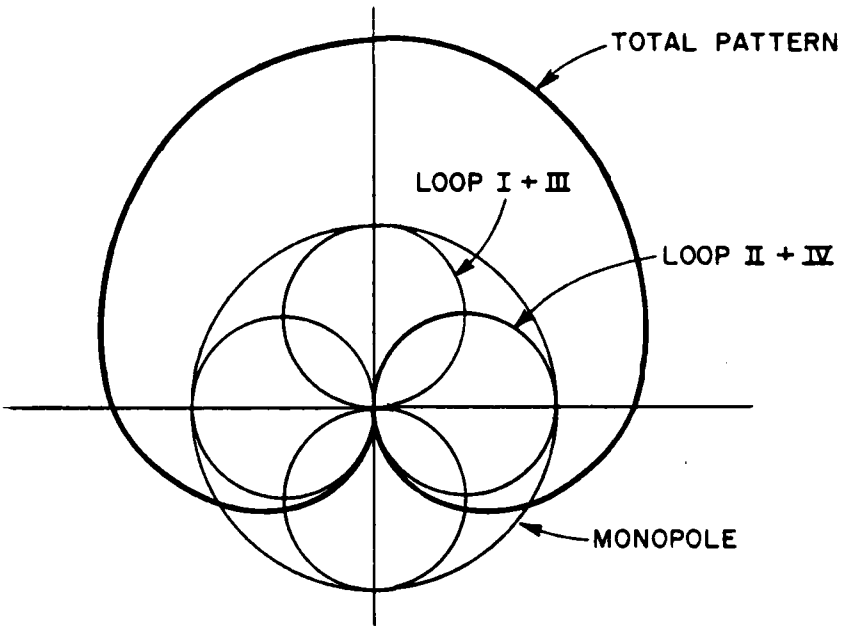

(a)

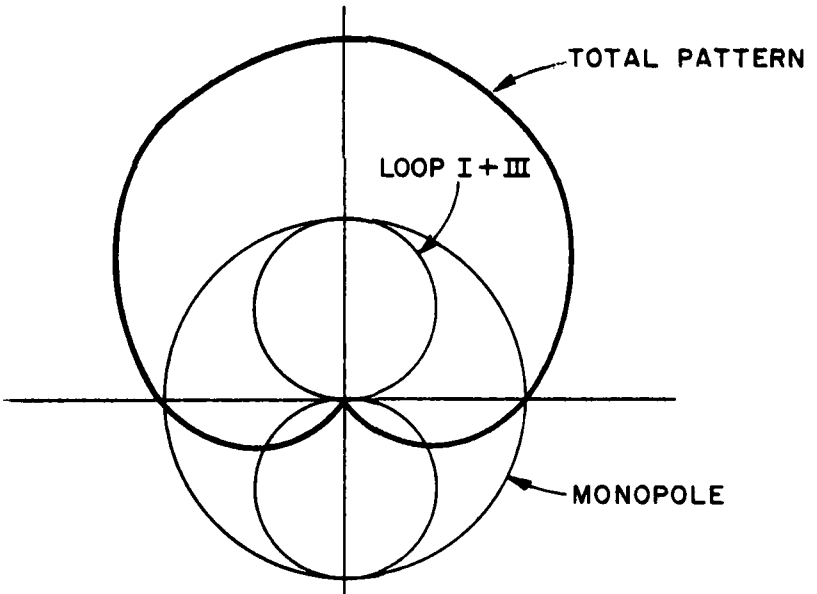

(b)

Figure 17a. The cardioid pattern created by the monopole pattern and all four loops.

b. The cardioid pattern created by the monopole pattern and only two loops.

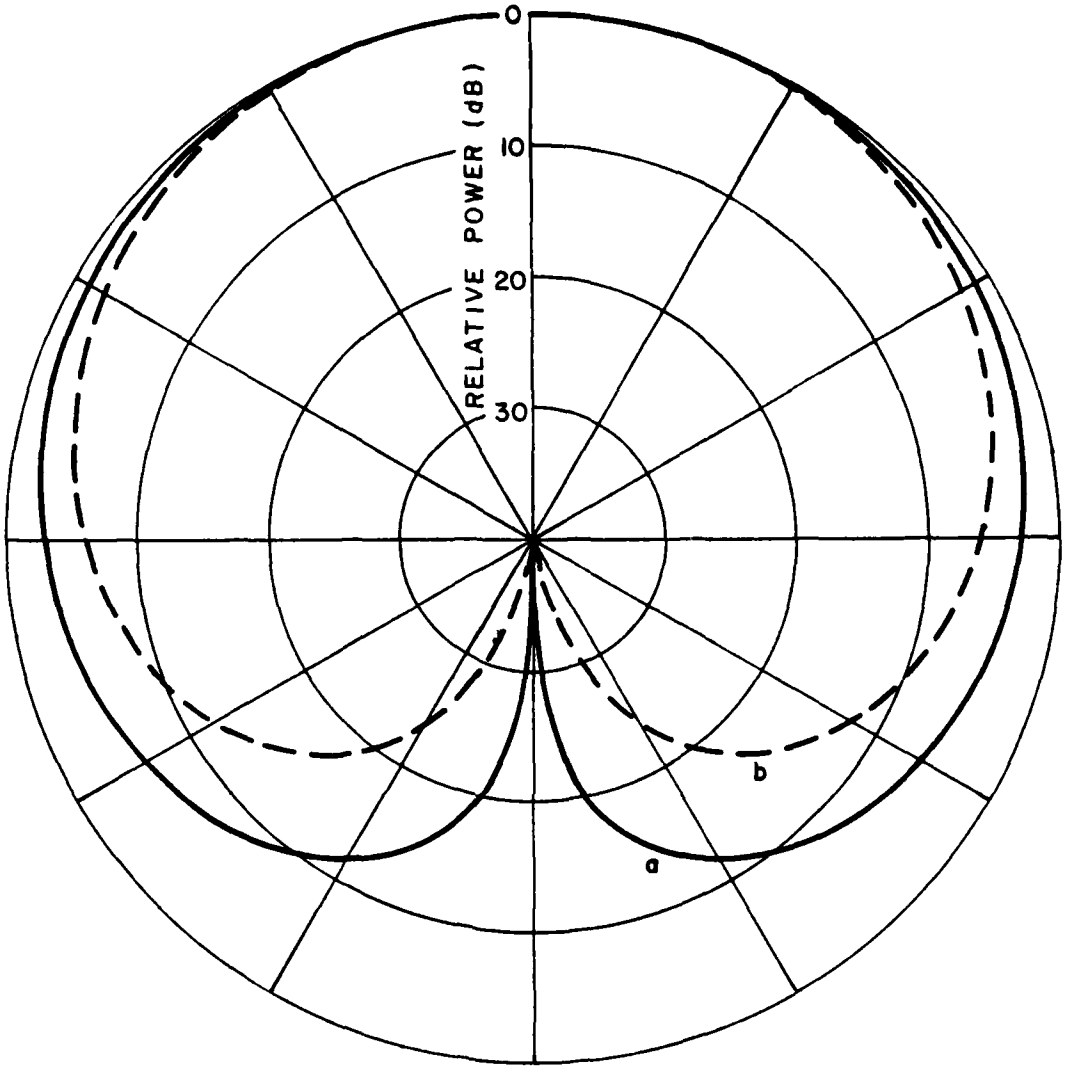

Figure 18. Calculated radiation pattern for the two versions of Design II.

Curve a: Monopole and all four loops fed in phase rotation (Design IIa)

Curve b: Monopole and just two opposing loops fed 180° out of phase (Design IIb).

four loops would change by 360^{o}. Thus, at a certain direction in the horizontal plane the "Loop-field" and the monopole field will be exactly in phase while they, in the opposite direction, will be exactly out of phase. If further the two fields are of the same magnitude, a complete cancellation will take place in this direction.

A more complete understanding is perhaps best obtained by inspection of Figure 17a. Here we show the two figure eight pattern from loop pair 1+3 and 2+4. Since they are fed in quadrature they will combine into a circular pattern coinciding with the monopole pattern in amplitude. The total pattern also shown in Figure 17a can be obtained by simple use of phasors. It is also clear by inspection of Figure 17a that loops 2+4 not only "waste" all their radiated power out to the sides of the radiation pattern but also deliver no energy in the forward direction. Consequently we might as well not excite loop 2 and 4 and thus arrive at the modified pattern shown in Figure 17b (Design IIb). If we compare the two patterns in Figure 17a and b, we note that curve a is down only 3 dB at $\Phi=\pm 90^{o}$, while curve b is down 6 dB in the same directions. What is perhaps even more important is the fact that the null in the back direction is considerably broader for curve b than for curve a. In fact a more exact set of curves from Reference [1] and shown in Figure 18a and b bears this statement out very well. Whats more, curve "b" has more directivity than "a" (estimated to $\sim$2 dB). On the other hand, the advantage by design IIa is that if we continuously change the phase difference between the group of four loops and the monopole, the null in the back direction will continuously rotate correspondingly in the horizontal plane, while design IIb is more suitable for stepwise rotation. However, when we consider that design IIb is lower than 15 dB over an angular sector larger than 90^{o} (see Figure 18 curve b), this drawback becomes less important. Based on the above considerations, we decided to actually develop model IIb which would be somewhat simpler, lighter and cheaper to build because we would not need a special 3 dB 90^{o} hybrid feeding the two sets of loops. It should also be emphasized that design IIb could always be relatively easily modified into design IIa if it later was found desirable.

IV. DEVELOPMENT OF DESIGN IIb

Design IIb can be considered as made of two subantennas interlaced into each other, namely one subantenna consisting of two loops producing the figure eight pattern and the monopole producing the omnidirectional pattern. In order to produce a perfect figure eight pattern, the two opposing loops are fed in series rather than in parallel. This will assure that the two loops are always fed 180^{o} out of phase as illustrated in Figure 19a. For contrast we also in Figure 14b show the two loops being fed in parallel leading to in phase feeding. [The notation in phase and out of phase refers here to a cylindrical coordinate system with vertical axis.]

Feeding the two loops 180^{o} out of phase as in Figure 19a requires the use of a balun. The first model is shown in Figure 20a. It can be viewed as a strip line version of the coaxial version shown in Figure 20b which has been used earlier by one of the authors with excellent results. Basically it consists of two transmission line sections each of length $\sim\lambda/4$. They are grounded at their far ends to the ground plane where the unbalanced input is located. By connecting the inner conductor to the opposite outer conductor as shown, we obtain the balanced output in the middle of the construction.

As mentioned above, the coaxial version of this balun has been used before; however, the strip line version shown in Figure 20a was less than successfull; it radiated. In an attempt to eliminate this problem we modified the stripline design into a microstrip design, however, to no avail. Also, moving the two outer conductors closer to the ground plane only showed minor improvements, if any. We also thought that perhaps the unbalanced input leading from the balun to the right edge of the ground plane in Figure 20a could somehow excite the entire "ground plane" which consisted merely of slightly more than the cavity bottom (i.e., a 8x8" square). To this end we remounted the input connector

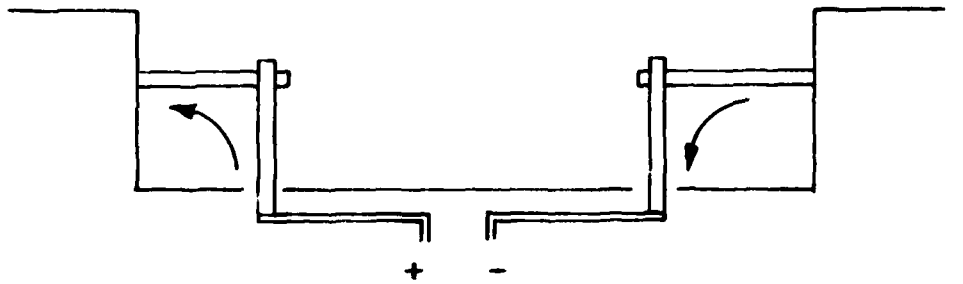

(a)

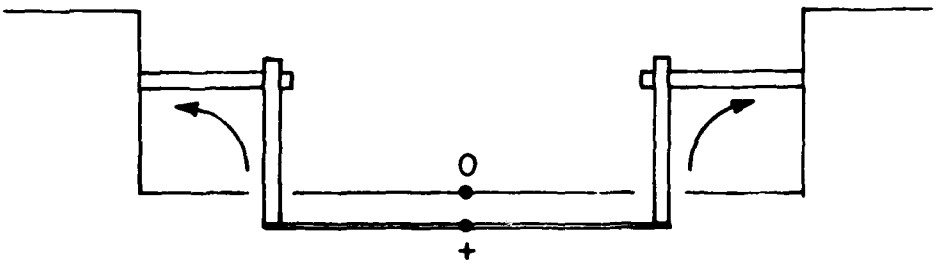

(b)

Figure 19a: Two opposing loops being fed 180^{0} out of phase by being fed in series (requires a balun).

b: Two opposing loops being fed in phase by being fed in parallel.

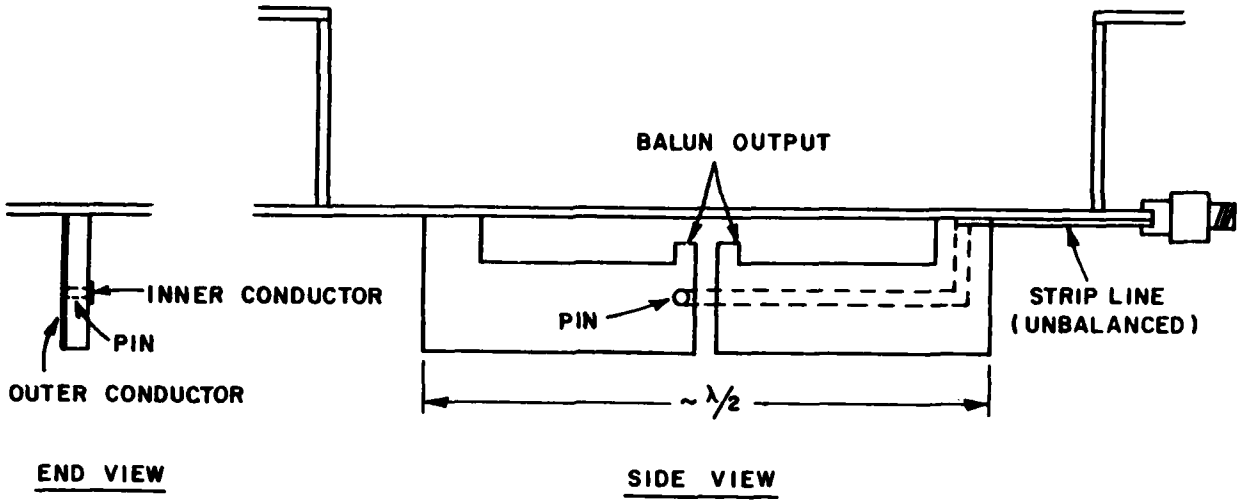

(a)

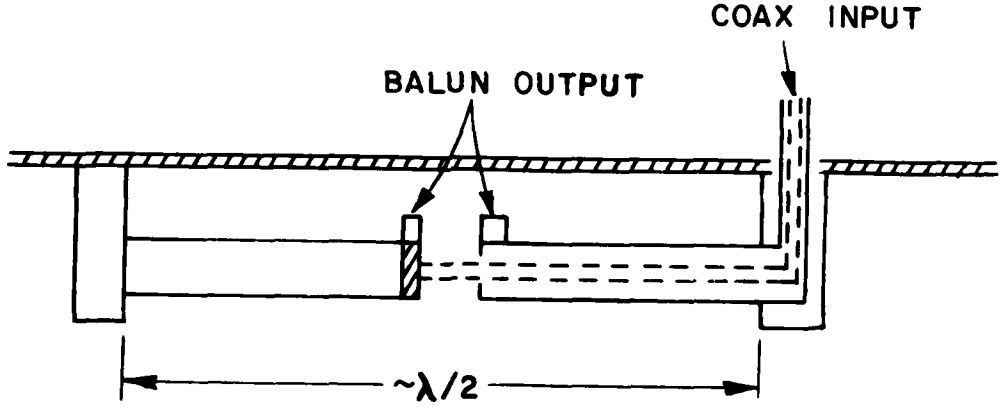

(b)

Figure 20 a: The first balun made in strip line.

b: The more wellknown coaxial forerunner for for the strip line version above.

at the edge of the ground plane as before but this time in the plane orthogonal to the plane of the balun. Since this plane is electrically neutral, it was considered a better place to mount the input connector, however, again this move was disapointing.

We finally decided that the ground plane available was too small for this type of balun to work satisfactorily, and we consequently decided to change to another type balun. Although this new type ultimately proved successful as we shall see below, we are in retrospect not quite sure that putting the blame on the size of the ground plane was correct. The fact is that the new balun also radiated independently of the ground plane but was subsequently brought under control as explained later.

The new type of balun is shown in Figure 21 and is seen to be merely a strip line version of the well known Roberts balun. This type will provide a balanced output from "DC" up to frequencies when the transmission line deteriorates because of higher modes. Its bandwidth limitation in practice is determined by the fact that the length of the slit should be approximately an odd multiple of a quarter wavelength in order not to affect the impedance properties of the antenna connected to the balanced output. This was no limitation in the present case ($\sim$25%), in fact the reactance from the slit in parallel with the antenna impedance at the balanced output can often be designed to make the combined "distorted" impedance more broadbanded than the antenna impedance alone.

When this new balun was connected to a single pair of loops, we obtained quite acceptable radiation pattern, i.e., nicely shaped symmetric figure eight with more than 20 dB deep nulls. However, when we next started taking pattern of the monopole in the middle (see Figure 16) we ran into a multitude of problems.

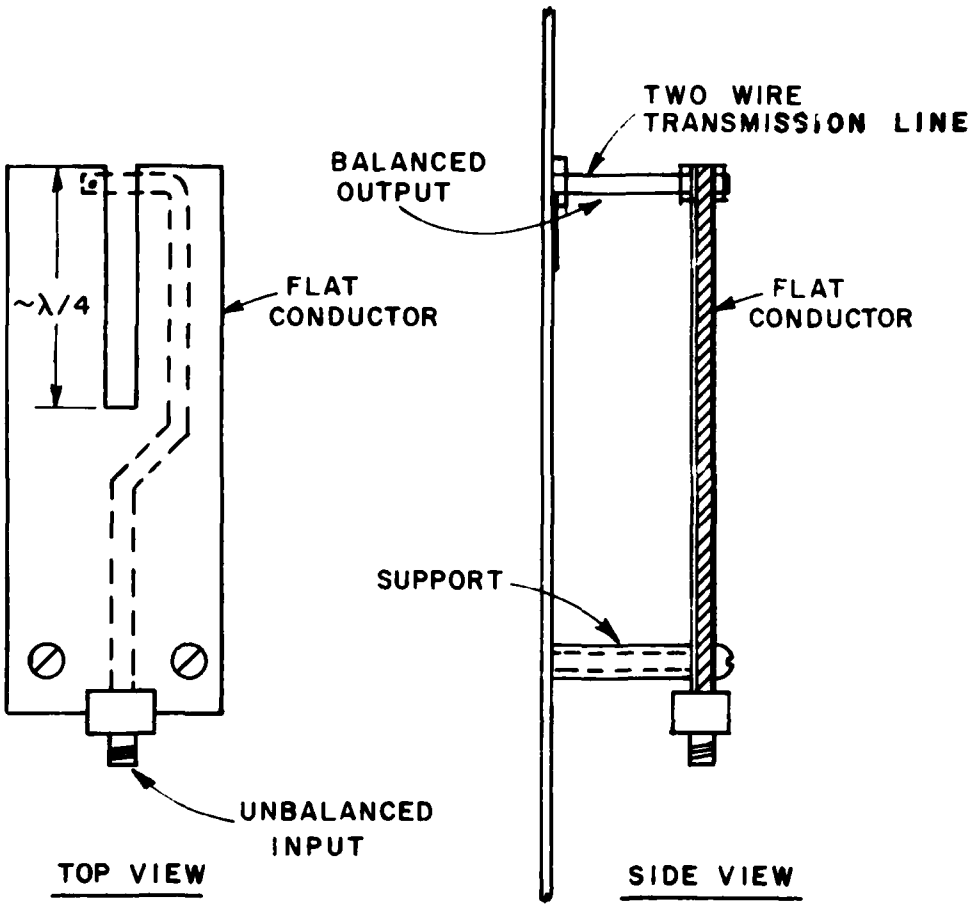

Figure 21. The second balun which is merely a strip line version of the well-known Roberts balun.

First of all, the radiation pattern of the monopole was not omni-directional but oval shaped (at least at some frequencies). Secondly, the balun was "hot", i.e., it radiated. The first problem was caused by the parasitic excitement of the two loops. The second was caused by the fact that the voltages induced in the two loops from the monopole was in phase rather than 180^0 out of phase. This phenomenon is illustrated in Figure 22. We observe that while the push push mode with actually never will enter <u>through</u> the balun to the unbalanced input terminal, they will excite the entire balun in a push push mode with respect to ground (i.e., the circuit board in Figure 22).

The parasitic excitation of the loops leading to a distorted pattern of the monopole will of course depend very much on the load condition of the loops. It was determined experimentally that short circuiting the two loops close to these inputs to ground (i.e., at point A and A' in Figure 22) produced the best monopole pattern. In other words what was needed was a device which would short circuit the loops to ground when the voltages on the two loops produced push push currents as shown in Figure 22, while it would let the push pull currents produced by a voltage at the loop input pass unobstructed.

A. <u>The Push Push Traps</u>

This action can possibly be accomplished in a number of ways. However, we believe the simplest and most direct approach consists of merely connecting the two loops with a transmission line of length $\sim\lambda/2$. This is illustrated in Figure 23 and works as follows:

Imagine first that a push push signal is applied to the "balanced" input (coming from the loops, or whatever) as illustrated in Figure 23a. From each end of the interconnecting cable a wave will now travel toward the center where the two voltages will meet in phase, i.e., add together just like the interconnecting cable was open circuited at this

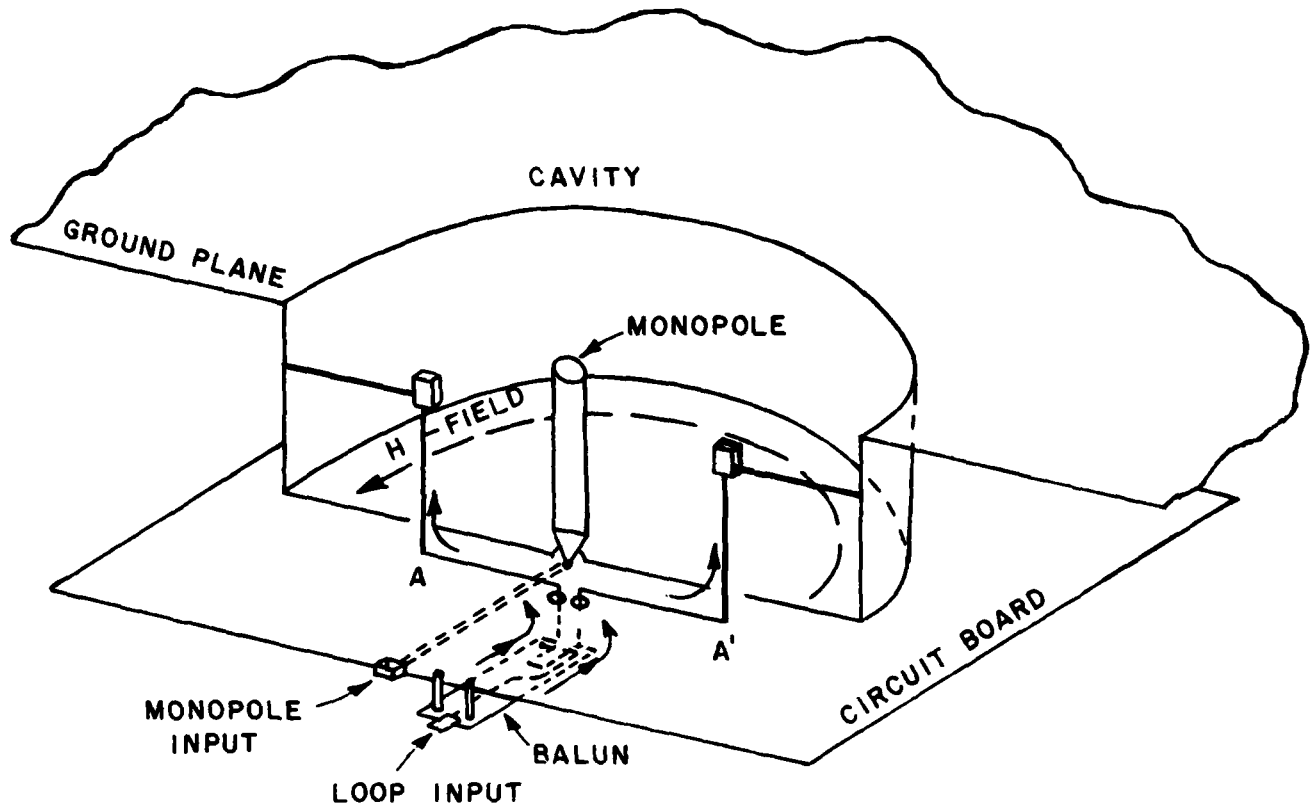

Figure 22. The H-field from the monopole excites the two loops in phase which subsequently makes the balun "hot" with respect to the ground plane (circuit board).

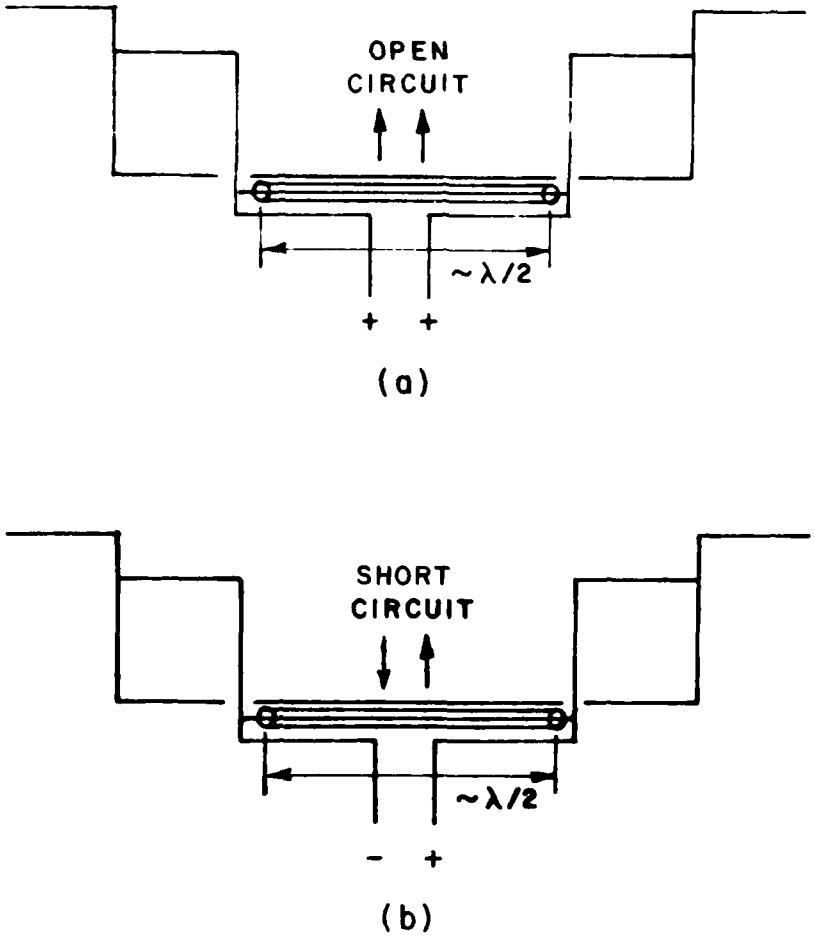

Figure 23. The working of the Push-Push Traps.

a: A push push signal will cause voltages to meet in phase in the middle of the interconnecting cable resulting in an electrical short-circuit at the loops.

b: A push pull signal will cause voltage to meet out of phase in the middle of the interconnecting cable resulting in an electrical open circuit at the loops.

point. Since the distance from this "open circuit" to the two ends is $\lambda/4$, we will at the two endpoints obtain the equivalent of a short circuit, i.e., the push push mode on the transmission line will be stopped. On the other hand, if a push pull mode is applied to the input as shown in Figure 23b, the voltages meeting at the center of the transmission line will now be 180^{o} out of phase, i.e., they will cancel producing an equivalent short circuit at the center of the inter-connecting cable. Consequently an equivalent open circuit is produced at the two ends of the interconnecting cable and the push pull mode on the feeding lines will pass unobstructed.

In the practical execution of the push push traps we used RG-58U cable stripped of the PVC coating. Care should be taken to ensure good contact between the braids and the ground plane to prevent the trap from radiating.

B. The Actual Layout

We are now ready to show the strip line layout of the antenna circuitry as shown in Figure 24. There are two inputs (to be combined later) namely one for the monopole and one for the loops. The latter is as explained earlier at the balun and from here the balanced output is seen to be connected to all four loops. However, only one set of loops should be excited at a time and this is accomplished in the following way:

To each of the four loops is connected a transmission line $\lambda/4$ long (switching traps) which is terminated in a switching diode. When a pair of diodes are open (i.e., non conducting), we obtain short circuits at these two loop inputs, i.e., the energy cannot be radiated by these particular loops. Contrary, if a pair of diodes acts as short circuit (i.e., conducting), the impedance of the switching traps at the loop inputs is infinite and will permit energy transfer between the loops to the feeding lines. Note an additional feature in Figure 24, namely

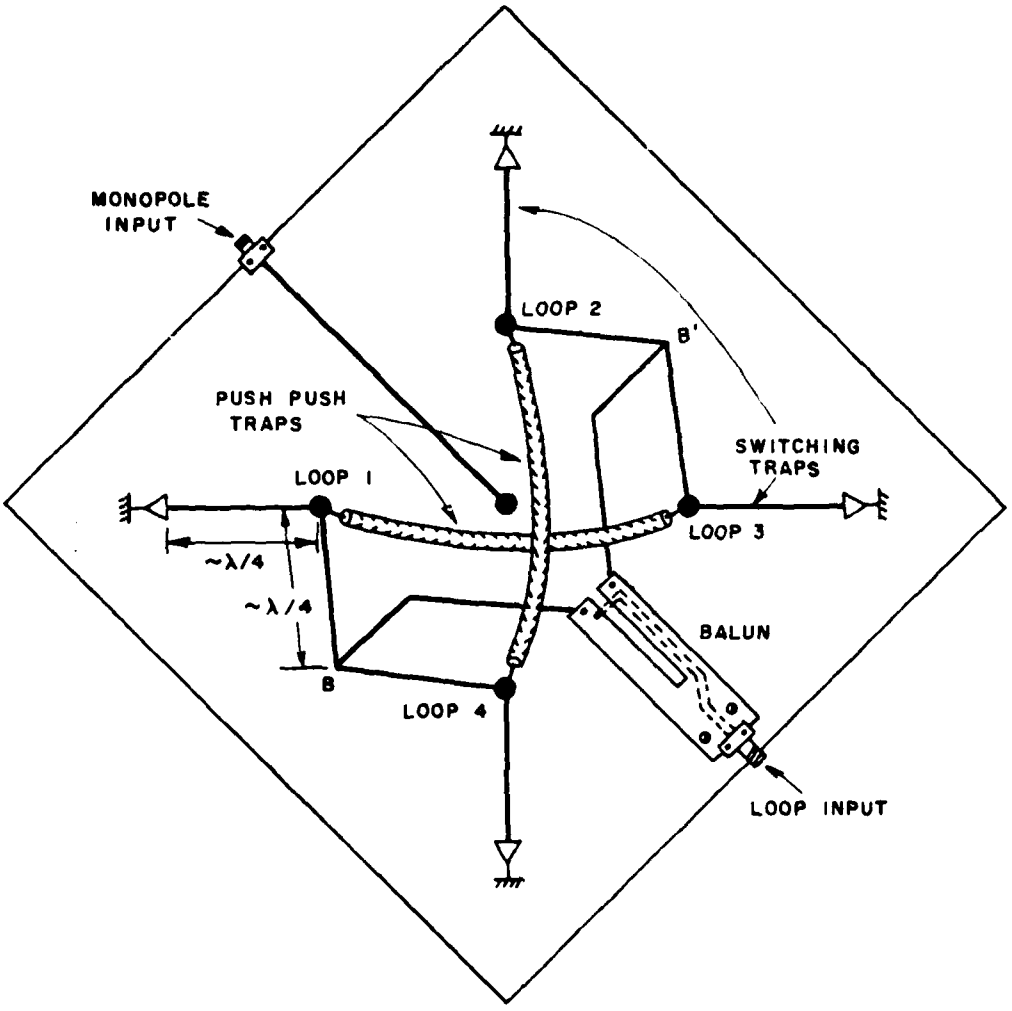

Figure 24. Bottom view of the actual layout of the circuit board feeding the monopole and the four loops from the balun. Also note the switching traps activating the loops. In the model screws were used instead of diodes.

that the transmission lines from the loops to the two branch points B and B' are all $\sim\lambda/4$ long. The reason for this is simply that when the switching traps act like short circuits at the input of one set of the loops, a high impedance will be produced at point B, i.e., the energy transfer to the other set of loops will not be disturbed.

C. Phase Reversal in the Balun

As can be seen from the description above, the switching traps determine which set of loops is going to be radiating. If we further excite the monopole with proper amplitude and phase, a beam will be formed in one of the four directions East, West, North or South. In order to shift the beam from, for example, North to South, we merely have to change the phase of loops 2 and 4 180° with respect to the monopole. This could be accomplished by a simple $\lambda/2$ transmission line which could be short circuited by a diode. However, due to the relatively large bandwidth desired ($\sim$25%), the electrical length of the transmission line would probably vary more over the frequency band than could be tolerated in order to maintain a good null in the back direction of the pattern (see later). This problem is avoided by performing the phase switching in the balun as illustrated in Figure 25. Instead of a single "inner conductor" we have split it up into two in parallel each of which has a total length of $3/4\lambda$. We have further at points B and B' connected a pair of transmission lines $\lambda/4$ long and each terminated in a switching diode. Let us now assume that the diode to the left is open circuited and the one to the right short circuited. That will result in a short circuit across the transmission line at point B, while the energy can pass unobstructed along the feed line going through point B'. Furthermore, since the distance from point B to the branch point A is $\sim\lambda/4$, the short circuit at B will produce a high impedance at point A, i.e., the energy will flow freely through the transmission line to the right. Finally, since the distance from point B to point C (at the balanced terminal at the top) is $\sim\lambda/2$, the short circuit at B will

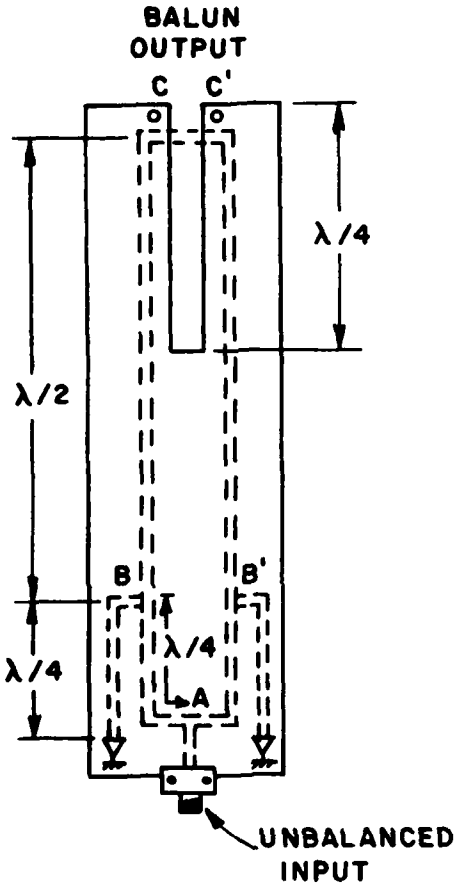

Figure 25. A modified Roberts balun provided with switching traps enabling us to change the phase 180°.

also produce a short circuit at point C between the "inner and outer" conductor, which is precisely what is required for the proper operation of a Robert balun (in fact, the frequency dependence of the $\lambda/2$ transmission line will partly compensate for the frequency dependence of the $\lambda/4$ fork at the balanced output).

By reversing the conducting condition of the two diodes in Figure 25, we can lead the power transfer along the transmission to the left. The important point is now to note that this will change the phase of the signal at the balanced output by exactly 180°, i.e., the beam will

rotate by 180^{o} in the horizontal plane. Note further, that due to complete symmetry of the balun in Figure 25, the frequency sensitivity of the balanced output is the same for the two phase positions. As we shall see later, this is important in order to maintain a good null in the back direction of the radiation pattern.

D. The Final Model of Design IIb

We are now going to present measured radiation patterns and impedances. We shall limit ourselves to what we consider pretty much as the final development model. Although this was proceeded by numerous other variations, we have in the previous section attempted to give more of a background and explanation rather than a substantial collection of data.

Thus, we first show in Figure 26 a drawing of the antenna to be delivered. Note in particular that although the previous models were mostly made with the open micro strip line, this final model was redesigned for the closed strip line in order to minimize any radiation from the feed lines etc. We also note that the cavity is quite deep, namely 5" ($\sim\lambda/2$). This was done to improve the isolation between the monopole in the center and two pairs of loops. Mounting the loops in the same cavity but half way up produced a very serious coupling problem. This was somewhat startling since it was realized that the H-field is actually zero here ($\lambda/4$ away from the cavity bottom). We believe the reason for this descrepancy was the fact that the loops were of the unbalanced type and may have picked up the E-field being very strong midway up in the cavity. Considerable unsuccessful experimenting was done in order to reduce the height of the cavity without sacrificing the coupling. We finally decided to stay with the 5" cavity in order to have "something that worked". At the end of this successful development we decided to go back and attempt once more with our greater

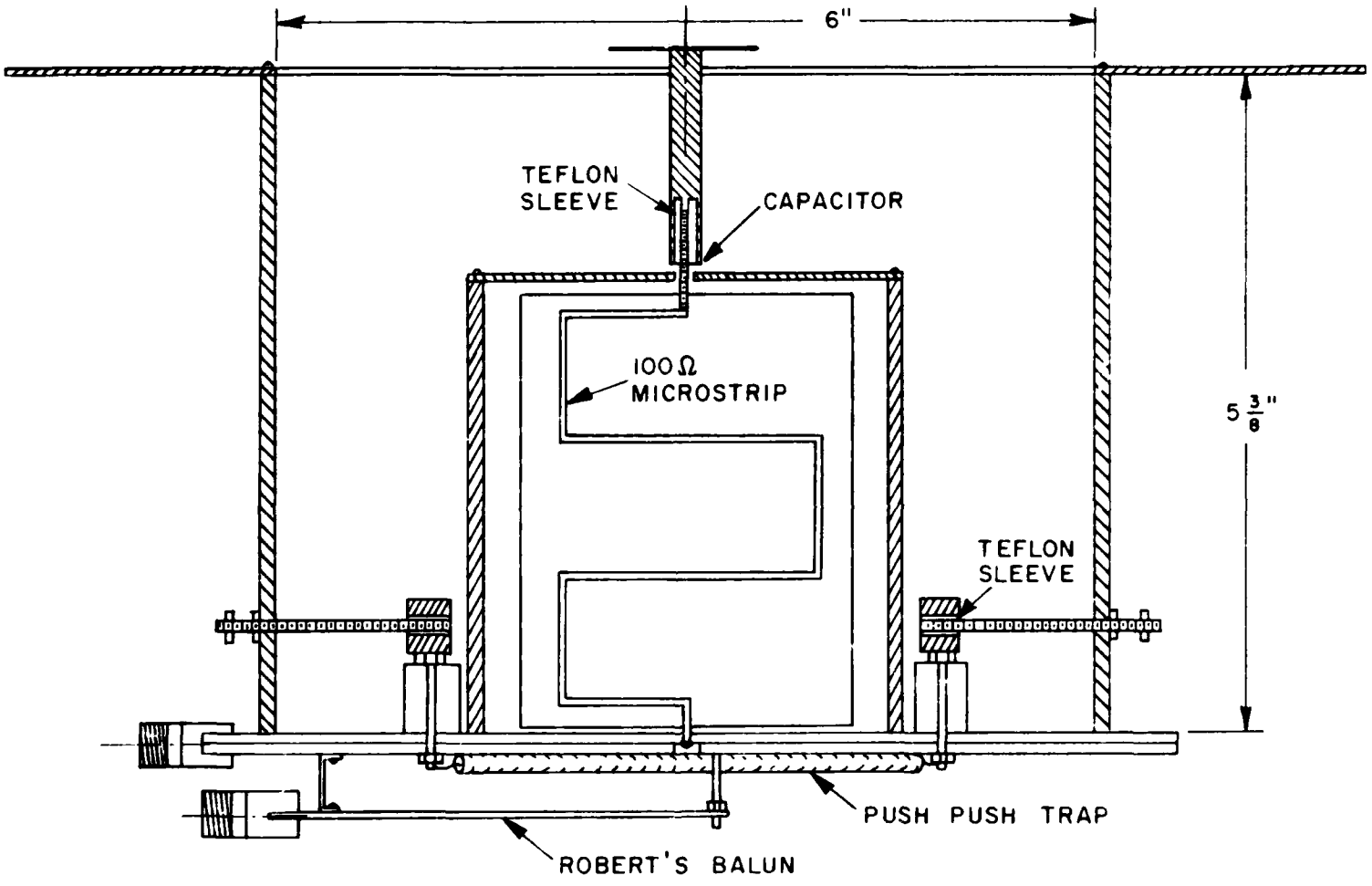

(a)

Figure 26. A sketch of the final model of Design IIb.

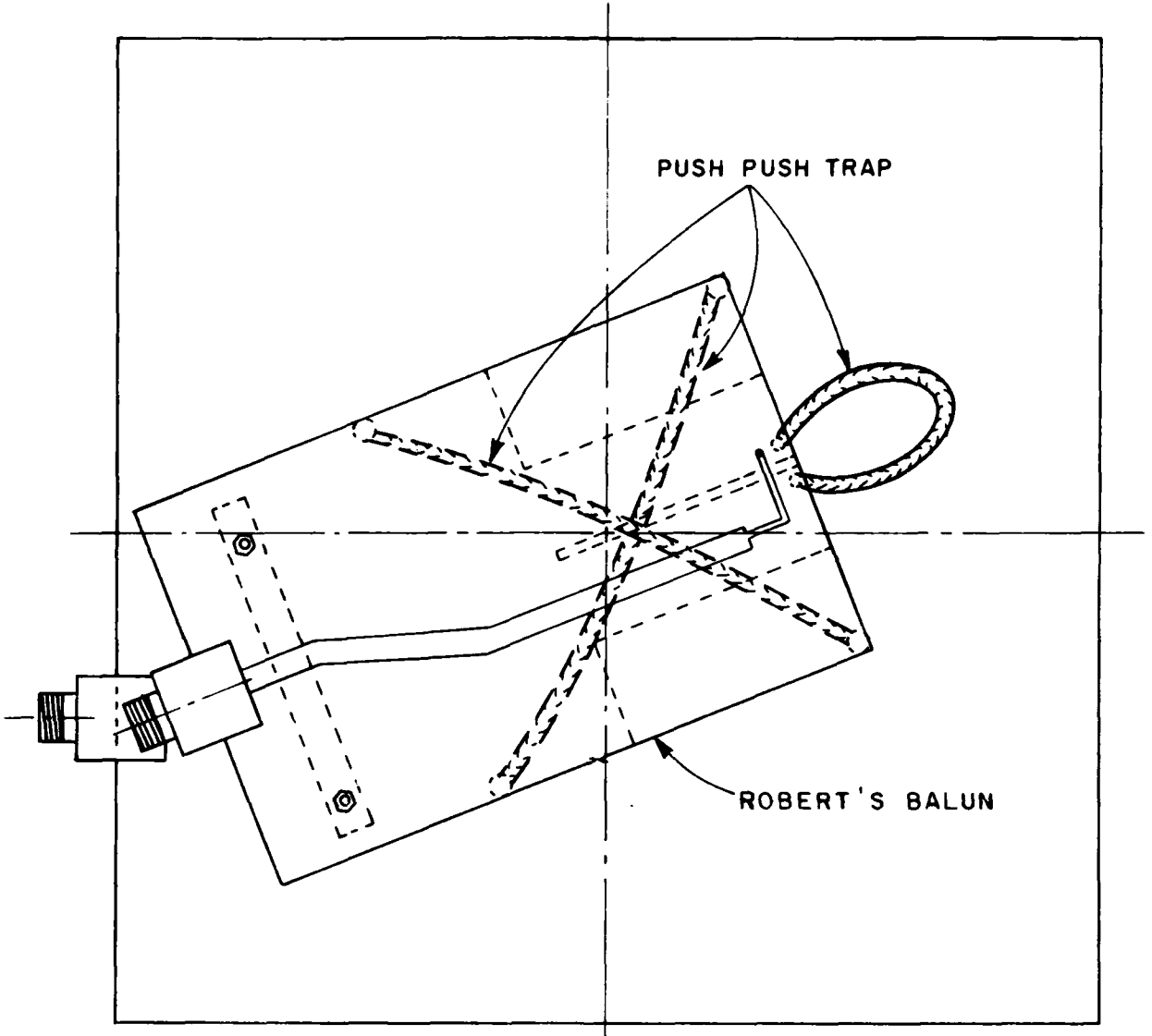

(b)

Figure 26. (Continued).

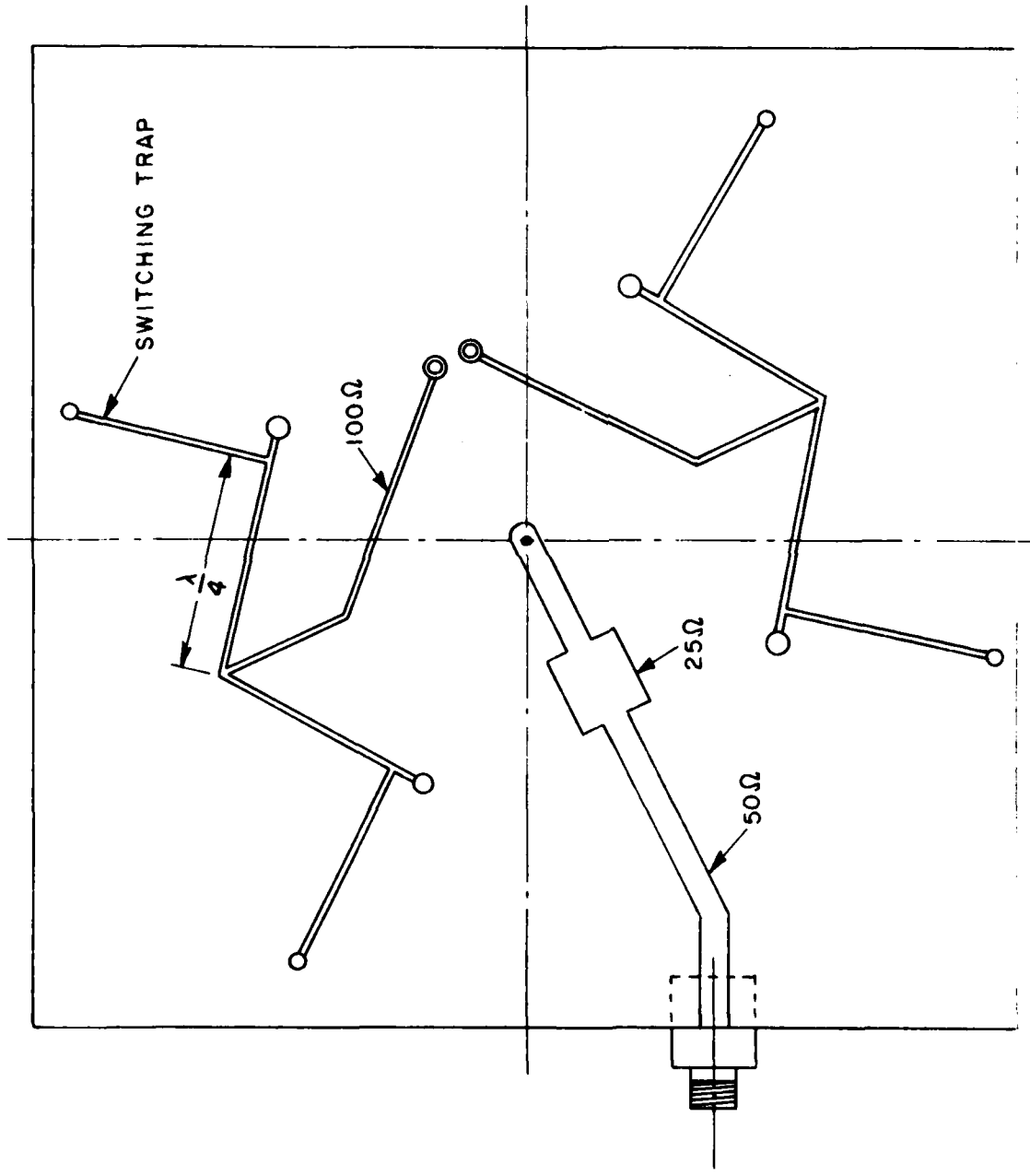

(c)

Figure 26. (Continued).

experience to build a considerably shallower version. Although not as good as the deep model it looked promising and will be discussed in more detail in Appendix B.

In Figure 27 we show the radiation pattern for various frequencies for a set of loops activated and the other set deactivated by the switching traps as explained above. Note that the radiation level in the front and back direction is fairly much the same. This is quite important when we recall that the field from the monopole and the two loops shall cancel each other simultaneously in both the front and back directions.

A necessary condition is a near perfect balun. While the first balun described earlier gave us some problems in that respect, we never experienced any balance problem with the Roberts balun (in its printed version). What is further of utmost importance for equal front to back radiation is that the impedances of the two activated loops be equal. As can be observed in Figure 26, the capacitance on each of the four loops can be varied individually, i.e., the impedance of each loop varied in a certain way of Figure 8. However, rather than to balance the two capacitors until the same field strength was obtained in front and back, they were simultaneously adjusted for minimum coupling between the monopole and the activated set of loops and the best impedance performance of the loops (on the network analyzer). This approach automatically leads to an acceptable front to back ratio and is much faster and more accurate than monitoring the fields.

We further note in Figure 27 that the nulls are reasonably deep and stable. While this in itself is not of utmost importance for the final pattern since the monopole radiates substantially in these directions, it is an indication that things are working as intended. It will be noted that the nulls are most stable and deepest in the middle of the band while some deterioration is observed at the upper and lower frequencies. The reason for this again is not any shortcomings of the balun but

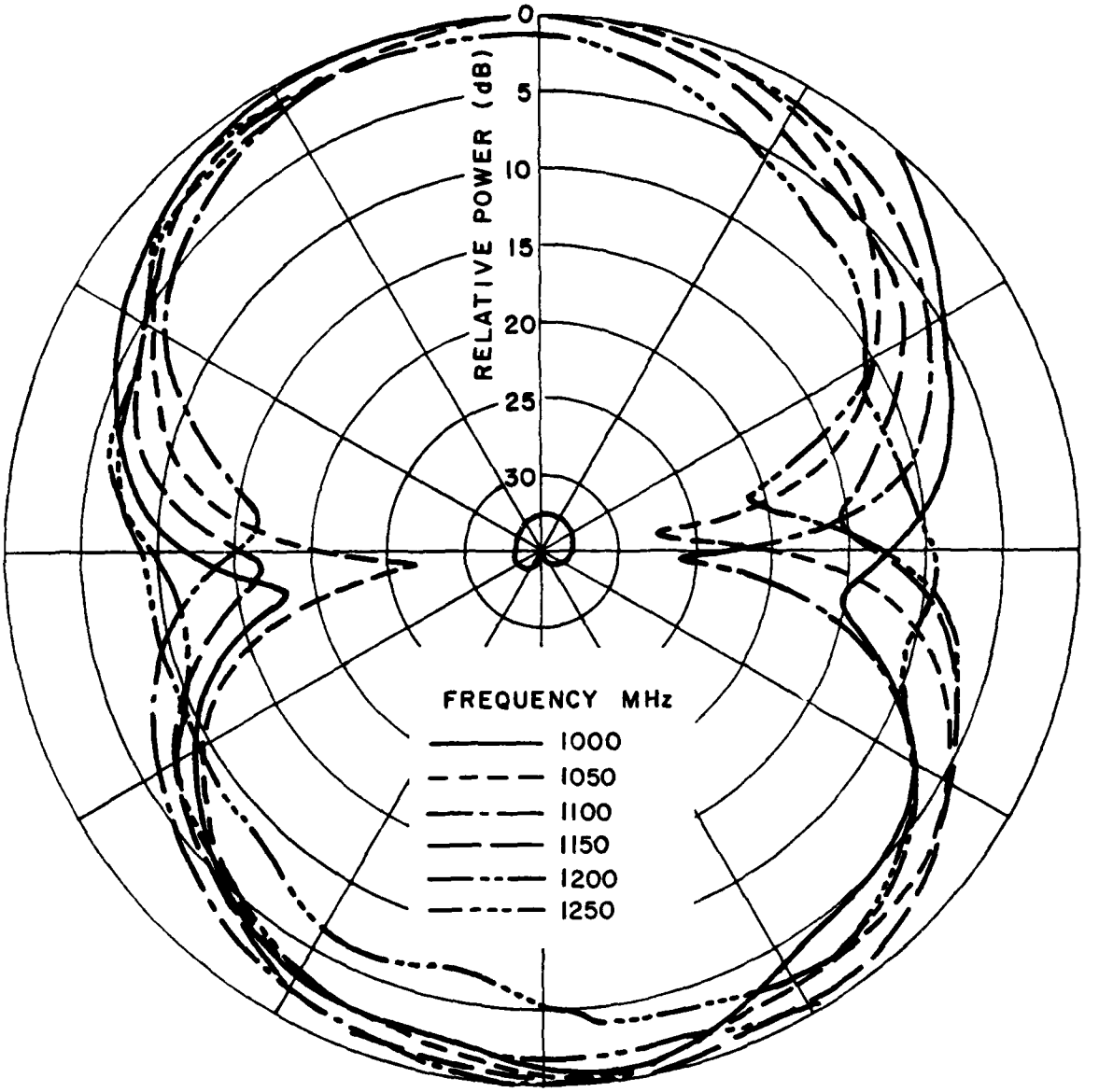

Figure 27. Radiation pattern of one set of loops activated by the switching traps while the other set is similarly deactivated.

was caused by some radiation from the deactivated set of loops. More specifically, recall that the switching traps were made by $\lambda/4$ transmission lines, i.e., they are perfect only when exactly $\lambda/4$ long. This conclusion was arrived at by simply removing the deactivated set of loops. The radiation pattern null now looked as though it were taken right out of a text book.

We next show in Figure 28 the radiation pattern of the monopole alone, and as can be seen it even looks like just that. These patterns turned out to be some of the most troublesome to obtain. As already indicated above, the problem was that the loops surrounding the monopole got parasitically excited causing the radiation pattern of the monopole to be oval shaped. We determined experimentally that the load condition of the loops which caused the least disturbance of the monopole pattern was a short circuit. In fact they should be slightly inductive which is why the switching traps are placed slightly down the feeding line as shown in Figure 26. Also close to the loop inputs are the push push traps discussed earlier. They act like short circuits for any voltage induced in the loops from the monopole field. Care should be given to the fact that both the switching traps and the push push traps act as perfect short circuits at only one frequency due to their physical length. If these "resonance" frequencies are different for the two traps, the reactances of the two traps will be of a different sign for all frequencies between the two "resonance" frequencies. At some specific frequency they will be equal in magnitude, and a high impedance will result which will have a most detrimental effect on the monopole pattern. The final design of the switching and push push traps was determined experimentally; in particular we should mention that the switching trap was modeled by use of conducting tape which could easily be cut to size.

It would in some sense be logical to present the total pattern made up by the phasor sum of the loop and the monopole pattern. However, since their individual signal strength depends to quite an extent on the degree of matching of the monopole and the loops, we shall shortly digress to present the input impedances of these two components.

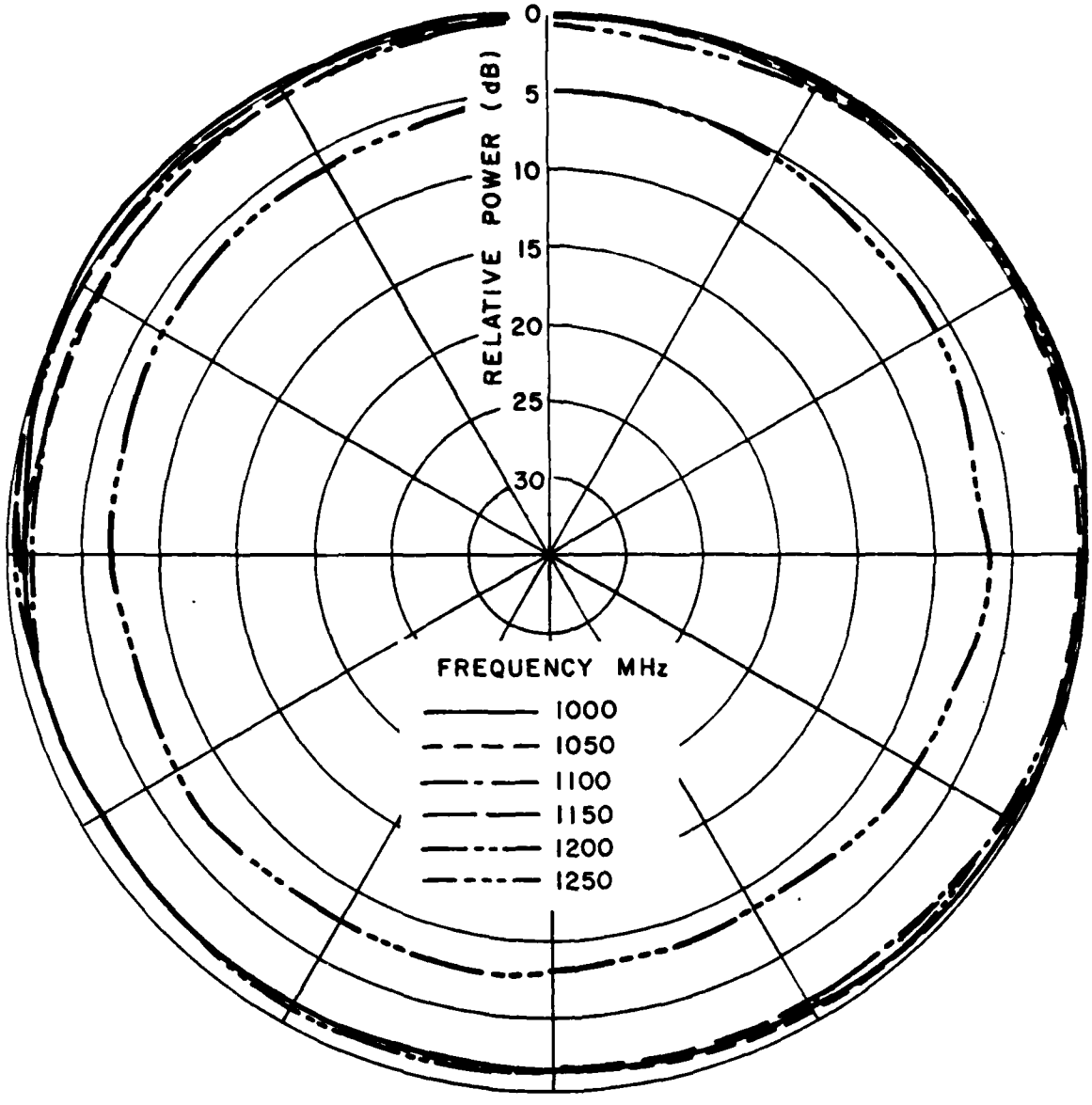

Figure 28. The radiation pattern of the monopole alone surrounded by the four loops.

E. The Input Impedance of the Loops

Since the loops used in the present design, IIb, are essentially identical to the ones used in the first less successful Design I, the impedance curve was similar to these earlier ones shown in Figure 8. Thus, they need not be repeated here although some change was observed, one reason being the different phase relationship between the loops. Another point worth emphasizing is that even a small change in the distance between the loops and the coaxial inner wall supporting the monopole makes quite a change in the impedance. Finally the reactances of the switching and push push traps are added in parallel to the loop impedances, which also modify the total impedance somewhat. The characteristic impedance of the feeding line leading from the individual loops to the balun is now chosen such that a compression of the loop impedance curve takes place (≈100 ohm). At the same time this value placed the impedance curve slightly off center of the Smith chart. The final centering was performed in the balun by chosing a section of the characteristic impedance equal to 100 ohm and having a length equal to 2.5 cm, see Figure 26. The final loop impedance as seen at the input of the balun when loop 2 and 4 are activated and loop 1 and 3 deactivated is shown in Figure 29, while Figure 30 shows the impedance in the opposite switch position. They should of course be identical and are except for the very lowest and highest frequencies within a VSWR<2. A substantial tuning of the loop impedances is possible by variation of the loop capacitors, however very little impedance change was observed by varying the height of the cavity provided the loops remained unchanged at the bottom of the cavity.

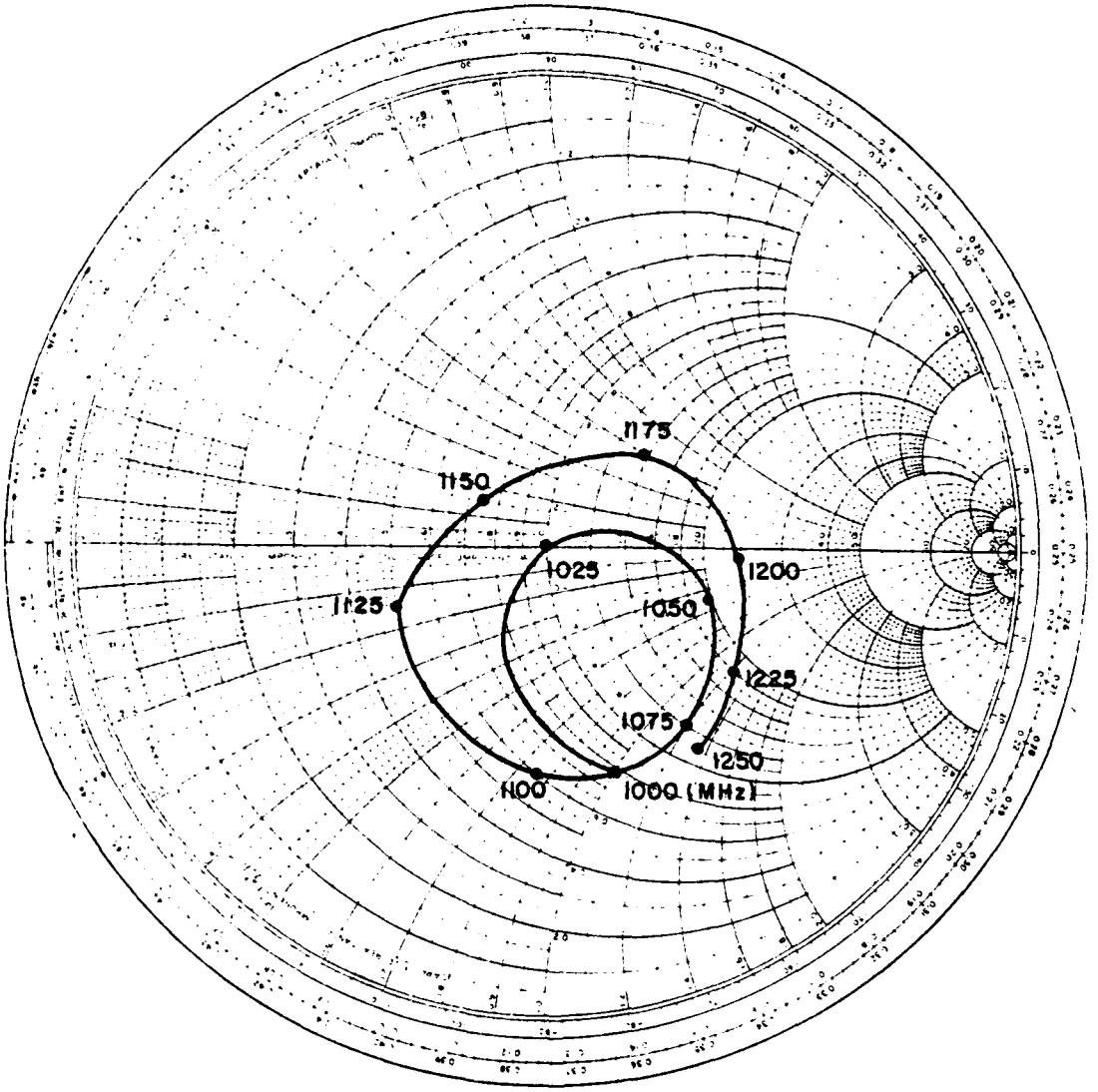

Figure 29. The input impedance at the balun with loop 2 and 4 activated and loop 1 and 3 deactivated.

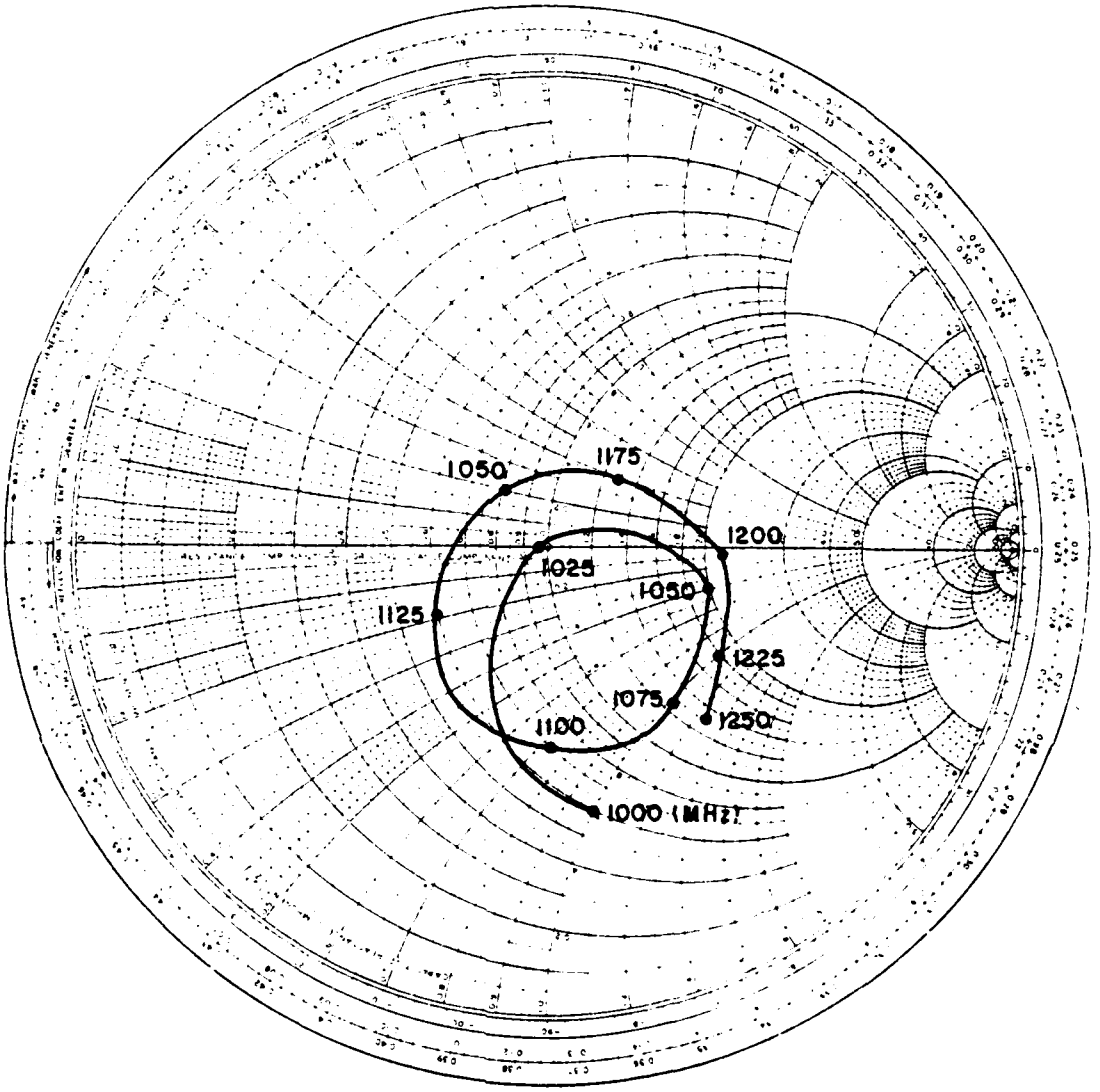

Figure 30. The input impedance at the balun with loop 1 and 3 activated and loop 2 and 4 deactivated.

F. The Impedance of the Monopole

Monopole impedances are usually relatively simple to match within a VSWR<2 with a 25% bandwidth. However, in the present case we did indeed have our fair share of problems. They can be summed up by stating that if the cavity surrounding the monopole was somehow shortcircuited (for example as shown in Figure 31 by placing wires from the upper edge A of the

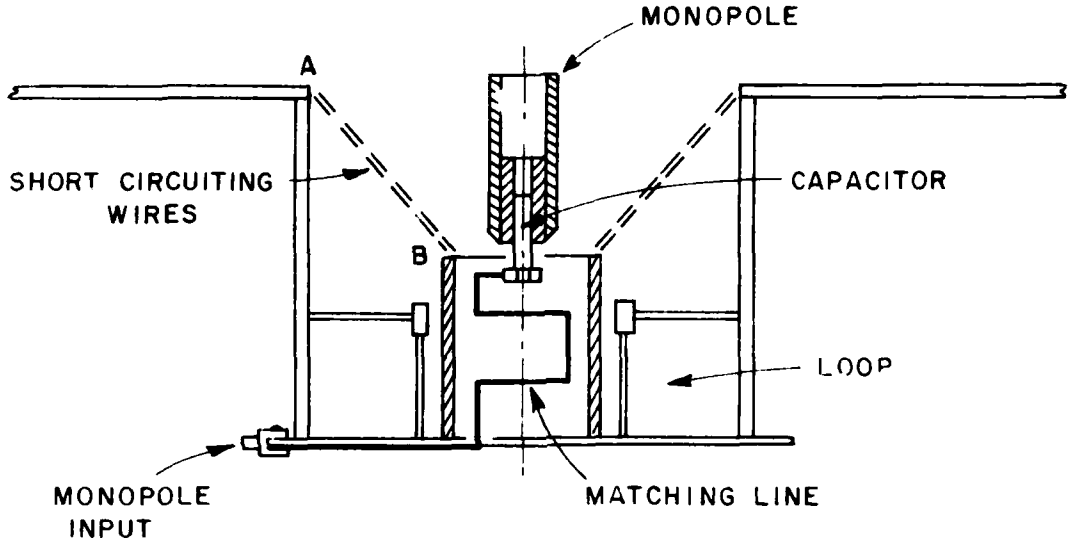

Figure 31. The monopole is being matched by an adjustable series capacitor and a section of 75Ω transmission line (strip line).

cavity to the base B of the monopole), the monopole impedance was "nice". However, as soon as the short circuit was removed, the cavity essentially could be viewed as a coaxial section short circuited at the bottom and with the upper part being in series with the ground plane and the base of the monopole. If the coaxial section is $\lambda/4$ deep, the impedance at the upper edge of the cavity is very high, and since it is in series with the monopole impedance makes the latter look very bad. On the other hand, if the cavity is $\lambda/2$ deep, a low impedance will be obtained at

the upper edge, and the monopole impedance looks acceptable although not as good as without a cavity.

Several attempts were made to shorten the $\lambda/2$ deep cavity. The most obvious was to load the cavity in some fashion, for example, as shown in Figure 32, where a low impedance section has been introduced

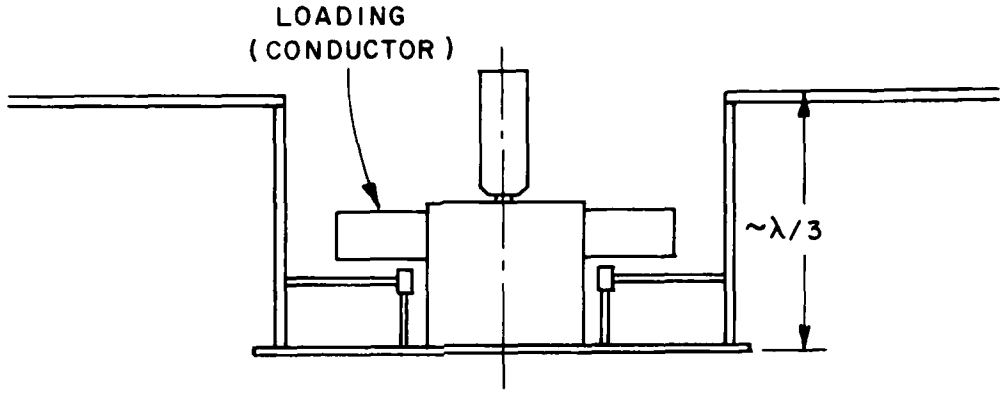

Figure 32. The height of the cavity can be reduced by using a low impedance section in the middle of the cavity.

in the middle of a cavity reduced to a depth of $\sim\lambda/3$. This approach did indeed produce an acceptable monopole impedance, however, the loop impedance became so detuned that it was deemed beyond ever tuning back to VSWR<2. Several degrees of loading was tried; however, the problem was always with the loop impedances which was greatly "disturbed" by anything on top of them, although they as reported earlier improved by the presence of the inner coaxial section supporting the monopole.

It was seriously considered to load the cavity with a dielectric. However, merely placing dielectric slabs in the middle of the cavity had only a minor effect on the monopole impedance, and filling the entire cavity with, for example, wax was discarded since it would make any adjustment of the loops rather cumbersome. However, for a production model this approach would seem quite feasible.

Another approach would have been to make the cavity quite shallow ($\sim\lambda/8$). However, at this point we were running out of time, and we consequently decided, at least for the time being, to stay with the $\lambda/2$ deep cavity in order to have "something that worked". Fortunately, we did at the end of the contract return to the shallow cavity approach as described shortly in Appendix B.

The actual matching of the monopole (see Figure 31) is obtained by use of a series capacitor at the very input of the monopole in order to reverse the impedance curve similarly to the loop case as explained in Figures 6, 7 and 8. This is followed by a section of 100 ohm transmission line of length $\sim 0.4\lambda$. The capacitance is seen in Figure 31 as being created between a screw extension of the "inner-conductor" of the feed line and the inside of the monopole. It is adjustable by simply screwing the monopole up or down.

The final impedance of the monopole referred to the edge of the circuit board as shown in Figure 33. It has an acceptable USWR in the first half of the desirable band while it is somewhat lacking in the second half. However, we shall later see how this impedance combined with the loop impedance can be improved to an acceptable level over the entire band.

G. Combining the Loops and the Monopole

Horizontal Pattern

As was explained earlier the monopole and one set of loops now has to be combined such that their fields add in the forward direction and cancel as much as possible in the backward direction. This is illustrated in vectorial form in Figure 34 where the fields from the loops and the monopole are denoted by $\bar{E}_{Loop}$ and $\bar{E}_{Mono}$, respectively.

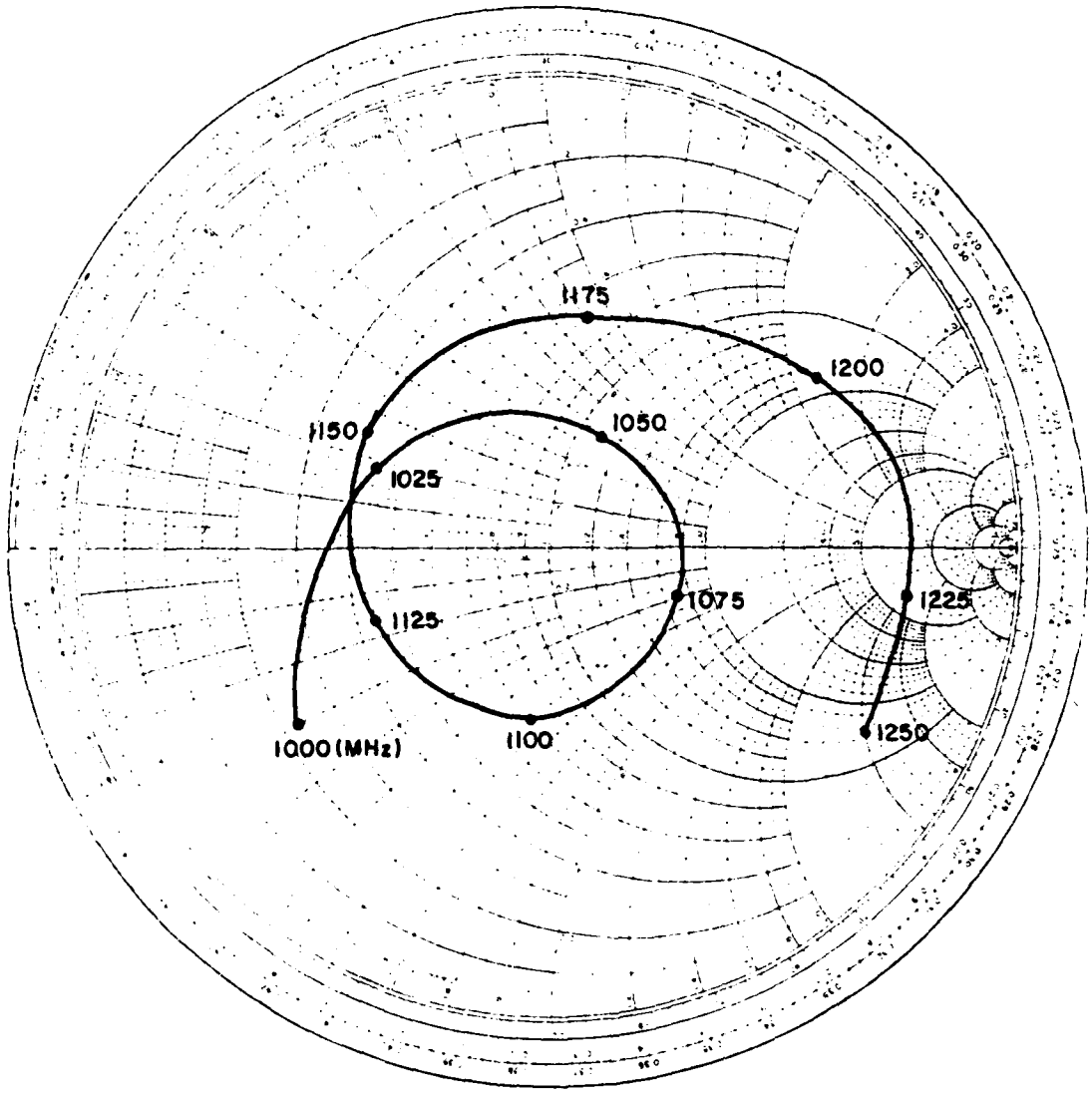

Figure 33. The impedance of the monopole as seen at the input connector.

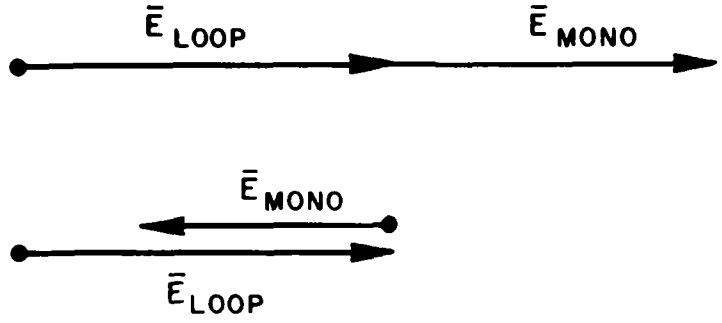

Figure 34. Phasor diagram showing the formation of the total signal to the front (top) and the back (bottom) when $\bar{E}_{mono}$ and $\bar{E}_{loop}$ are in perfect phase but of unequal magnitude.

For the two components being in perfect phase, the front to back ratio becomes

$$FB = \frac{E_{Loop} + E_{Mono}}{E_{Loop} - E_{Mono}} \qquad (1)$$

or

$$\frac{E_{Loop}}{E_{Mono}} = \frac{FB + 1}{FB - 1} \ . \qquad (2)$$

For a front to back ratio of 10 times (i.e., 20 dB), we must according to Equation (2) require

$$\frac{E_{Loop}}{E_{Mono}} = 1.22 \qquad (3)$$

i.e., E_{Loop} and E_{Mono} should be within 1.8 dB of each other.

Similarly we see from Figure 35 that if the two components E_{Loop} and E_{Mono} are equal in amplitude but differ in phase by ϕ_{L-M}, the front to back ratio becomes

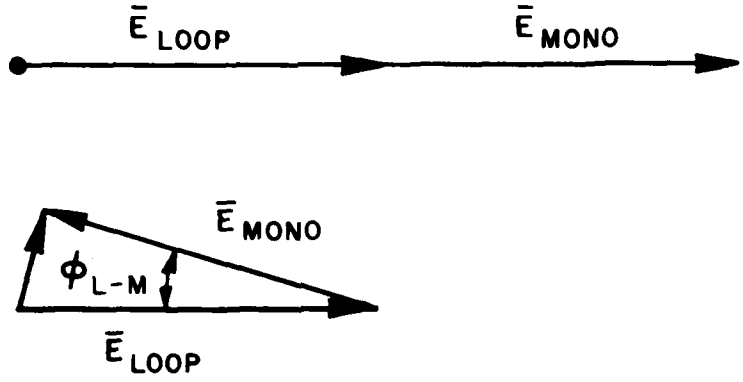

Figure 35. Phasor diagram showing the formation of the total signal in the front (top) and back directions (bottom) for $|\bar{E}_{mono}| = |\bar{E}_{loop}|$ but imperfect phase relationship.

$$FB = \frac{1}{\sin \phi_{L-M}/2} \quad . \tag{4}$$

For FB=10 (i.e., 20 dB) we obtain

$$\phi_{L-M} = 2 \sin^{-1} 0.1 = 11.6^{o}. \tag{5}$$

As can be observed from the numbers calculated in Equations (3) and (5), it is necessary to maintain a rather close tracking both in amplitude and phase between the two fields radiated by the loops and the monopole. Rather than obtain this in a trial and error way, we decided to pursue this problem in a systematic way, namely, simply by measuring the amplitude and phase difference of the far fields of the loops and the monopole. The setup for this purpose is shown in Figure 36. A stable transmitter checked by a frequency counter is connected to a source antenna as well as a reference cable running to a network analyzer. This was first connected to one set of loops at the balun input and

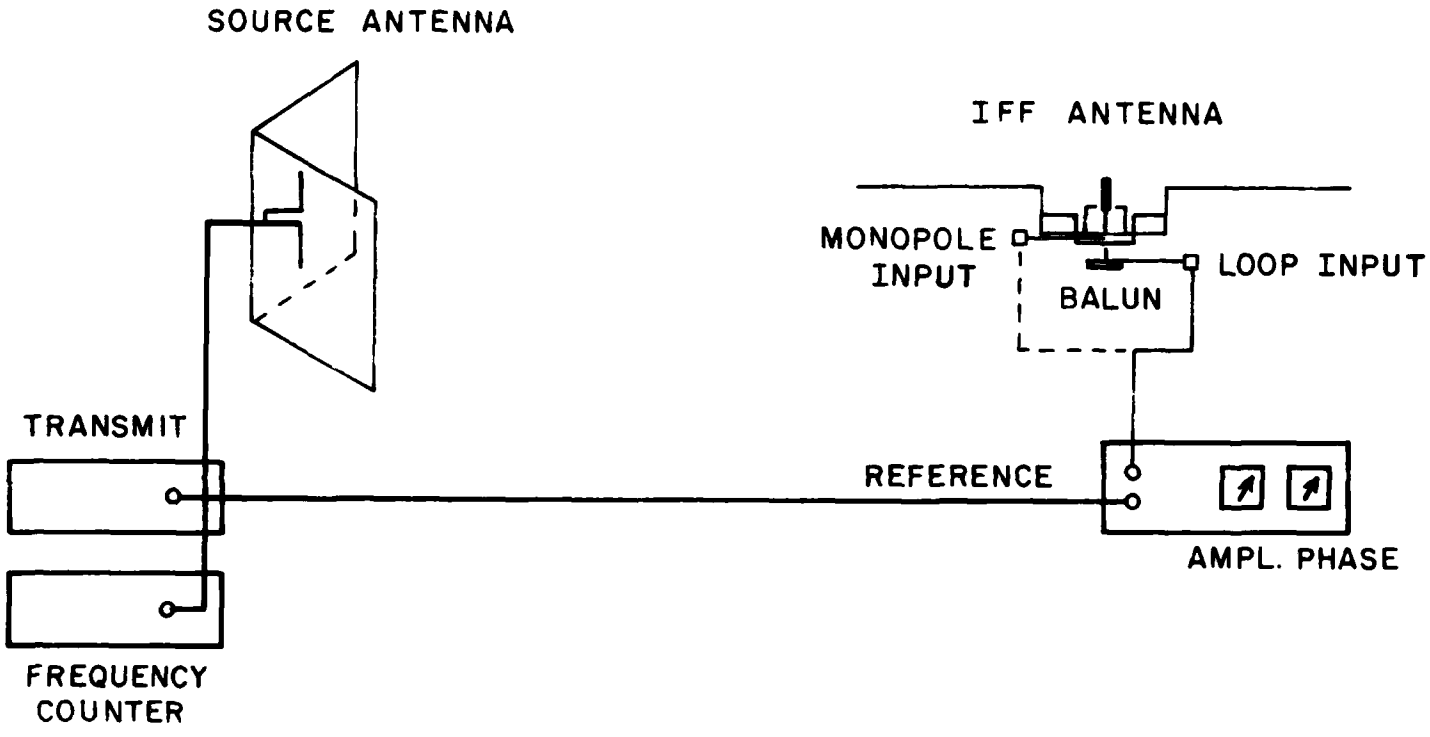

Figure 36. The setup for measuring the amplitude and phase difference between the fields from the monopole and loop sections.

subsequently to the monopole. We recorded their relative amplitude and phase difference as shown in Figure 37 over the entire frequency band 1 to 1.25 GHz for every 20 MHz. If we would connect the loops and the monopole to a common 3 dB hybrid, we would feed these two components with 0 dB difference. As indicated in Figure 37, this design would satisfy Equation (3) above only in the upper half of the frequency band. If instead, however, a 4 dB coupler was used, we would as shown in Appendix A obtain a difference in power level between the monopole and loops of 1.7 dB, and as indicated in Figure 37 this would constitute a reasonable compromise over the entire frequency band. Since 4 dB hybrid does not appear to be readily available, we decided to make our own rather than wait for a manufacturerer to make one for us. The entire design and manufacturing only took us a day, and the details are given in Appendix A.

We also note in Figure 37 that the average phase of the monopole with respect to the loops differ by -90^{o} as should be the case if we use a 90^{o} hybrid. We also observe, however, an average slope which changes the phase $\sim 30^{o}$ across the band from 1.00 to 1.25 GHz, which ideally should not be the case. If we change the difference in the feed cables from the hybrid to the loops and the monopole by one wavelength, the average phase delay at the center frequency will remain -90^{o} as before, however, we will obtain an additional slope of $\pm\ 360^{o}\ \frac{1250-1000}{1125} = \pm\ 80^{o}$(the sign depending on in which feed line we insert the additional cable). Obviously, this will only make the phase-variation across the band even worse. If instead we let the feed line length differ by an additional half wavelength, the phase difference between monopole and loops will be $+\ 90^{o}$ while the slope will be $\pm\ 40^{o}$. This simply means that the beam will rotate 180^{o} which is trivial and a slight improvement in phase slope across the band could be obtained resulting in a better pattern. However, at this point considerable cable cutting had already taken place and, anxious to see the combined pattern, we decided to leave the results shown in Figure 37 as they were.

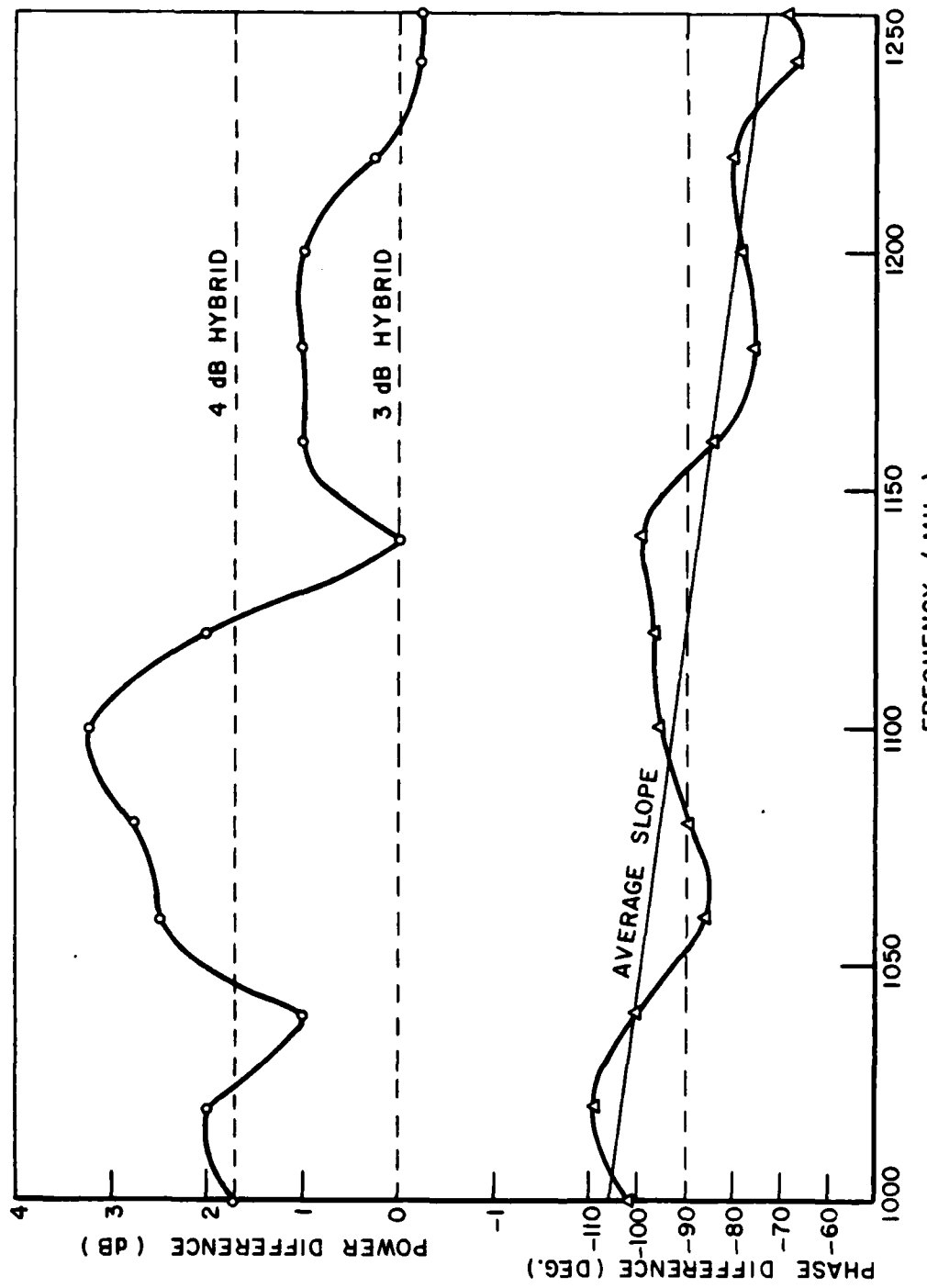

Figure 37. The amplitude (top) and phase (bottom) difference between the monopole and one set of loops measured on the setup shown in Figure 36.

These combined pattern (cardioid) are seen in Figure 38a, b and c taken for every 20 MHz in the entire frequency range 1000 to 1250 MHz. To facilitate the inspection of these patterns we have in Figure 39 shown the front to back ratio. It is seen to exceed 15 dB in more than the desired frequency band 1000-1250 MHz, and also to exceed 20 dB in the range 1040-1160 MHz. Also, observe that the low radiation in the back remains quite low over a 90^{o} broad sector which makes directing the beam in finer increments than 90^{o} superfluous. We finally show in Figure 40a, b and c the total pattern for other sets of loops activated by the switching traps as explained above. They are observed to be very much like the first set in Figure 38a, b, and c except they are rotated 90^{o}. Unfortunately time did not permit the balun to be modified to switch the phase 180^{o}, i.e., we did not take all four sets of radiation pattern.

Vertical Pattern

All the horizontal patterns above were recorded at elevation angle 8^{o} above the horizontal plane. While this is considered a good average value for an antenna mounted on top or bottom of an airplane, it is of course of considerable interest to know the pattern in the entire vertical plane. These are shown in Figure 41a, b and c; they are taken in the vertical plane going through the front and back direction and the polarization was parallel to this plane. Observe that the high front to back ratio is maintained over a significant sector in the back direction while the front direction is approximately 6 dB below the peak, a well known fact resulting from the finite ground plane (diameter = 4 feet).

Cross Polarization Pattern

Cross polarized patterns are always of interest; in particular in the present case where we are trying to obtain low radiation in the back direction to avoid interference. A complete set in the horizontal

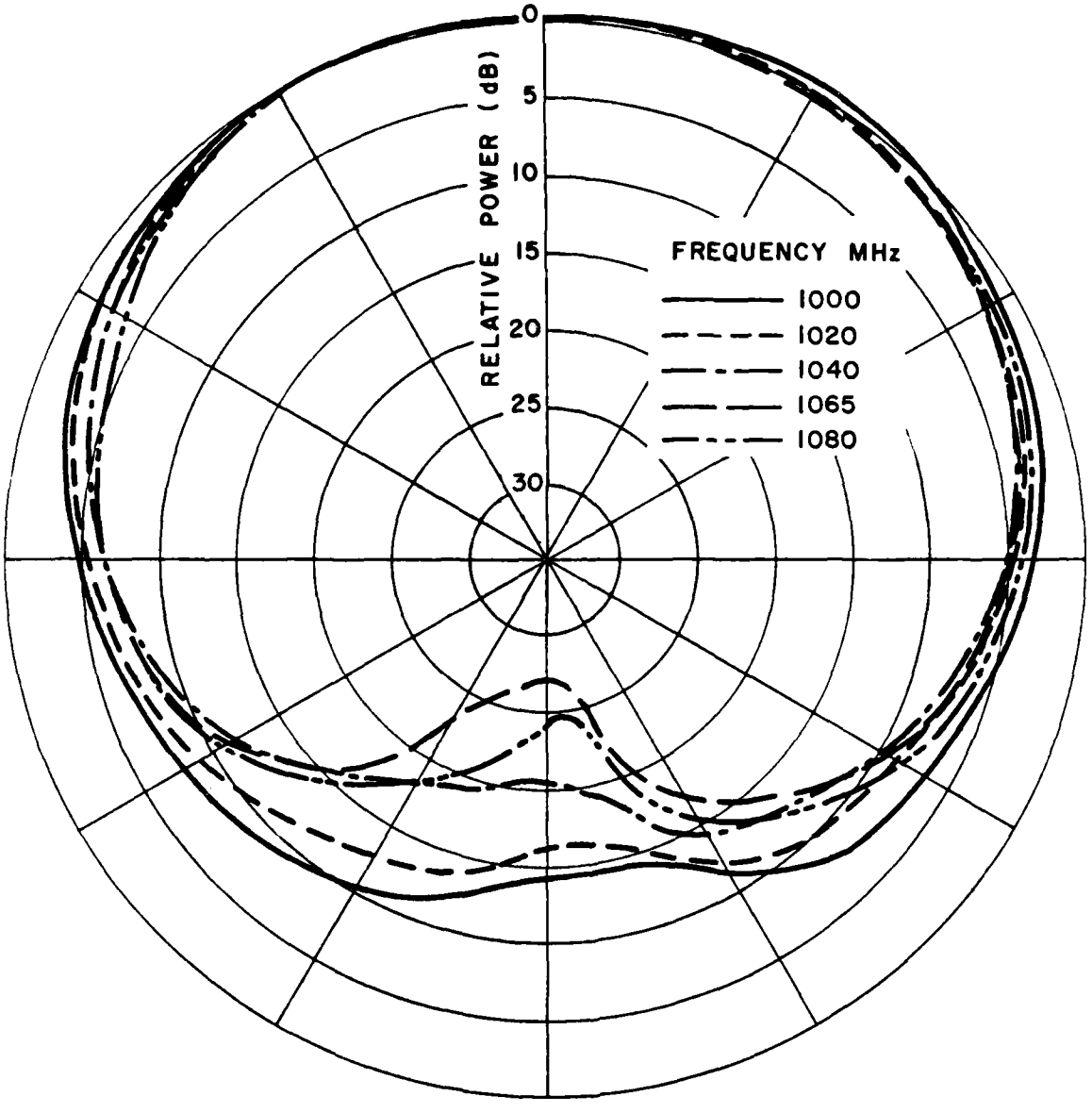

Figure 38a. Cardioid pattern of the IFF antenna.
Frequencies 1000-1080 MHz.
Taken at elevation 8° above horizon.
Loop 1+3 activated.
Vertical Polarization

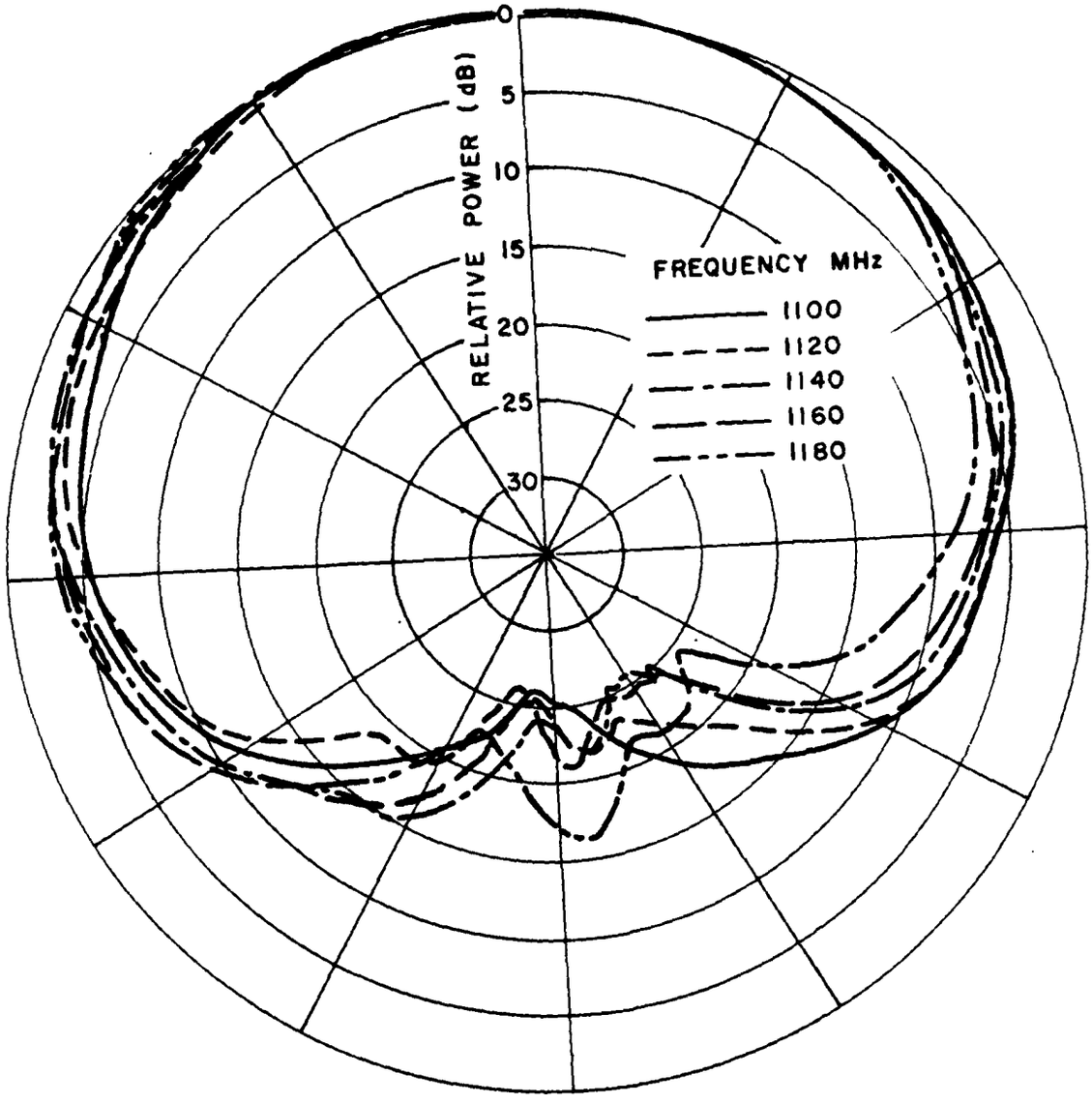

Figure 38b. Cardioid pattern of the IFF antenna.
Frequencies 1100-1180 MHz.
Taken at elevation 8^{o} above horizon.
Loop 1+3 activated.
Vertical Polarization

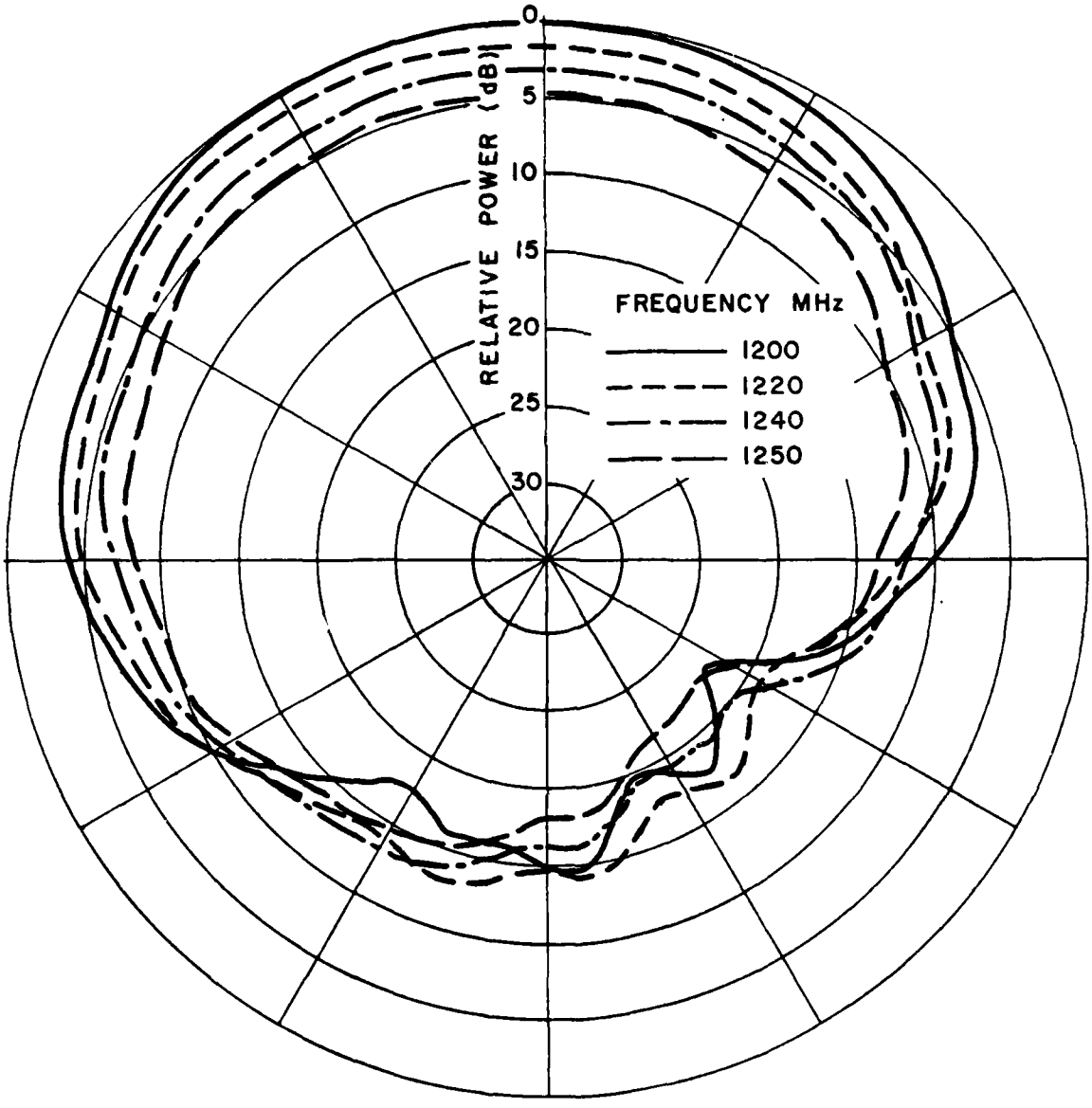

Figure 38c. Cardioid pattern of the IFF antenna.
Frequencies 1200-1250 MHz.
Taken at elevation $\sim 8^{0}$ above horizon.
Loop 1+3 activated.
Vertical Polarization.

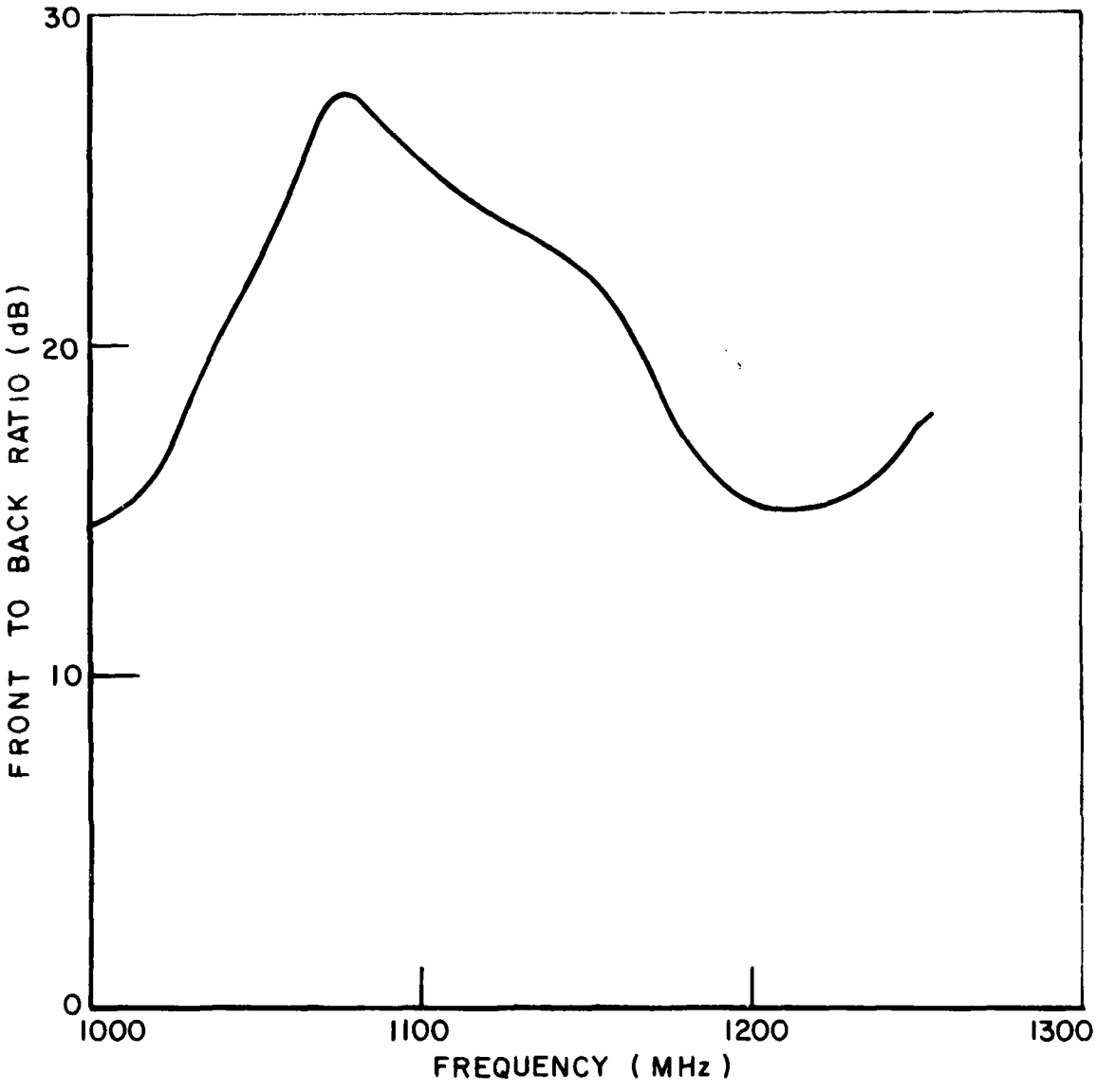

Figure 39. The FB-ratio as a function of frequency taken from the measured pattern in Figure 38.

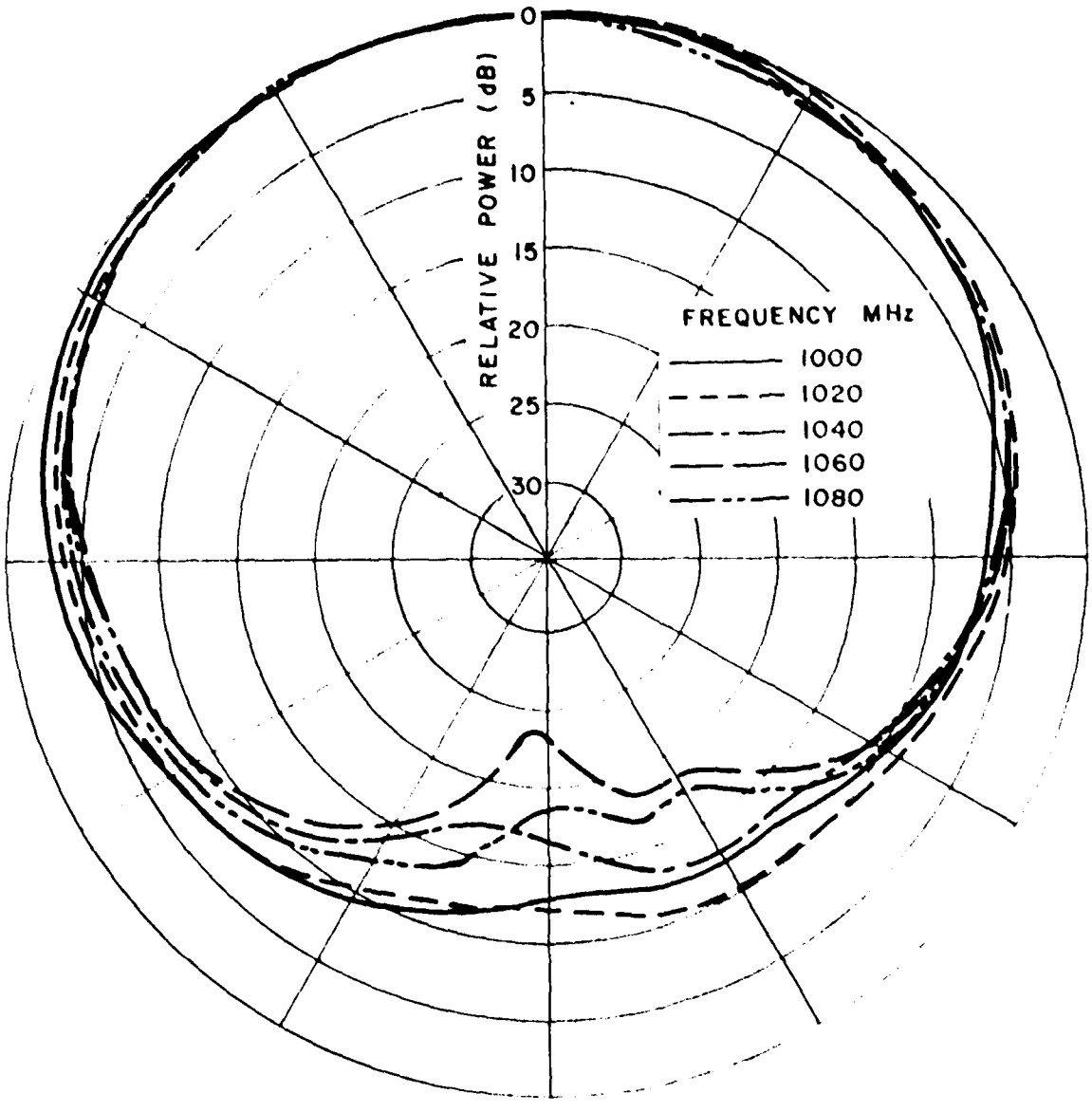

Figure 40a. Cardioid pattern of the III antenna.
Frequencies 1000-1080 MHz.
Taken at elevation $+8^{0}$ above horizon.
Loop 244 activated.
Vertical Polarization.

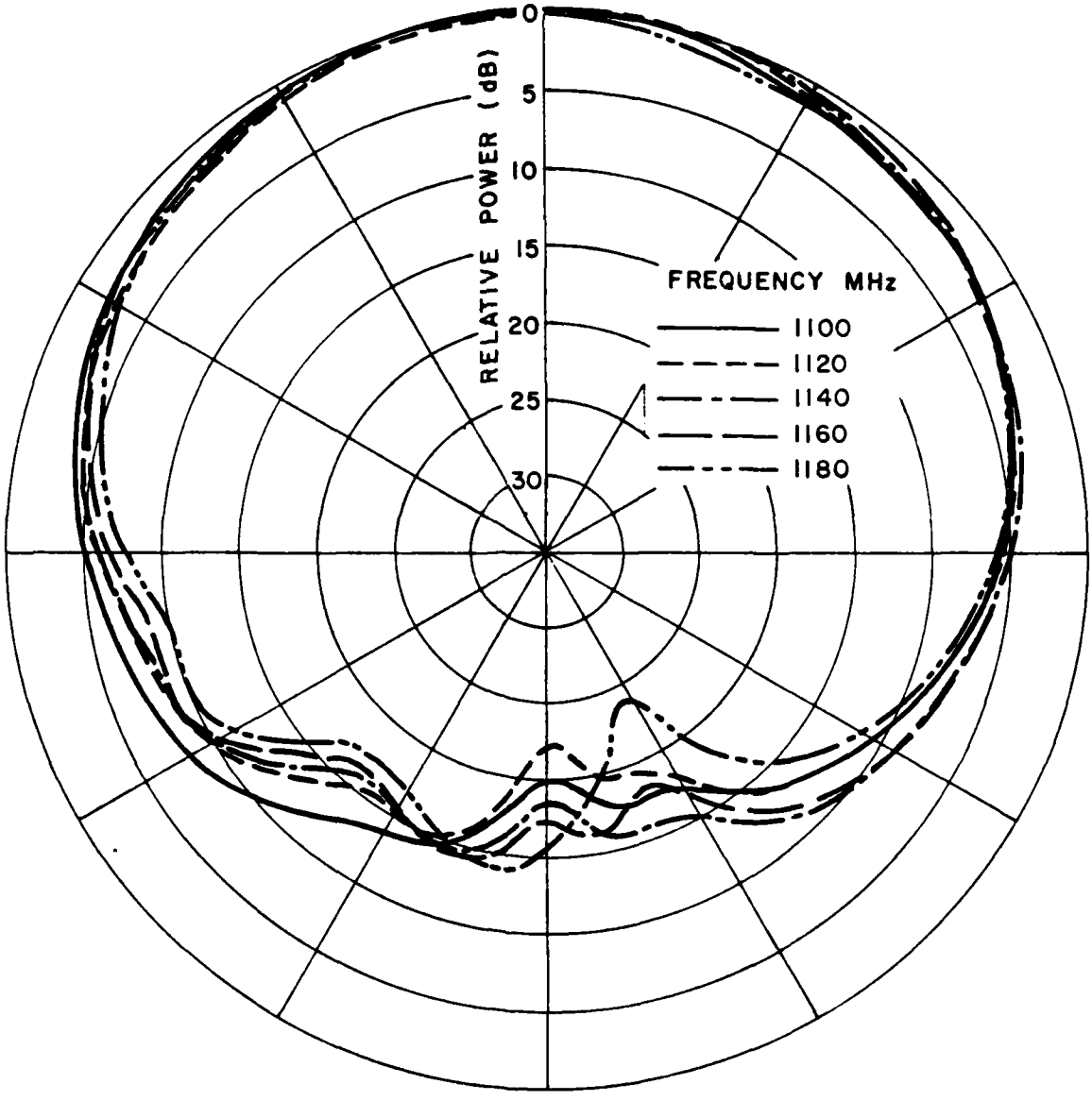

Figure 40b. Cardioid pattern of the IFF antenna.
Frequencies 1100-1180 MHz.
Taken at elevation $\sim 8^{\circ}$ above horizon.
Loop 2+4 activated.
Vertical Polarization.

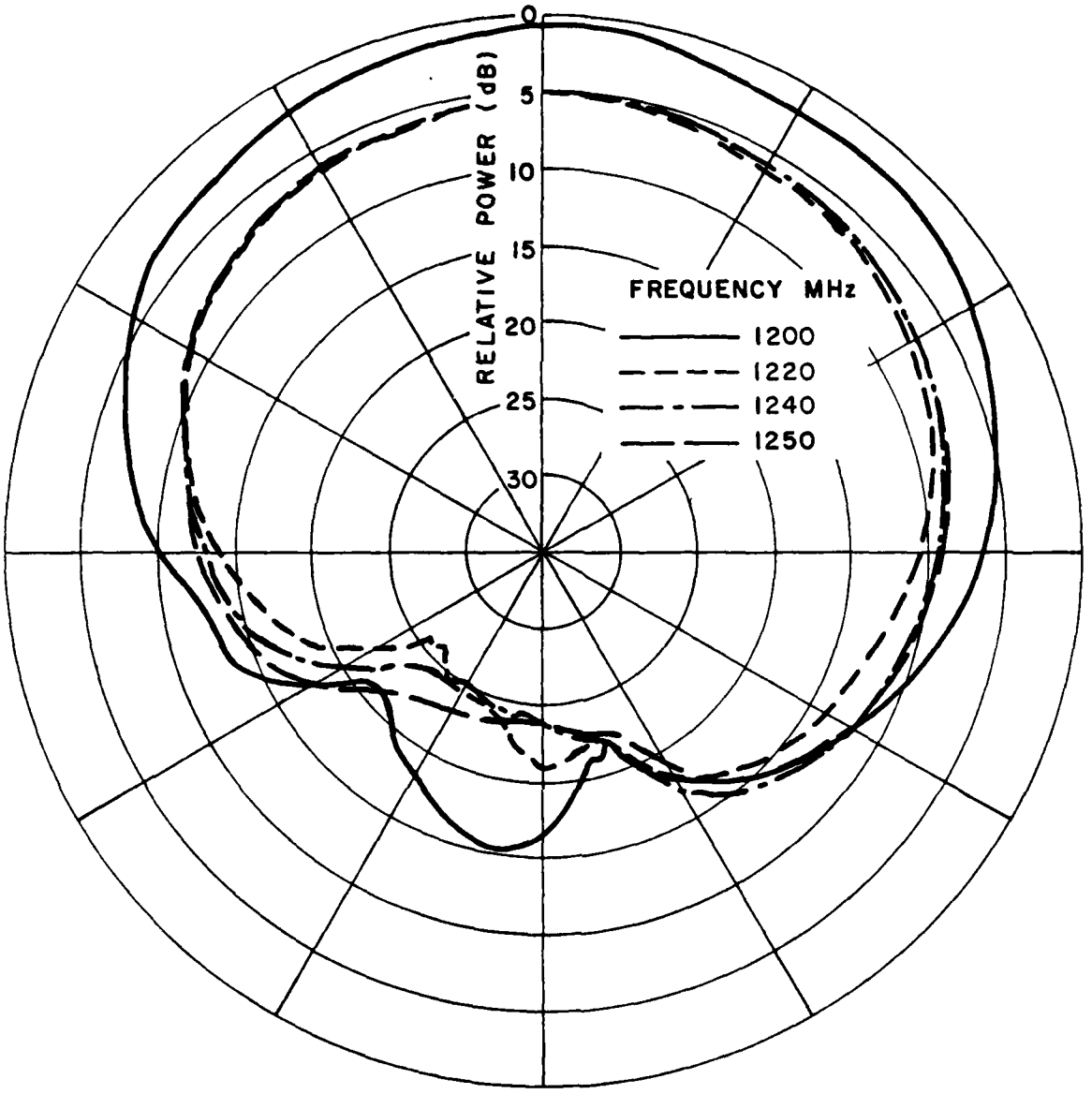

Figure 40c. Cardioid pattern of the IFF antenna.
Frequencies 1200-1250 MHz.
Taken at elevation $\sim 8^{o}$ above horizon.
Loop 2+4 activated.
Vertical Polarization.

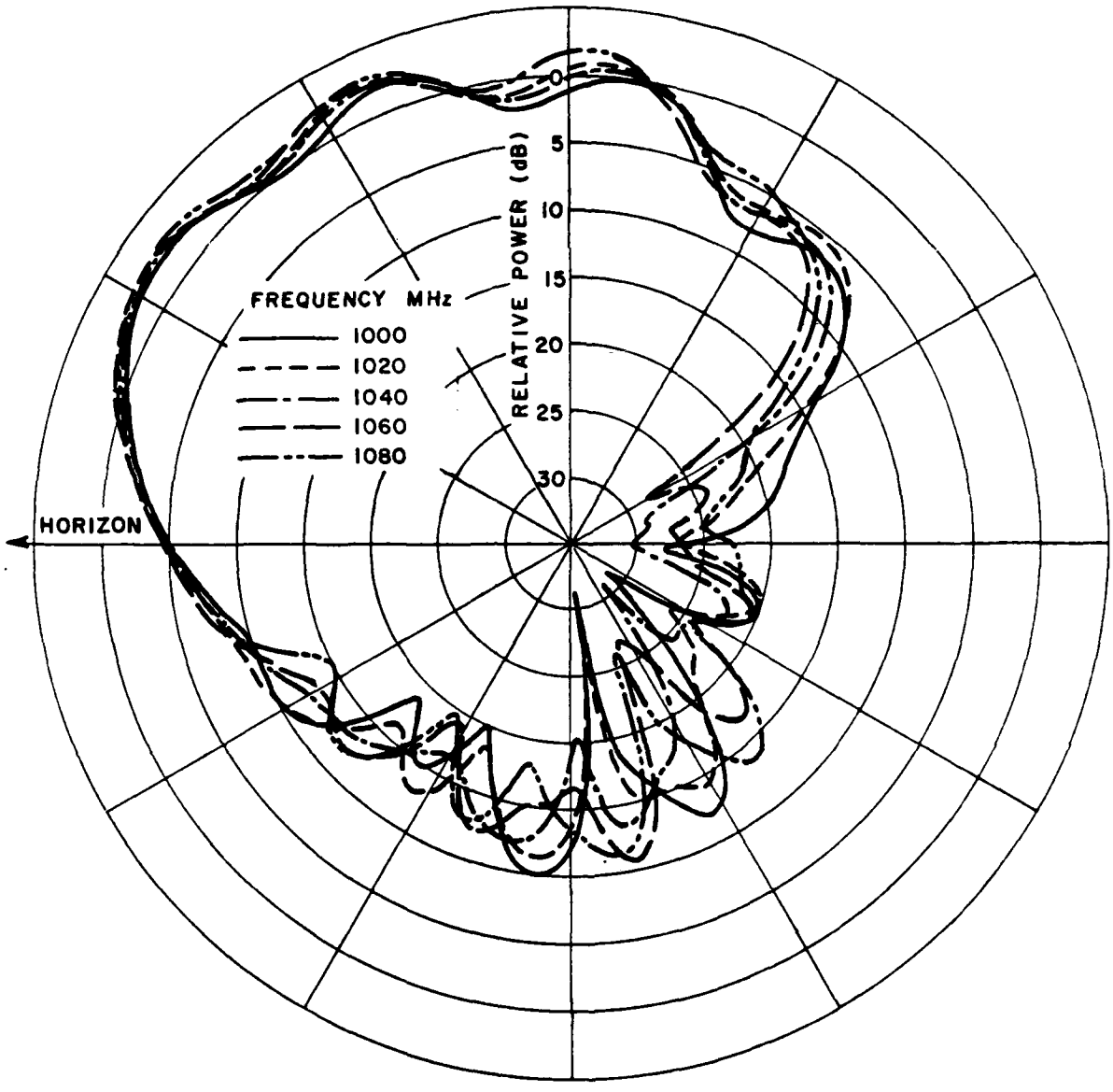

Figure 41a. Vertical pattern of the IFF antenna taken through the plane of symmetry. Frequency 1000-1080 MHz. Loop 1+3 activated. Vertical Polarization.

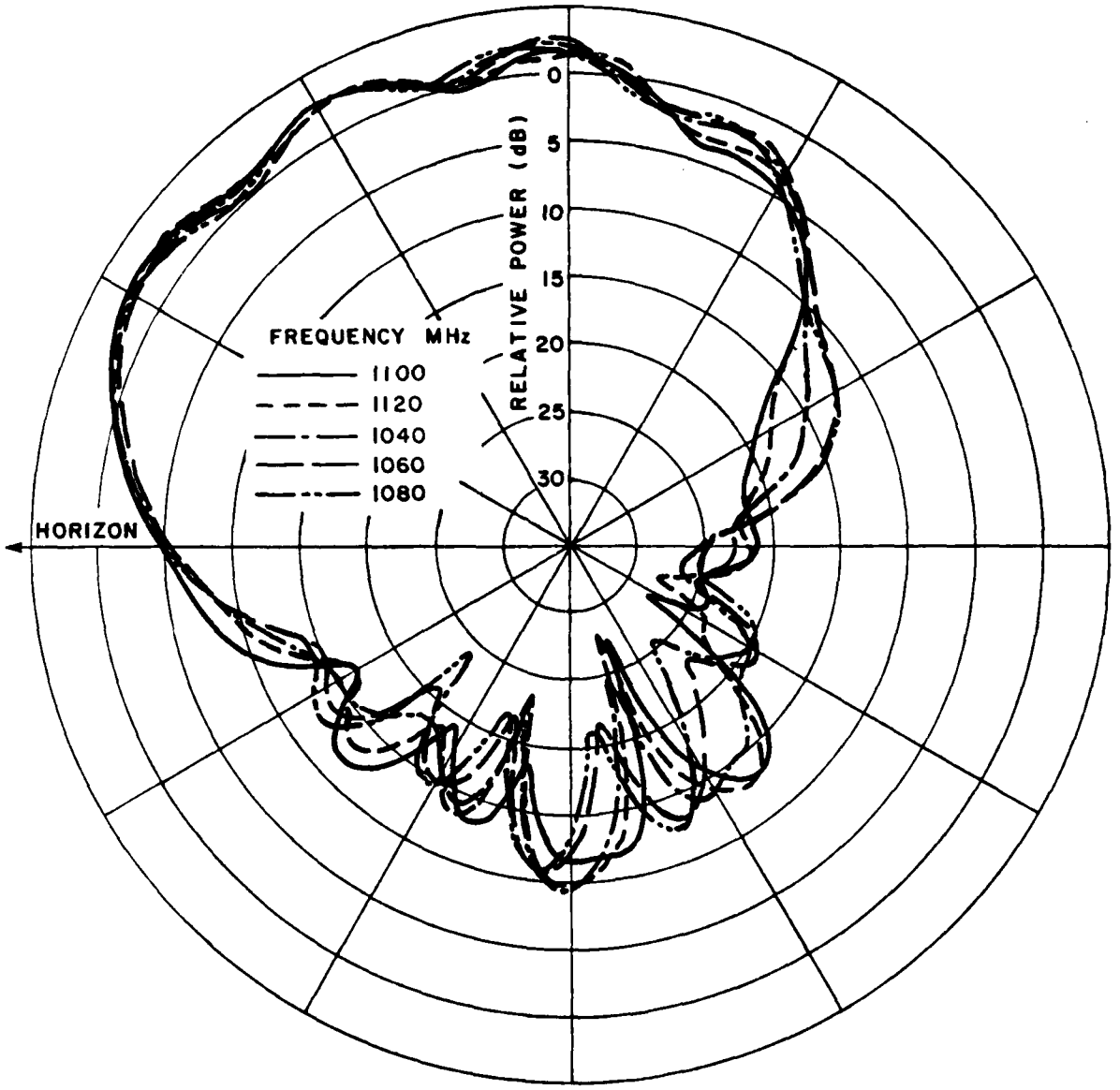

Figure 41b. Vertical pattern of the IFF antenna taken through the plane of symmetry. Frequencies 1100-1180 MHz. Loop 1+3 activated. Vertical Polarization.

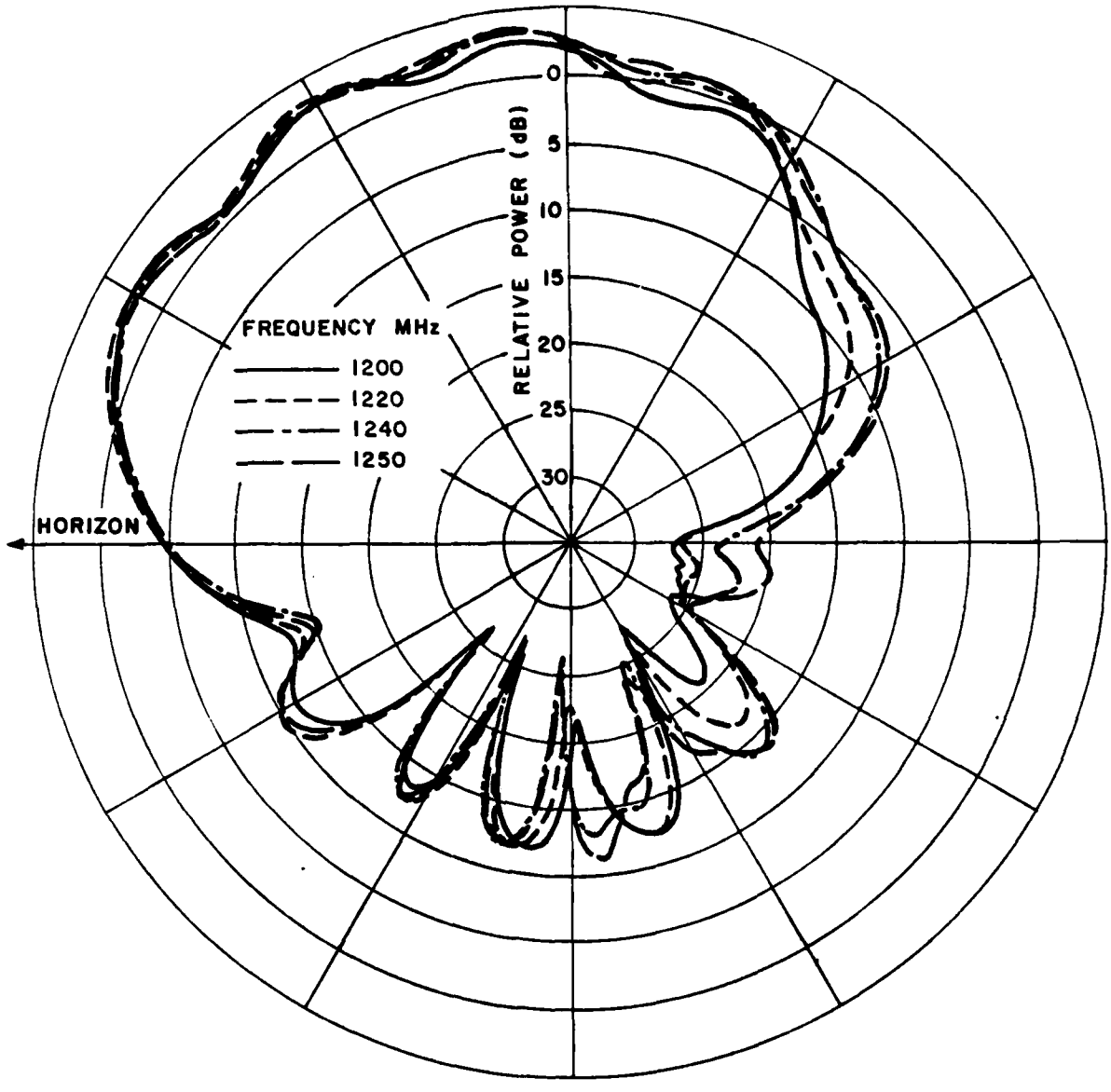

Figure 41c. Vertical pattern of the IFF antenna taken through the plane of symmetry. Frequencies 1200-1250 MHz. Loop 1+3 activated. Vertical Polarization.

plane (actually 8^{o} elevation) is shown in Figure 42 for every 50 MHz in the range 1000-1250 MHz. The level in the back direction is seen to be more than 20 dB below the parallel polarization in the front which is considered very acceptable. Only in the side directions do we have a level worse than 15 dB, however this is of little consequence since the parallel pattern itself is only down around 6 dB with respect to the signal in the front direction.

Gain

The measured gain of the new antenna with respect to a standard IFF antenna used by the U. S. Navy (AT-740/A) is seen in Figure 43. Considering that a "passing grade" is considered a tie between the two, we must state that an average gain of $\sqrt{2}$ dB of the new antenna is more than satisfactory.

VSWR of Final Antenna

We have earlier shown the VSWR of both the input of the monopole and the input of the balun leading to the two sets of loops. These are as explained earlier connected to a specially made 4 dB hybrid. The input impedance of this hybrid connected to the monopole and the balun is shown in Figure 44. Except for the first 15 MHz and the last 50 MHz the VSWR of the entire antenna is well within 2:1.

Effect of Flush Mounting

As pointed out earlier the monopole extends approximately 3/8" above the ground plane and several attempts to get it below this level was detrimental to the monopole impedance. However, during a meeting at the ElectroScience Laboratory it was suggested by Messrs. Gerry Hart and Paris Coleman from NRL, that perhaps a compromise could be obtained if the diameter of the cavity was somehow increased at the very top.

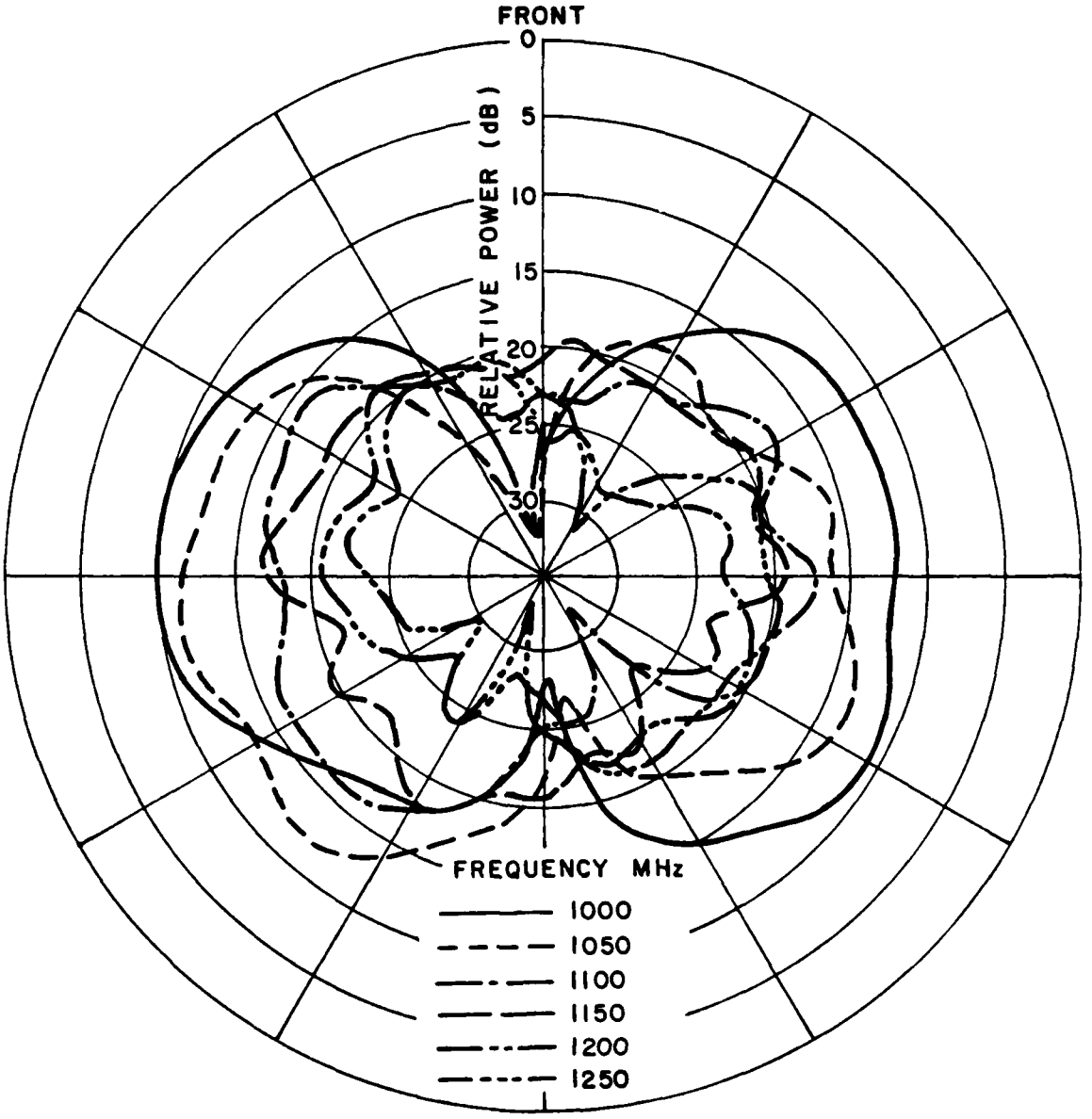

Figure 42. The cross polarized radiation pattern of the cardioid pattern shown in Figure 38. Elevation 8^{o}.

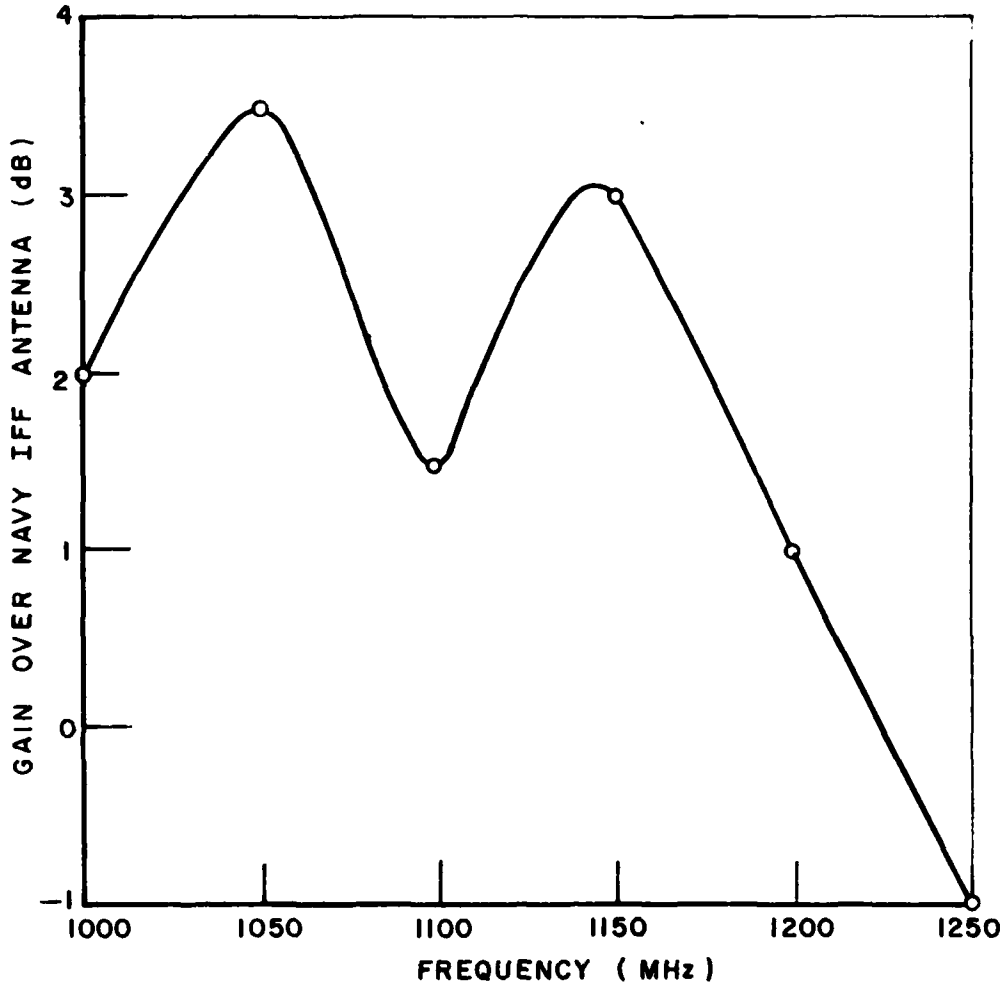

Figure 43. The gain of the new IFF antenna measured with respect to old IFF antenna type AT-740/A.

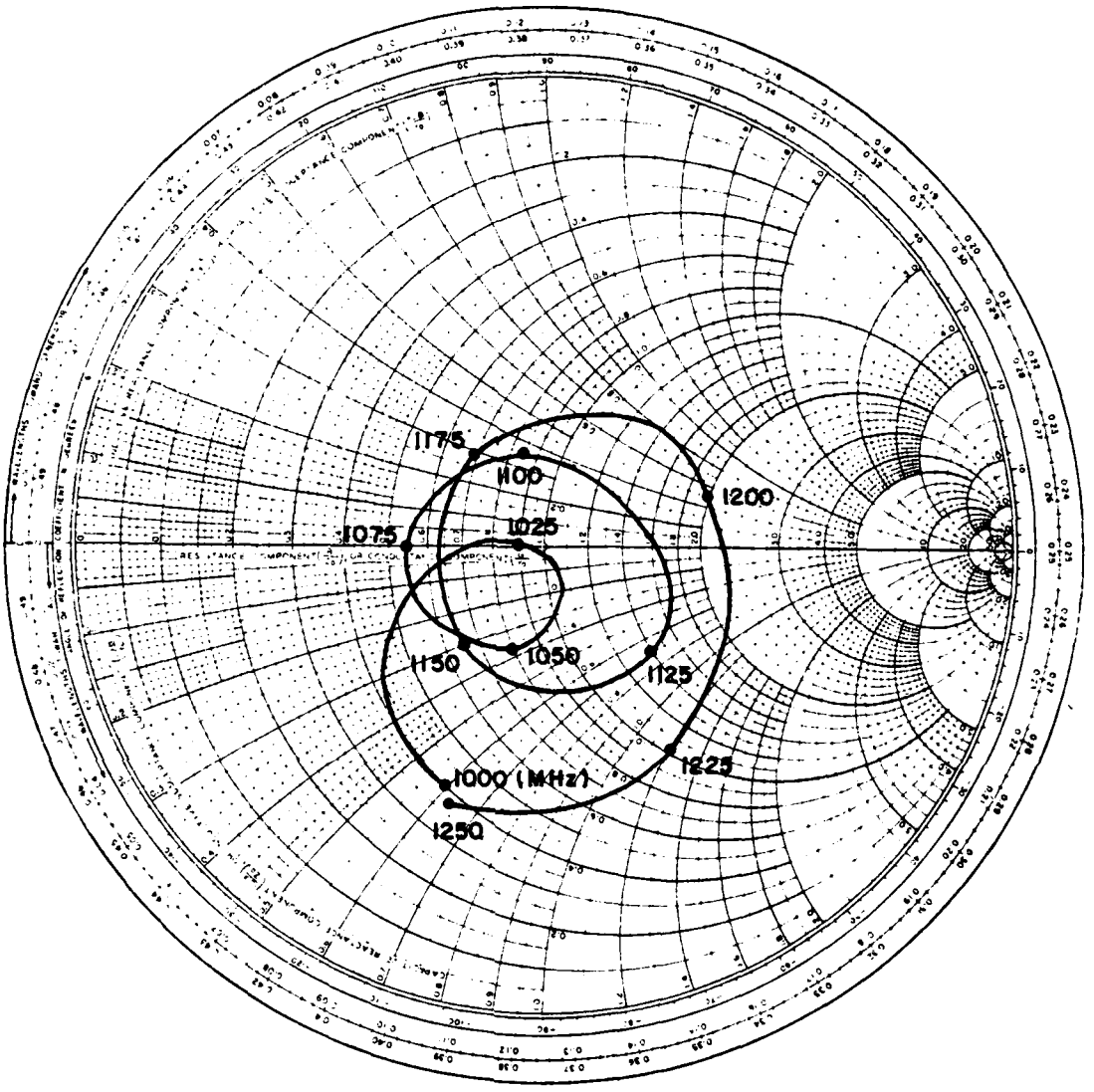

Figure 44. The impedance seen at the 4 dB hybrid connected to the monopole and a pair of loops via the balun.

To this end we modified the antenna and ground plane as indicated in Figure 45 by a build up of the ground plane as shown by the broken lines.

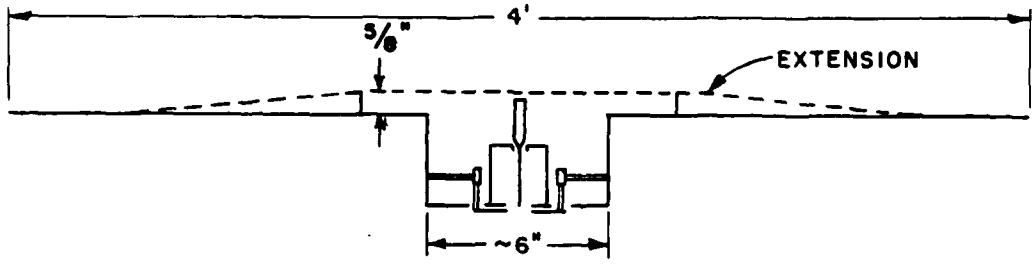

Figure 45. The buildup of copper sheets around the IFF antenna making the monopole flush with the airplane skin.

We were not too surprised by observing no significant change in the impedance. However, we were particularly impressed by observing only minute changes in the radiation pattern as can be seen in Figure 46a and b where the former shows the radiation pattern with the "build up" ground plane and the latter the plain ground plane as before where the monopole is protruding ~1/2".

CONCLUSION

We have produced a flush mounted cavity antenna with a diameter of 6" for the frequency band 1000-1250 MHz. The radiation pattern was a cardioid with a front-to-back ratio better than 15 dB in the entire band and better than 20 dB from 1040-1160 MHz. The beam can be directed in four directions in the horizontal plane with 90^{o} intervals. This should be adequate considering that the 3 dB beam width in the forward direction is $\pm 60^{o}$ and also that the width of the section in the back yielding low back radiation is roughly $\pm 45^{o}$. The level of the cross polarized signal with respect to the parallel signal was 20 dB or more

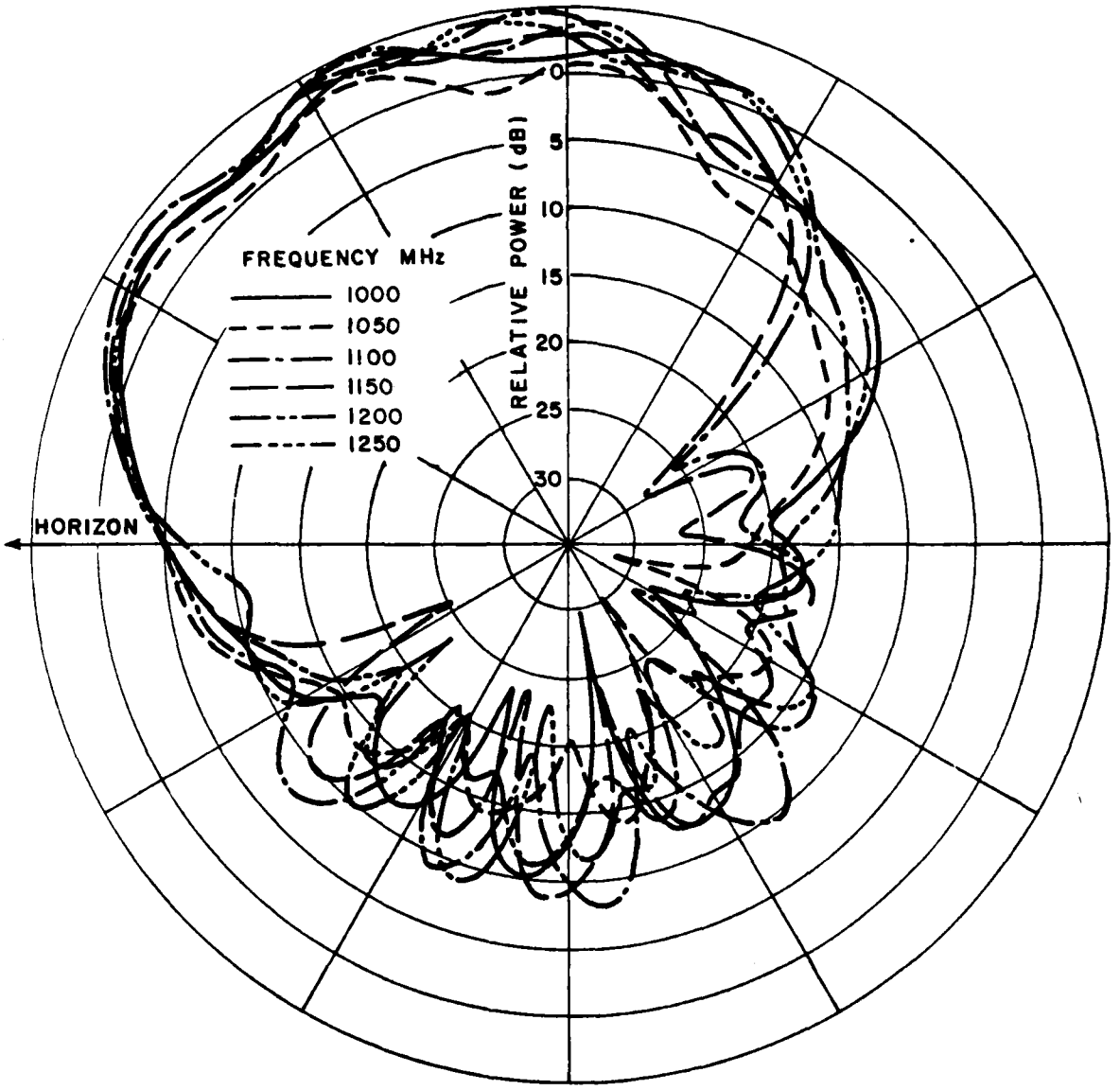

Figure 46a. The vertical pattern of the IFF antenna with the "buildup" as shown in Figure 45.

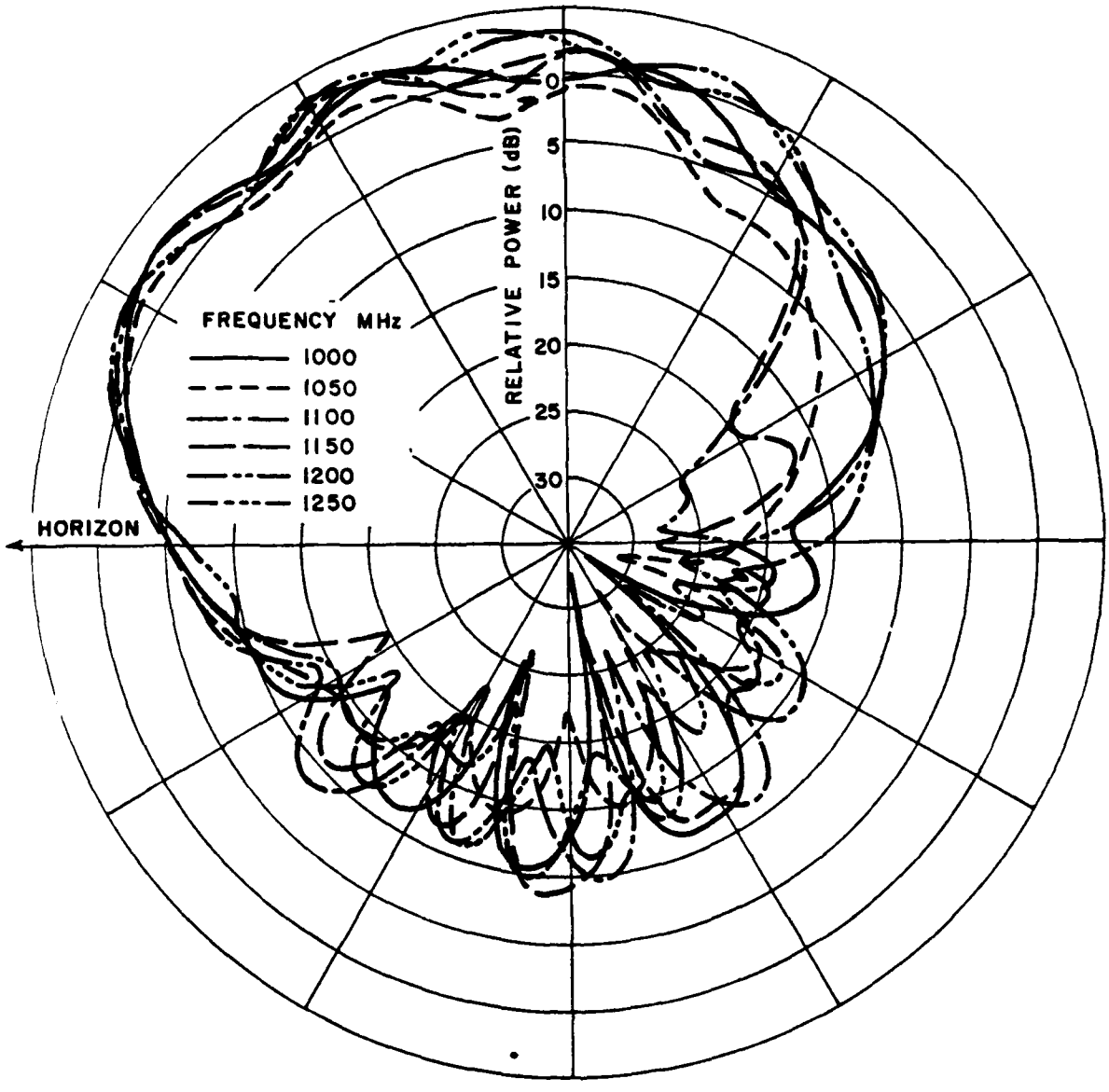

Figure 46b. The vertical pattern of the IFF antenna without the "buildup" as shown in Figure 45.

below in the forward direction and lower or equal to in the back direction. Finally, the gain of this new antenna was about 2 dB more than a monopole. Thus, all in all we have produced a flush mounted antenna that very much satisfied the design goals stipulated by NRL. We do regret that the cavity was 5" deep (although no stipulation to this effect was given in the contract). However, since some concern in this matter was raised by Messrs. Gerry Hart and Paris Coleman at a meeting at ElectroScience Laboratory, we decided (time permitting) to reduce the size of the cavity. This effort is described in Appendix B. We may conclude that this model having only a 2" deep cavity could quite possibly be made workable with a somewhat reduced bandwidth (like 1000-1160 MHz). The perfection of this antenna must await some time in the future.

REFERENCES

1. Koichi Ayoke and B. A. Munk, "Annular Slots with Cardioid Type Pattern," Report 711559-1, The Ohio State University ElectroScience Laboratory, Department of Electrical Engineering; In preparation under Contract N00014-78-C-0855 For Department of the Navy, Office of Naval Research.

2. George L. Matthaei, Leo Young and E. M. T. Jones, Microwave Filters, Impedance-Matching Networks and Coupling Structures, McGraw Hill, 1964, pp. 795-797.

APPENDIX A
DESIGN OF A 4 dB HYBRID

As mentioned in the text we decided to make our own 4 dB hybrid used to connect the monopole and the set of loops. The design of the hybrid is described in Reference [2] and is known as a transmission line coupler using interleaved strips. Two couplers were designed and constructed with nominal couplings of 3.5 and 4.5 dB. Measurements of the couplers using a network analyzer showed a coupling of 4.0 and 5.0 dB. These results were quite good considering that the strip lines were not done photographically. Over the years the authors have become proficient at using Scotch tape, a straight edge and an X-acto knife in laying out microstrip and strip lines. The nominal dimensions of the 4 dB hybrid are given in Figures A-1 and A-2.

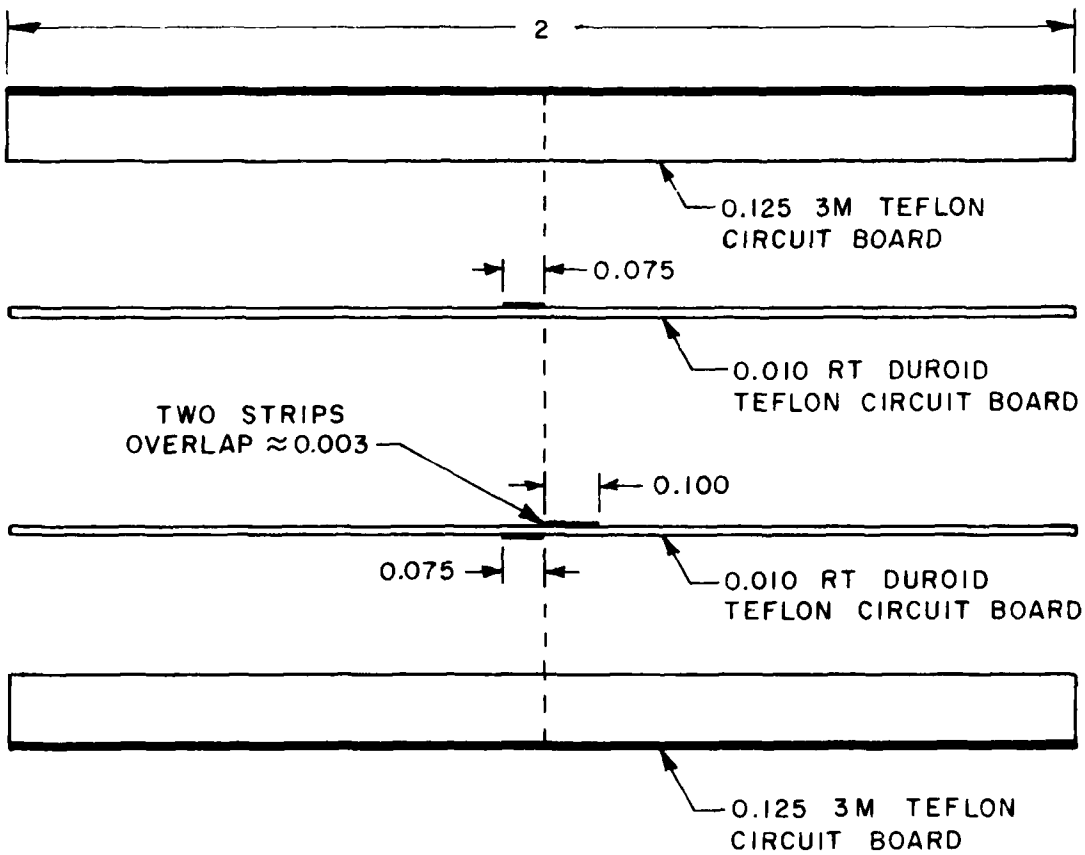

Figure A-1. Edge view details of construction of 1125 MHz 4 dB coupled-transmission-line directional coupler using interleaved strips. All dimensions in inches.

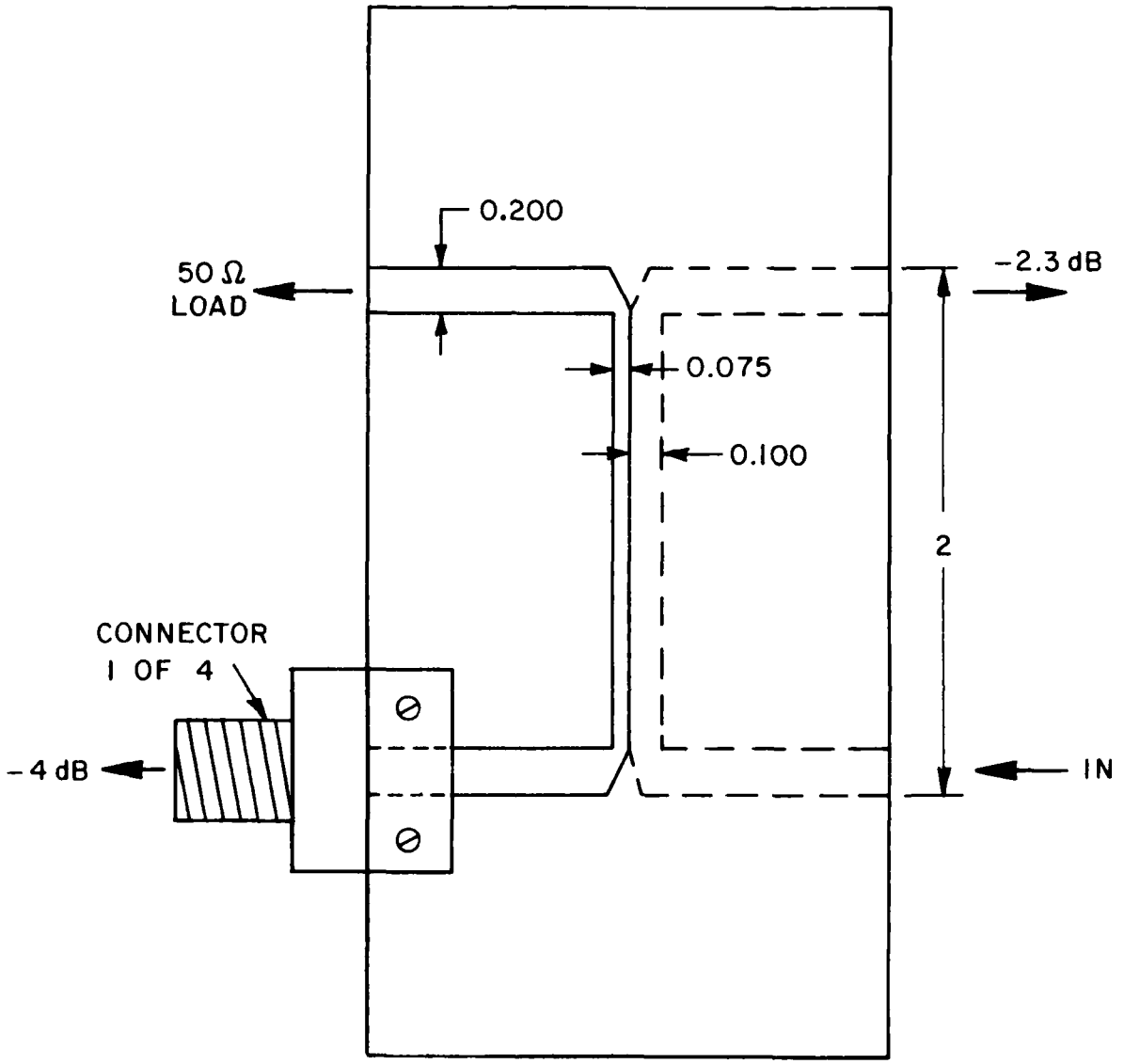

Figure A-2. Top view details of 4 dB hybrid.
All dimensions in inches.

APPENDIX B
THE SHALLOW VERSION

After learning what and what not to do on the one half wavelength deep cavity we briefly reinvestigated a shallow version of the antenna. Our primary problem with earlier versions was that the cavity was about one-quarter wavelength deep. Since the cavity impedance was in series with the monopole's terminal impedance, (see text) it makes the total impedance more reactive and changes rapidly as a function of frequency. Another problem is the series resonant circuit formed by the inductance of the horizontal part of the loop and the capacitance between the vertical part of the loop and the inside wall of the cavity. The unfortunate thing is that when the loops are properly matched the series resonance occurs in the operating band. This resonance short circuits the cavity making the cavity less deep. If the cavity is about one-half wavelength deep a small change in the cavity depth changes the impedance of the cavity a small amount. However, if the cavity is about one-quarter wavelength deep a small change in the cavity depth will change the impedance of the cavity a lot. Since the cavity impedance is in series with the monopole impedance we do not want the cavity impedance to vary a lot. Since we would like to avoid one-quarter wavelength deep cavities, the depth of the cavity was reduced to about one-eighth wavelength. A cross sectional view of this antenna is shown in Figure B-1. The feed network for the loops was the same as the feed network of the one-half wavelength version. No attempt was made to match the loop impedance because the VSWR only deteriorated from 2:1 to 4:1 over the band. The monopole impedance changed significantly and the impedance was modified by changing the base capacitance, the top hat capacitance and the monopole length. Figure B-2 shows the best impedance obtained.

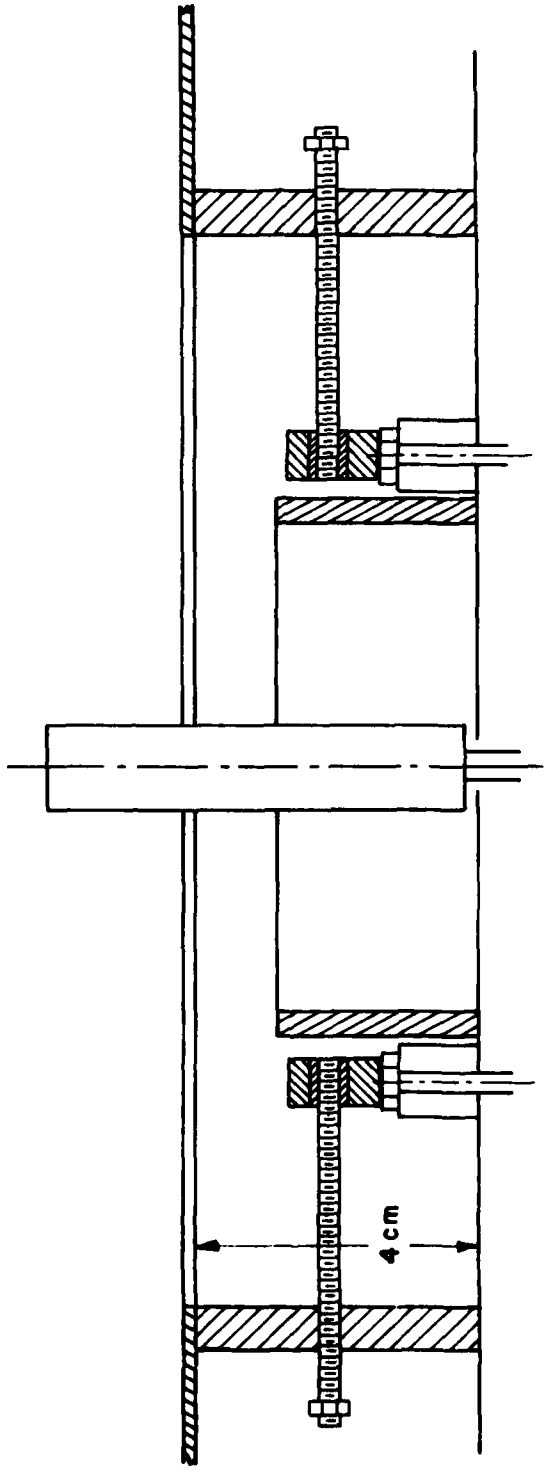

Figure B-1. The cross sectional view of the shallow cavity.

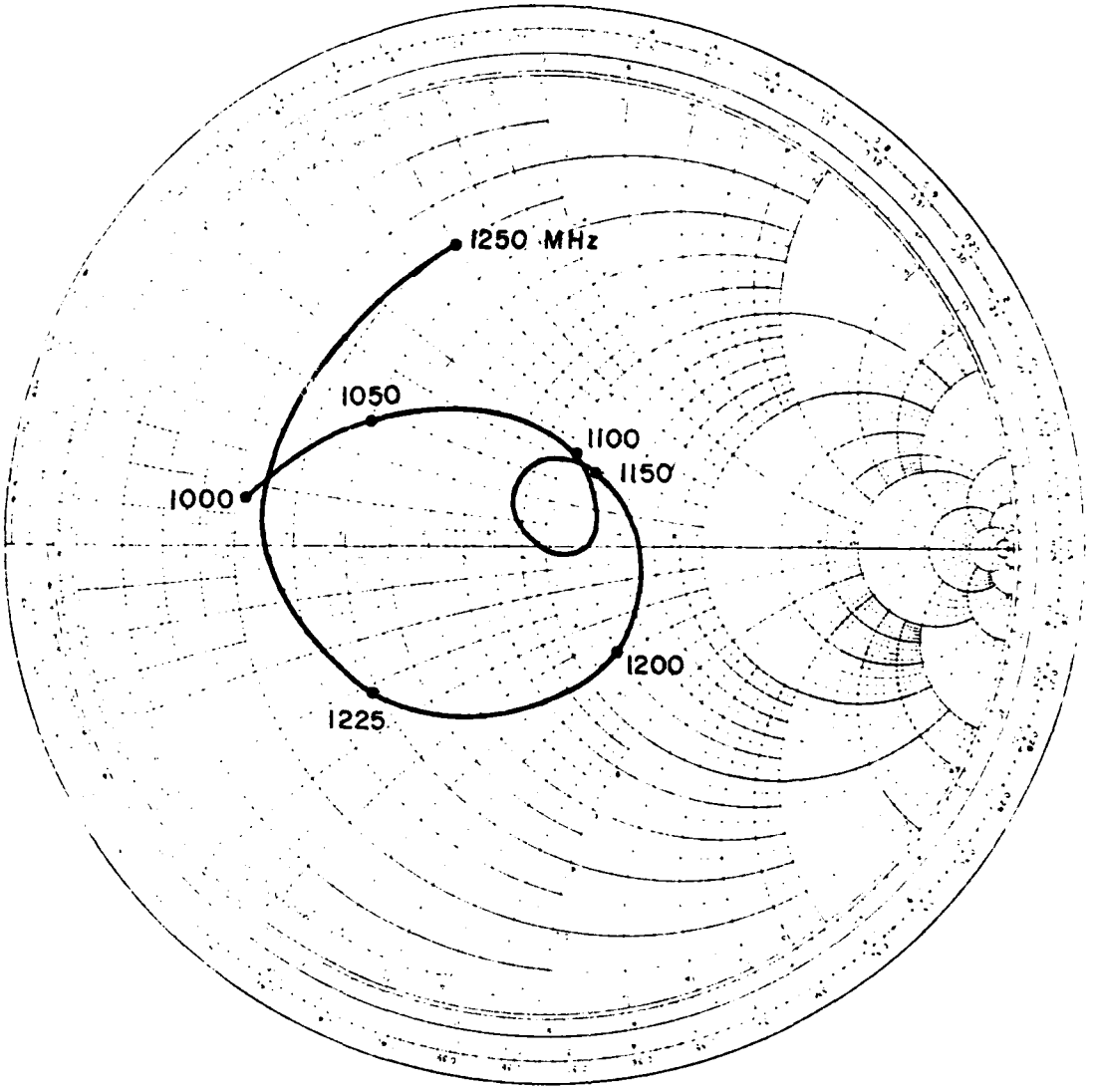

Figure B-2. Input impedance of the monopole of the shallow cavity version.

With the previous shallow version we had some difficulty obtaining good patterns for the monopole and the loops. Figures B-3 and B-4 are the new patternes obtained with the shallower version. In Figure B-3 one immediately notices that the patterns of the monopole are good except at the band edges where the deviation from a perfect circle is $\pm$ 1.5 dB. However, the loop patterns shown in Figure B-4 are not very good. These patterns show an imbalance in the loops at the high end of the band which is probably due to the feed network and/or the loops.

The impedance and pattern measurements indicate that the shallow cavity version could be made to work but over a smaller bandwidth. The smaller bandwidth is primarily due to the impedance of the loops and monopole being harder to match. We feel the reduction in bandwidth would be about 50 to 100 MHz.

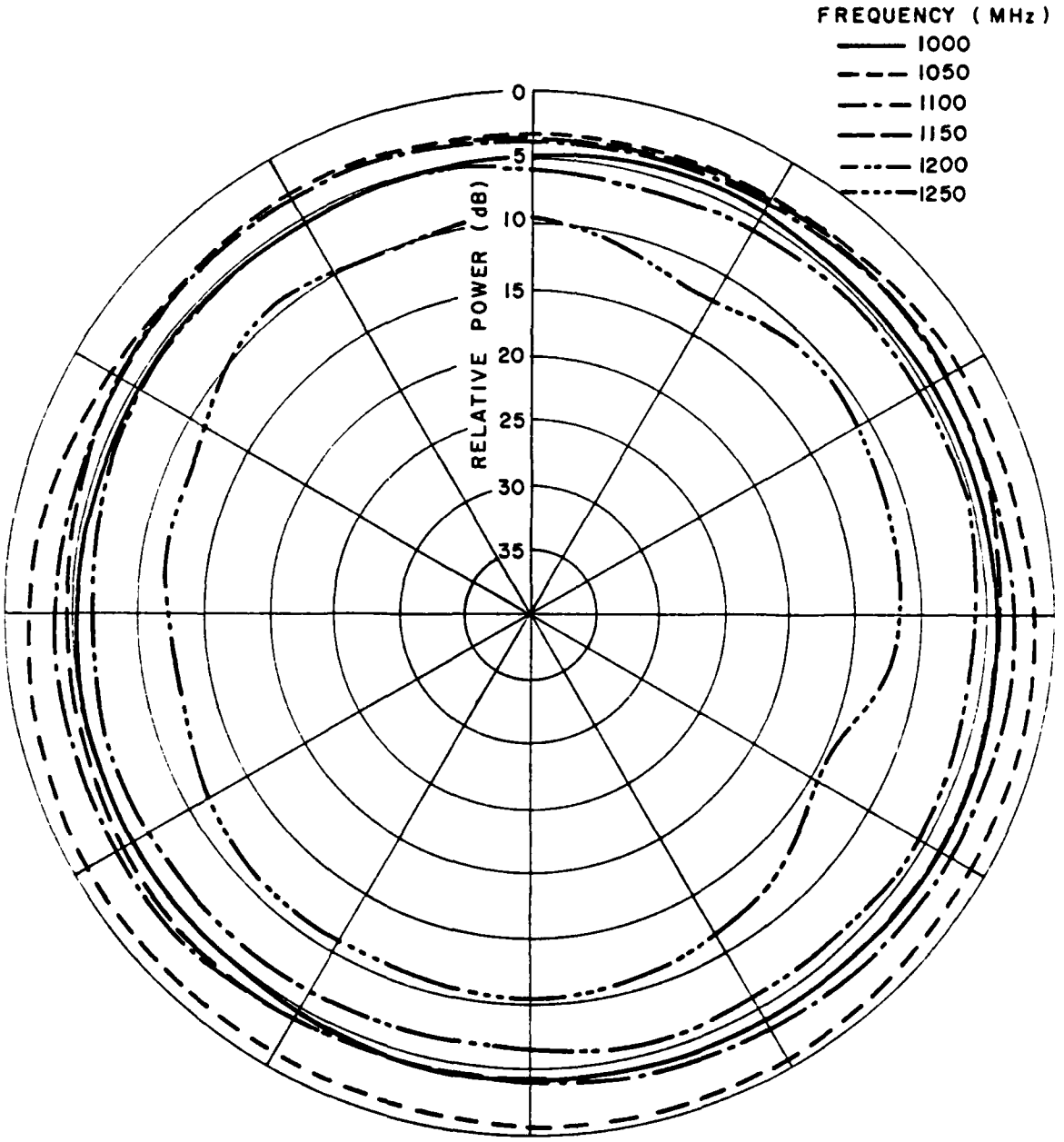

Figure B-3. Measured monopole pattern of the shallow cavity version with the 4 foot diameter ground plane.

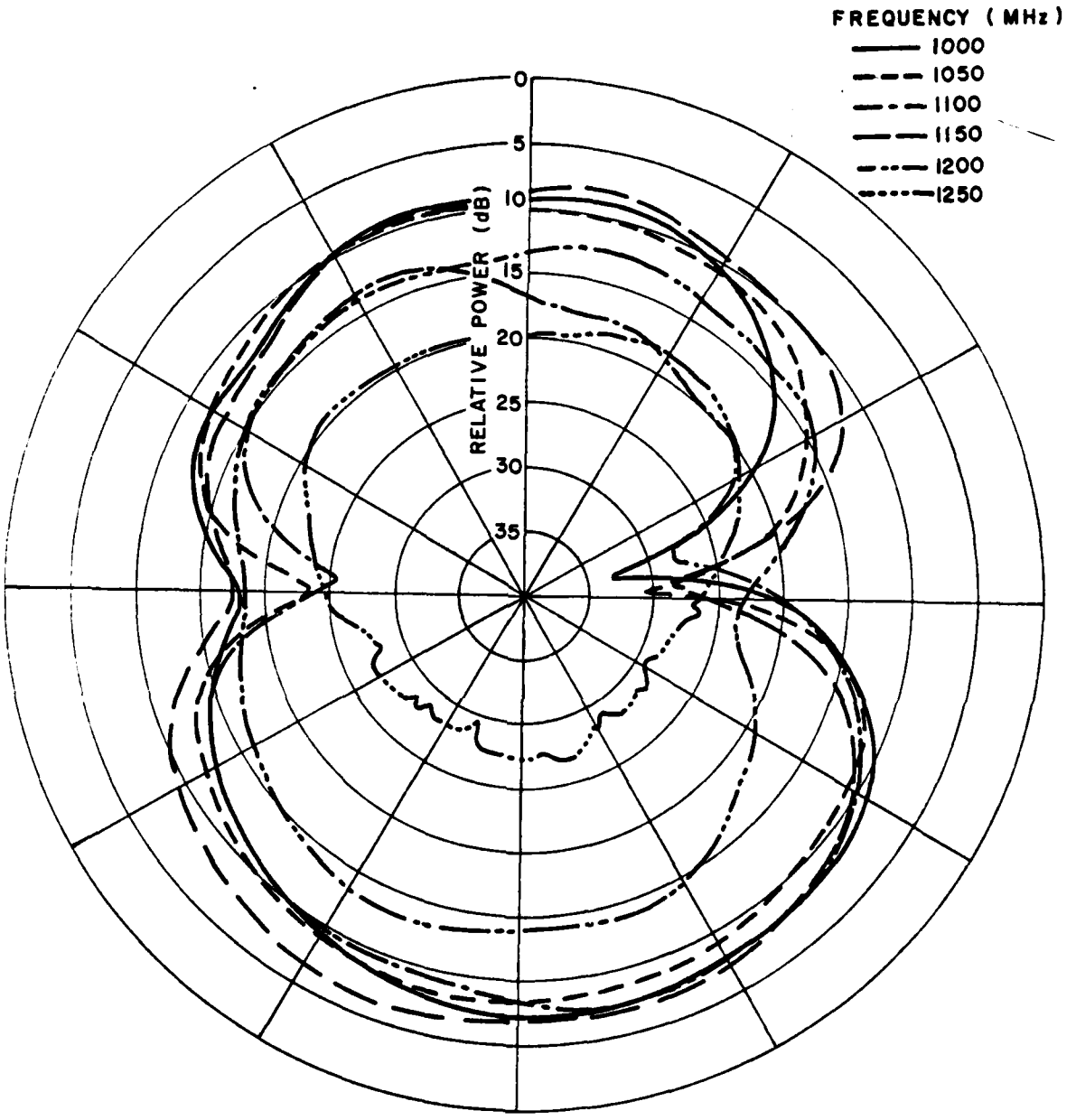

Figure B-4. Measured loop pattern of the shallow cavity version with the 4 foot diameter ground plane.